Beam Column Connections for Multi-storey Timber Buildings

A Report

submitted in partial fulfulment

of the requirements for the Degree

of

Master of Engineering in Civil

in the

University of Canterbury

by

Robert Hugh Fairweather

University of Canterbury

1992

ABSTRACT

This report concerns the testing of 8 connections constructed using steel dowels epoxy bonded into glulam timber. Tests were conducted under simulated seismic loads. Three different types of connection were tested; epoxied steel dowels only, epoxied threaded rods embedded into the members and bolted to the joint made from a prefabricated steel hub and thirdly, epoxied threaded rods embedded into the members but bolted to two steel side brackets, one each side of the column. Two types of bar were used: mild steel deformed reinforcing bars and high strength threaded rods. Several different arrangements of bars within the joint were examined; two different sizes of deformed bars and two different epoxy types were also used.

Several connections exhibited excellent ductile behaviour and could be designed using a capacity design procedure.

TABLE OF CONTENTS

LIST OF FIGURES

PAGE

PAGE

PAGE

LIST OF TABLES

PAGE

ACKNOWLEDGEMENTS

This project would not have been possible without the material and financial support given by several organizations. All the glulam timber was donated by three manufacturers under the auspices of the Structural Engineered Timber Manufacturers Association (SETMA); Hunter Laminates Ltd of Nelson, Peter Stevens Ltd of Christchurch and McIntosh Timber Laminates Ltd of Auckland. The epoxy was donated by Adhesive Technologies Ltd of Auckland and Hylton Parker Fasteners of Christchurch. Financial support came from two scholarships awarded by the Timber Design Society for Pacific Timber Engineering Scholarship and the New Zealand National Society for Earthquake Engineering for the Earthquake Engineering Research Scholarship.

My thanks to all the above contributors for their support. It was greatly appreciated.

I would like to thank my supervisors, Dr John Dean and especially Dr Andrew Buchanan for their encouragement and enthusiasm through out this project. A special thanks goes to David Macpherson for his valuable input and enthusiasm in preparing and testing the specimens. Other technical assistance from Mark Stuart-Jones, Paul Murphy and John Maley in preparing the connections was appreciated. I would also like to thank Geoff Hill for his input on laboratory procedures.

Finally I would like to thank my wife, Rowena for her unselfish support and encouragement during this project. This project would never have started without her backing. Not only did she help with the typing of this report and its final preparation, but she did more than her fair share of the work at home while I was busy working on this project.

NOTATION

γ	=	Total joint shear strain
Δ	=	Deflection (mm)
δ_1, δ_2	=	Measured vertical displacements due to column rotation (mm)
δ_3, δ_4	=	Measured horizontal displacements due to beam rotation (mm)
δ_5, δ_6	=	Measured displacements on the diagonal clip gauges due to joint distortion (mm)
$\delta_{b(flexure)}$	=	Flexural component of beam deformation (mm)
$\delta_{b(shear)}$	=	Shear component of beam deformation (mm)
$\delta_{b(sliding\ shear)}$	=	Sliding shear deformation in the beams (mm)
Δ_c	=	Column deflection (mm)
$\delta_{c(flexure)}$	=	Flexural component of column deformation (mm)
$\delta_{c(shear)}$	=	Shear component of column deformation (mm)
$\delta_{c(sliding\ shear)}$	=	Sliding shear deformation in the column (mm)
$\Delta_{c,b}$	=	Column deformation due to beam flexure and shear (mm)
$\Delta_{c,b(flexure)}$	=	Column deformation due to beam flexure only (mm)
$\Delta_{c,b(shear)}$	=	Column deformation due to beam shear only (mm)
$\Delta_{c,c}$	=	Column deformation due to column flexure and shear (mm)
$\Delta_{c,c(flexure)}$	=	Column deformation due to column flexure only (mm)
$\Delta_{c,c(shear)}$	=	Column deformation due to column shear only (mm)
$\Delta_{c,j}$	=	Column deformation due to the shear distortion of the joint region
$\Delta_{c,r}$	=	Column deformation due to hinge rotation of the beams and the column
$\Delta_{c,r(beam)}$	=	Column deformation due to hinge rotation of the beams only
$\Delta_{c,r(column)}$	=	Column deformation due to hinge rotation of the column only
$\Delta_{c,s}$	=	Column deformation due to sliding shear at the beam-column face
$\Delta_{c,s(beam)}$	=	Column deformation due to sliding shear of the beams only
$\Delta_{c,s(column)}$	=	Column deformation due to sliding shear of column only
Δ_{max}	=	Maximum column deflection (mm)
Δ_y	=	Column displacement at first yielding of the structure (mm)

θ	=	Angle of inclination between the diagonal and the horizontal (radians)
μ	=	Displacement Ductility Factor = Δ_{max}/Δ_y
ϕ_b	=	Rotation of the beam end (radians)
ϕ_c	=	Rotation of the column end (radians)
A_b	=	Cross sectional area of the beam (mm^2)
A_c	=	Cross sectional area of the column (mm^2)
A_{gh}	=	Gross area of the joint core in the horizontal direction (mm^2)
A_{gv}	=	Gross area of the joint core in the vertical direction (mm^2)
A_v	=	Shear cross sectional area (mm^2)
B	=	Breadth of the timber member (mm)
B_b	=	Breadth of the beam (mm)
B_c	=	Breadth of the column (mm)
C	=	Resultant compressive force in the dowels (kN)
d	=	Length of the diagonal clip gauge (mm)
D	=	Depth of the timber member (mm)
e	=	Horizontal distance between the vertical gauges (mm)
E	=	Young's Modulus of Elasticity for timber (MPa)
f_b	=	Bending stress in the timber (MPa)
f_s	=	Shear stress in the timber (MPa)
f_{sh}	=	Average horizontal shear stress in the joint region (MPa)
f_{sv}	=	Average vertical shear stress in the joint region (MPa)
F_{s1}, F_{s2}	=	Force in the steel bars (kN)
F_y	=	Yield strength of the steel bars (kN)
g	=	Vertical distance between the horizontal gauges (mm)
G	=	Shear Modulus for timber, which is usually taken as E/15 (MPa)
H	=	Storey height (mm)
h_b	=	Depth of the beam (mm)
h_c	=	Depth of the column (mm)
I_b	=	Moment of Inertia of the beam about the major axis (mm^4)
I_c	=	Moment of inertia of the column about the major axis (mm^4)
jd	=	Distance between the resultant steel dowel forces (mm)
k	=	Shear distribution factor = 1.5

K	=	Initial stiffness (kN/mm)
l_b	=	Clear distance from the end of the beam to the face of the column
L_b	=	Length of the beam to the centre of the column (mm)
l_c	=	Clear distance from the top of the column to the top of the beams (mm)
L_c	=	Length of the column to the centre of the beams (mm)
M	=	Bending moment in the timber member (kNm)
M_y	=	Measured bending moment in the timber member at first yield of the reinforcing steel in the connection (kNm)
M_y'	=	Theoretical bending moment in the timber member at first yield of the reinforcing steel in the connection (kNm)
P	=	Lateral load (kN)
P_y	=	Measured lateral load applied at the top of the column, resulting in first yield of the reinforcing steel in the connection (kN)
P_y'	=	Theoretical lateral load applied at the top of the column, resulting in first yield of the reinforcing steel in the connection (kN)
T	=	Resultant tensile force in the dowels (kN)
V_b	=	Shear force at the beam end (kN)
V_c	=	Shear force at the column end (kN)
V_{col}	=	Shear force in the column (kN)
V_{jh}	=	Horizontal shear force in the joint core (kN)
V_{jv}	=	Vertical shear force in the joint core (kN)
x_1, x_2	=	Lever arm between the bar groups (mm)
Z	=	Section modulus of the timber member (mm^3)

CHAPTER 1

INTRODUCTION

1.1 INTRODUCTION

In New Zealand, most of the timber used by the building industry is for domestic dwellings consisting of one and two storeys. While the amount of timber used in agricultural and industrial buildings has steadily increased over the past few years, there has been no growth in multistorey timber structures in the commercial sector (Buchanan, Deam and Dean, 1991). This indifference to timber buildings taller than two storeys is partly due to restrictive design codes, the lack of information on the feasibility of building such structures and the shortage of information on the design and performance of moment-resisting connections. Several recent studies (Halliday, 1991 and Thomas, 1991) have recently been conducted and indicate that multi-storey timber buildings up to six storeys are not only technically feasible, but economically viable.

A recent innovation in New Zealand is the use of steel dowels epoxy bonded into timber. This method comprises of drilling a hole in the timber about 6mm larger than the dowel diameter, centrally placing the bar in the hole and injecting epoxy into a grout hole positioned at one end, until it begins to flow out of an airing hole at the other end. Use of this technique enables steel bars to be placed at the top and bottom of the beams, forming a compression/tension couple which resists the column moment with the shear carried by dowel action. Recent uses in New Zealand include swimming pools (Buchanan and Fletcher, 1989) and a space frame roof (NZ Journal of Timber Construction, 1986).

Several advantages can be gained by epoxy bonding steel dowels into timber:

- the steel components are protected from corrosion
- allows high strength connections to be made, utilizing the full strength of the timber

- the epoxy provides a bond stronger than the timber
- increased stiffness of the joint
- excellent aesthetic appearance
- excellent fire resistance since the timber member protects the connection

Simple beam-column connections can be made using epoxied steel dowels. By using mild steel reinforcing bars, excellent ductile behaviour can be achieved. Connections designed for ductile behaviour should use a capacity design procedure. This approach ensures that the timber members have sufficient capacity to remain intact while the ductile deformations occur at specially designed elements, designed for that purpose. The ductile connections must be weaker than the connecting members.

Using a steel bracket and epoxied steel dowels gives a good solution to the problem of constructability. All holes are drilled, the bars placed and glued in place in the factory. The members are transported to the building site and bolted to the prefabricated steel bracket. This allows for very fast construction times. This type has the advantage, that if well designed, it will show excellent ductile behaviour and final failure will consist of damage to the steel flange plates and not the rods or timber members. A capacity design approach should be adopted to ensure the right failure mechanism. The benefits of this type of connection are that great savings in construction time will result due to faster erection of members.

1.2 SCOPE OF REPORT

This report on beam-column connections for multistorey timber structures carries on from and extends the technology developed in previous two reports describing the work undertaken in the Department of Civil Engineering, University of Canterbury, by Townsend (1990) and Buchanan and Townsend (1990). The main aims of this report are:

(i) to develop new and improved beam-column connections suitable for multistorey timber construction;

(ii) to provide designers of timber buildings with design information on the behaviour of

several connection systems;

(iii) to investigate the effects of member and joint deformations on the overall column displacement; and

(iv) to trial two new epoxy formulations.

1.3 OUTLINE OF REPORT

Chapter 2 consists of a literature review of recent experimental work in the use of epoxy bonded steel in timber, with particular reference to moment-resisting connections. Alternative connections using bolts, nails and dowels are also mentioned. Examples of recent uses of epoxy dowels are also documented.

Chapter 3 describes the different types of materials used during the project and the method of assembly used to construct the connections. The arrangement of the testing frame is discussed along with the testing procedure.

Chapter 4 outlines the theory used to analyze the test results.

Chapter 5 describes the tests carried out on different types of connections. The behaviour of each connection is examined and compared against the performance of the other connections. Several trends are discussed and a summary of made.

Chapter 6 consists of conclusions drawn from the testing programme. Several recommendations for design follow, ending with a list of further research needs.

CHAPTER 2

LITERATURE REVIEW

2.1 INTRODUCTION

Most of the timber used by the building industry in New Zealand is for domestic dwellings consisting of one and two storeys. The amount of timber used in agricultural and industrial buildings has steadily increased over the past few years, but there has been no growth in timber structures in the commercial sector. This indifference to timber buildings taller than two storeys is partly due to restrictive design codes and the lack of design information (Buchanan, Deam and Dean, 1991).

While New Zealand has had a long history of timber structures, there have been very few multi-storey timber buildings built. The earliest multi-storey timber building is the Government Buildings in Wellington, which was built in 1875 (Clark, 1984). Many buildings constructed during the early 1900s used timber internal frames with external masonry walls. Two examples of modern timber office buildings are the Carter Holt building in Auckland and the Odlins building in Wellington. Both buildings use large glulam members for framing with concrete or masonry walls used to resist the lateral loads (Smith, 1982).

Several recent studies (Halliday, 1991 and Thomas 1991) have suggested that multi-storey timber buildings up to six storeys are not only technically feasible, but economically viable, as long as adequate beam-column connections are available.

In the last few years, there has been renewed interest in timber building construction in Europe and North America, where building codes are not so restrictive. Several seven storey timber buildings have been built in North America; a wooden framed building in Anchorage, Alaska (Doyle, 1985) and an asbestos processing mill in British Columbia, Canada. A five storey wood frame building was built on the Campus of Stanford University (Bulleit, 1989).

Lembke (1991) reports on several recent projects in the United States, Japan and Europe where there is a trend towards multi-level, wood framed structures. In the United States, several five storey buildings have just been built; the "2900 on First" building in Seattle (apartments), the "Copperfield Hill" building in Minneapolis (a retirement community with 157 units) and the four storey "Hampshire Place Apartments" in downtown Los Angeles (259 units). In the United Kingdom, a five-storey frame structure was built (probably the first for that country) consisting of a 40 bed extension to a hotel in Inverness. In Holland, building permits for 25 four-storey timber frame structures have been issued, with 22 more to be issued later, all for urban housing projects.

2.2 EARTHQUAKE RESISTANCE

Two basic systems are available to multi-storey timber buildings for resisting lateral loads induced during earthquakes; structural walls and moment-resisting frames. Most timber buildings use structural walls lined with plywood as the primary lateral load resisting system. Moment-resisting frames have generally been ignored as the load resisting system for multi-storey timber buildings, although there is potential for frames in commercial buildings since large open spaces are required, making structural walls not a very practical solution (Buchanan, Deam and Dean, 1991).

Two methods are used in lateral load resisting systems to achieve adequate performance during earthquakes; designing for strength or ductility. During an earthquake, buildings must be able to suffer horizontal displacements without a significant loss of strength. Structures designed for strength are very stiff and exhibit little capacity for large deformations without exceeding the strength of the building, resulting in sudden brittle failures and possible collapse of the structure. Ductile structures perform much better as they can tolerate large deformations without producing excessive forces.

Design seismic forces recommended by codes are less for ductile structures than structures designed with no ductility. This is due to the ability of ductile structures to dissipate seismic energy by inelastic deformations.

Building frames designed for ductile behaviour should be the subject of "Capacity Design". A Capacity design procedure ensures that there is sufficient capacity in the brittle materials to remain intact while ductile deformations occur at specially selected elements, detailed for that purpose. It is essential that ductile connections be provided that are weaker than the connected members (Buchanan and Dean, 1988).

Connector ductility found by full-scale testing must be used with care as most connections increase load capacity as deflections beyond first yield are increased. Hence in a building, yielding of the first connection may be followed by failure elsewhere before the first connection reaches its expected ductility capacity (Buchanan and Dean, 1988).

For many large timber structures the connections are the crucial parts. As timber only comes in particular sizes and shapes, strong connections are required. The behaviour of the connection under severe loads like during earthquakes, influences the behaviour of the building. Because of this reason, Buchanan and Dean (1988) classify all timber structures into one of three classes (see Table 2.1), depending on the type of connection and its behaviour: elastic response, limited ductile response and ductile response.

Table 2.1 Ductility exhibited by different types of connections (Buchanan and Dean, 1988)

Ductility Factor	Classification	Joint Type
$\mu = 1$	Elastic	• Rigid glued joints • Strong connections • Toothplate nail joints • Large diameter bolts
$\mu = 2.5+$	Limited Ductility	• Steel plates buckling under compression only • Nailed steel side plates
$\mu = 4$	Ductile	• Nailed joints • Small diameter bolts • Nail-on plates • Shearwalls with nailed sheathing.

2.3 MECHANICALLY FASTENED CONNECTIONS

The types of joints available for use in multi-storey timber buildings is extremely varied, depending on the application, aesthetic, environmental and fire conditions. The standard joints include nailed gusset plates made from steel or plywood or a combination of the two, mild steel bolts by themselves or combined with tooth plates, split rings and shear plates. Tightly fitted steel dowels, steel insert plates with drift pins have also been used in multistorey timber construction. Several concealed joints have been used to either hide or blend into the structural members. Some examples are the hooked plate system and glued dowel joints as shown in Figure 2.1 and Figure 2.2. Many examples of joints are given in the Timber Design and Construction Sourcebook (Gotz et al).

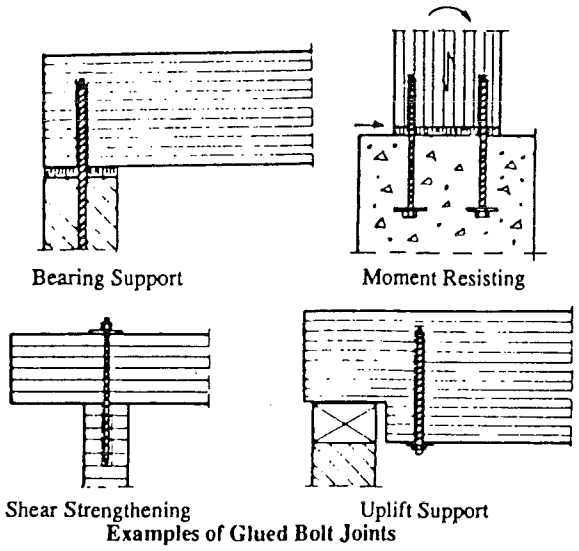

Figure 2.1 Examples of Glued Bolt Joints (Syme, 1989)

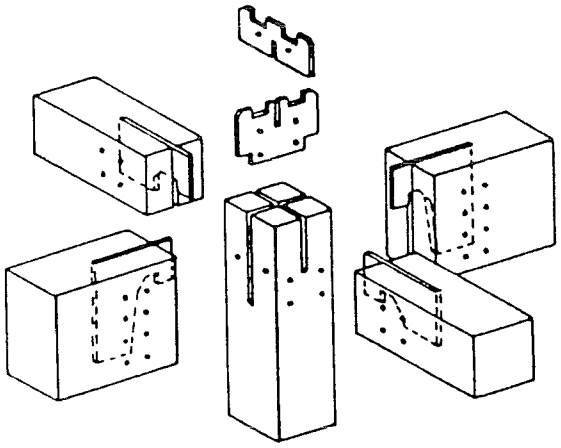

Figure 2.2 Internal hook plates

In moment-resisting timber frames, two types of connections can be constructed (Halliday, 1991) and are as follows:

- interior joints which are characterised by a deep beam that transfers high moment across the joint and a small square column taking low moment and high axial load, and

- exterior joints which usually consists of a deep beam resisting low to moderate moment with a wide column taking moderate moments and axial loads.

The following sections review current research into moment-resisting connections that have the potential to be used in multi-storey frame construction. Most of the recent work completed involves quantifying the performance of particular types of connections by full scale testing combined with analytical modelling.

2.3.1 NAILED CONNECTIONS

In New Zealand, nailed gusset connections are the most popular method of making moment-resisting joints. These joints are very easy to construct, but they are unattractive and behave poorly in fires unless covered with a suitable fire resistant material.

Boult (1988) describes tests completed on multi-nailed connections to determine if current design methods used for nail joints are overly conservative. Testing consisted of computer modelling using finite element method combined with experimental results. Peak nail loads were calculated using rivet group analogy and computer model. Tests determined the influence of nail pattern, the density of nails, the loading and friction between the plate and the timber.

Hunt & Bryant (1988) report on recent developments at Auckland University on moment-resisting nail plate joints.

Batchelar and Hunt (1991) report on tests completed on moment-resisting composite plywood/steel gusset plates.

2.3.2 BOLTED CONNECTIONS

Tokyo University (Inayama and Sakamoto, 1989) developed a new rigid joint using steel plates through the column with the beams being connected to plates using shear rings and high

strength bolts (shown in Figure 2.3). A beam-column joint and column base were tested and it was concluded that it would provide adequate resistance for a three storey rigid frame.

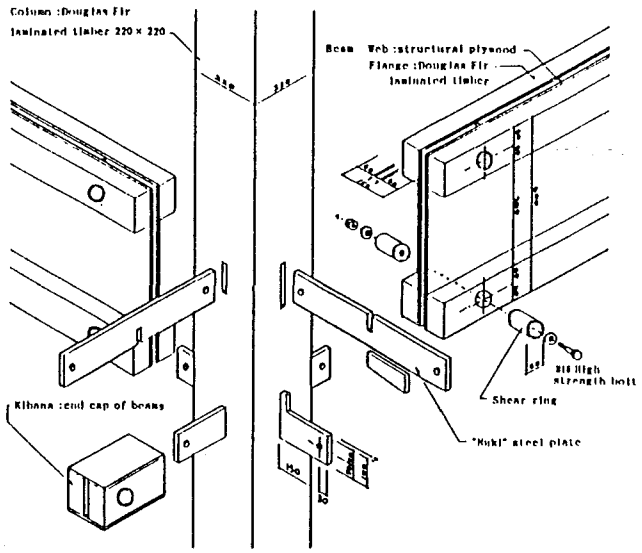

Figure 2.3 Connection using steel plates and shear rings with bolts (Inayama and Sakamoto, 1989)

Ohashi and Sakamoto (1989) report on cyclic tests completed on T-shaped connections using a column and twin-beam arrangement assembled using bolts and shear fasteners (shown in Figure 2.4). Three types of shear fasteners in several different arrangements were tested; split rings, shear plates and bulldog dowels. All connections produced significant ductility.

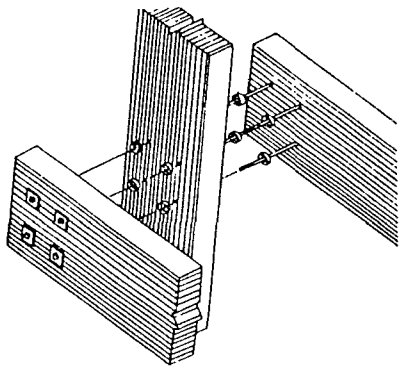

Figure 2.4 Connection using bolts and shear fasteners (Ohashi and Sakamoto, 1989)

2.3.3 DOWEL CONNECTIONS

Ceccotti and Vignoli (1988) carried out tests on several beam-column connections using steel dowels placed in a double ring pattern to resist moment as shown in Figure 2.5. The behaviour of dowelled connections in two and three storey timber frames were investigated to determine seismic performance.

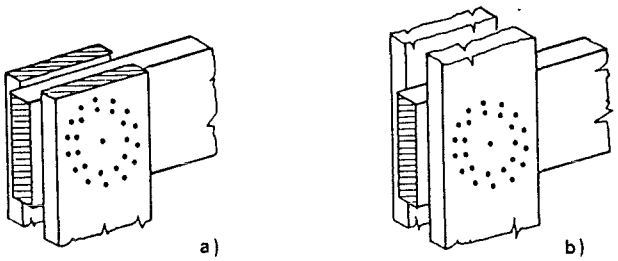

Figure 2.5 Types of moment-resisting dowel joint (Cecotti and Vignoli, 1988)

2.3.4 OTHER TYPES OF JOINTS

Komatsu (1989) reports on push-pull cyclic tests done on two types of mechanical connections; the first using drift pins with steel insert plates and the second with nail plate connections. Continued testing by Komatsu et al (1990) involved push-pull cyclic tests, duration of load tests and fire performance tests.

Komatsu et al (1991) describes a glulam moment-resisting connection using steel side plates bolted to steel insert plates which were embedded into the glulam members and fixed using drift pins. This connection is illustrated in Figure 2.6. Several full scale connections were tested using several different drift-pin sizes and patterns to determine the best arrangement of pins.

This joint was successfully applied to the three storey Obihiro Forest Management Centre building in Japan. This building was probably the first three storey glulam structure built in Japan with a floor area greater than 3000m^2. A photograph of the beam-column connection used in this building is shown in Figure 2.7.

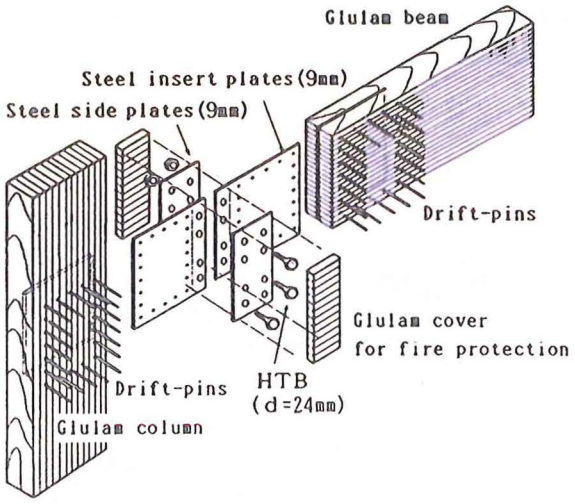

Figure 2.6 Modified glulam moment-resisting joint (Komatsu et al, 1991)

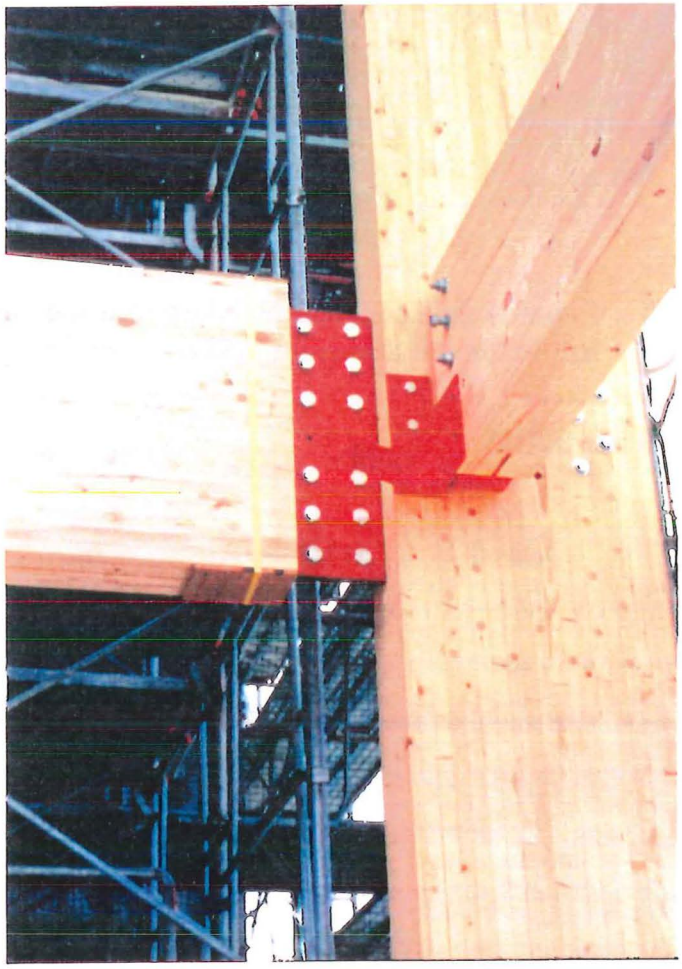

Figure 2.7 Detail of the moment-resisting connection used in the Obihiro Forest Management Centre

Touliatos (1991) describes several beam-column connections using prestressed springs acting as shock absorbing mechanisms to dissipate seismic energy during earthquakes and to permit independent displacements to take place between structural and non-structural components. The connection shown in Figure 2.8 has been used in a timber framed sports hall in Greece.

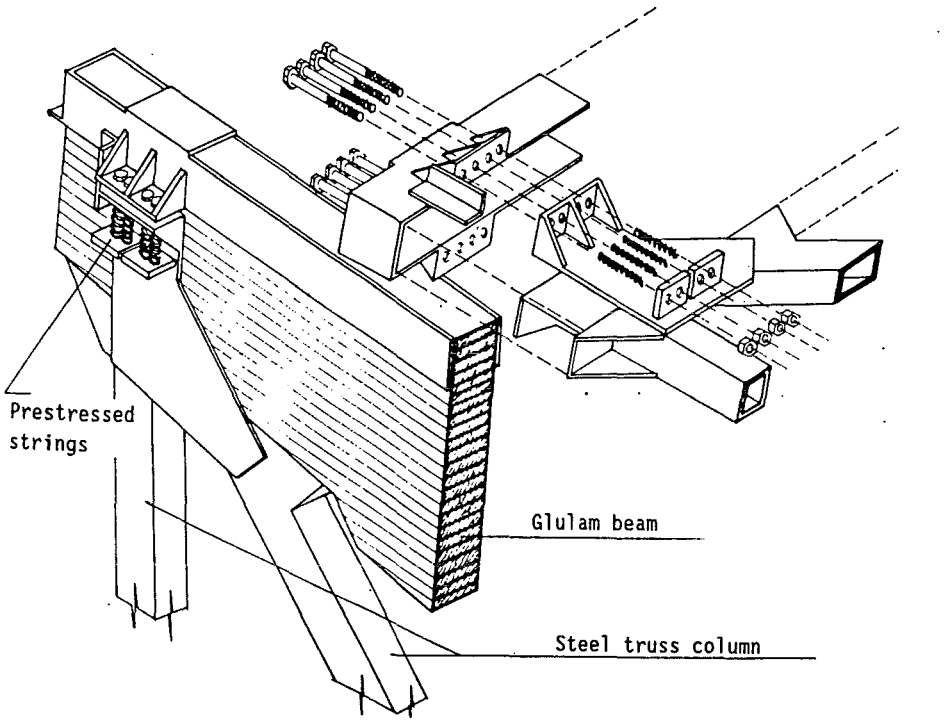

Figure 2.8 Detail of the beam-column connection used in a sports hall in Greece (Touliatos, 1991)

2.4 EPOXIED STEEL RODS

Joints using glued-in bars inclined at an angle to the grain have been investigated and developed in the USSR since 1975 (Turkovsky, 1991). The tests considered loading in both tension, compression, bending and shear. The method consists of placing reinforcement in predrilled holes, running at an angle to the grain of the timber, in holes 4 or 5mm larger than the bar diameter and injecting epoxy cement into the holes. This system has been widely used in the USSR for reinforcing glue laminated structures (see Figure 2.9 and Figure 2.10). It has been used to make a 100m continuous multispan beam in the roof of a public centre, rigid joints for a skating rink, in 24m trusses for an industrial building, and has been used to make cornice joints and for connecting the columns to the foundation on a 50m span sports hall.

Turkovsky et al (1991) reports on the use of glued-in bars for restoring delaminated beams, increasing the shear strength of members and strengthening beams using external reinforcement.

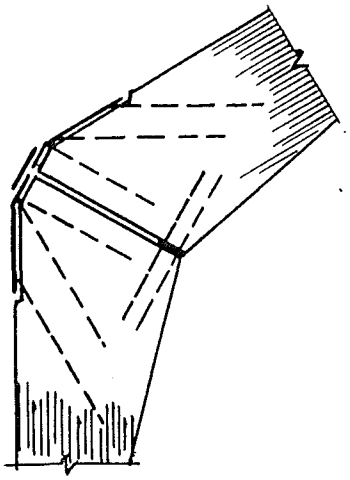

Figure 2.9 Cornice joint of frame (Turkovsky, 1991)

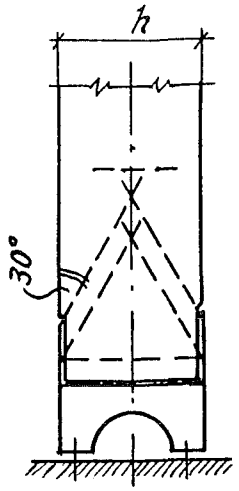

Figure 2.10 Joint of column with foundation (Tukovsky, 1991)

In the late 1970s, Gougeon Brothers (1980) conducted tests on small and large diameter fasteners epoxy bonded into timber for use in boat construction. Small fasteners were epoxied into plywood to determine the relative effects of surface area, type of screw, using standard or oversized holes, shear capacity and tension withdrawal loads. The size of the fastener and the hole were varied for several different types of screw; flathead wood screws, flathead machine screws and self tapping sheet metal screws. Some screws were also put into resin-soaked pilot holes. Large diameter bolts were also tested in several different species of wood. It was found that bonding significantly increases the capacity of the fasteners.

Gopu (1981) studied the behaviour of cracked pitch cambered beams that were repaired using epoxied radial reinforcement. Similar studies were carried out by Law and Yttrup (1989) in Australia on the repair of curved glulam beams and is shown in Figure Figure 2.11.

An investigation into the factors influencing the strength of epoxy repaired timber lap-joints was conducted by Advent (1986). Several factors were examined including the member thickness, grain orientation, glue line thickness, age of the timber, the length of the joint overlap and the effects of the mechanical connectors.

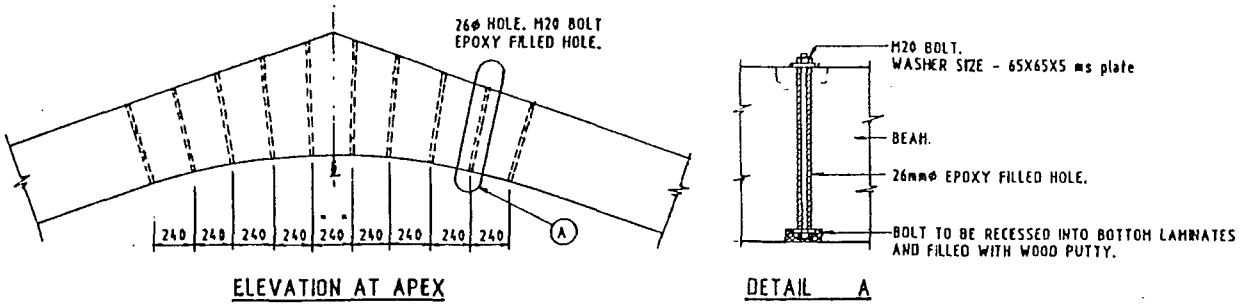

Figure 2.11 Repair of a curved glulam beam with epoxied steel dowels (Law and Yttrup, 1989)

Syme (1989) describes two methods of epoxying steel rods into glue laminated timber. The older technique uses threaded rods screwed into slightly undersized holes which are half filled with adhesive. The rods had a machined notch along the full length to allow mixing of the glue throughout the embedded length and permit excess glue to escape. The second, more recent technique has been extensively studied and developed in Denmark by Riberholt (1986). This system involves inserting rods in oversized holes and then injecting epoxy around the bars via a small hole at the base of the hole.

Riberholt (1986) completed tension and shear tests on dowels glued into the end grain of glulam beams. The report also describes tests on trimmer joints (see Figure 2.13) and moment-resisting connections for portal bases (see Figure 2.12) and knees (see Figure 2.14). A further report provides more test results (1988). Some empirical formulae for failure loads and empirical strength were developed and his findings were subsequently published in a report for proposals of CIB Code (Riberholt, 1988).

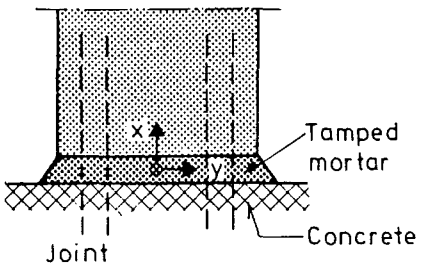

Figure 2.12 Column-foundation joint (Riberholt, 1986)

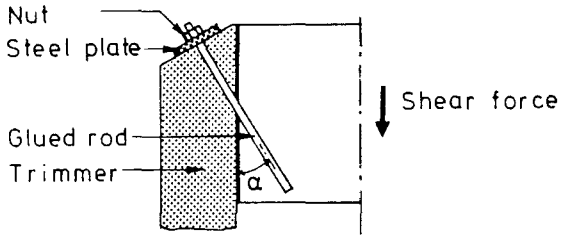

Figure 2.13 Trimmer joint (Riberholt, 1986)

Riberholt (1986) recommended a slightly flexible polyurethane adhesive rather than a rigid epoxy. Testing in New Zealand by Townsend (1990) used an Araldite K-2005 (Ciba-Geigy) that had similar properties as the polyurethane used in Danish tests. Investigations by Riberholt have shown that a slightly flexible polyurethane adhesive performed better than a rigid epoxy.

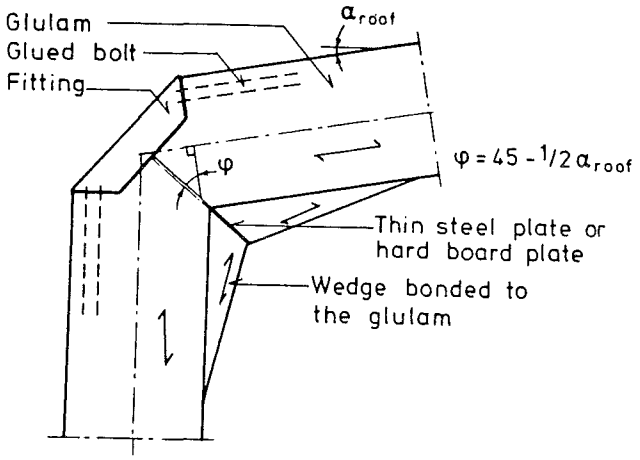

Figure 2.14 Portal knee moment-resisting connection (Riberholt, 1986)

Townsend (1990) carried out an extensive testing programm on epoxied steel dowels using New Zealand materials. The tests considered loading in both tension and shear, different types of epoxy and various rod geometries. High strength deformed reinforcing bars (Grade 430 steel) were used as the standard reinforcement in tests with threaded rods being used as a comparison. Although deformed bars are more readily available and less expensive than threaded rods, Townsend (1990) found that threaded rods performed better than deformed bars in pull out tests. Two epoxies were used; Ciba-Geigy K-2005 and Araldite K-80.

The main part of the testing programme consists of pull out tests of epoxied dowels in glulam timber conducted parallel and perpendicular to the wood grain. The arrangement used to test epoxied steel dowels parallel to the grain is shown in Figure 2.15. Several parameters were varied including the bar size, the embedment length, the edge distances and the glue type. The effect of dry and wet and timber on embedment strength was also investigated.

Townsend (1990) derived an equation from an empirical analysis of pull out test results of

deformed reinforcing bars embedded in glulam.

$$F = 9.2\ d\ l_g\ (r_d)^2\ \sqrt{r_e} \qquad (2.1)$$

where F = pullout force (N)

d = bar diameter (mm)

l_g = embedment length (mm)

r_d = ratio of hole diameter to bar diameter

r_e = ratio of edge distance to bar diameter, where the edge distance is measured from the bar centre-line

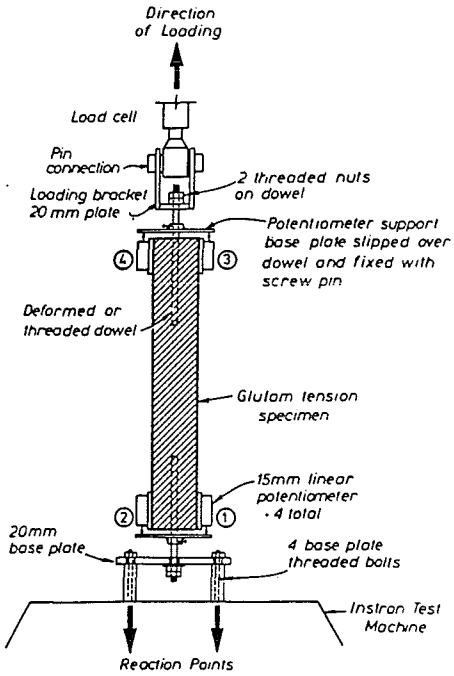

Figure 2.15 Test arrangement for tension parallel to the grain (Townsend, 1990)

Townsend (1990) also reports about several full size beam splices that were tested using high strength deformed bars in two different bar arrangments. The splices were either connected at mid-span or offset from the beam mid-span point. In both cases, the beams were loaded at the beam midspan. The beam splice connection performed very well and results showed they were generally stronger than the beams themselves.

Rodd (1988, 1989) investigates the use of epoxying circular dowel type fasteners into glulam timber to achieve stronger moment-resisting joints. By increasing the friction between the

surface of the fastener and the timber in which it bears, considerable increases in joint strength and ductility can be achieved. Initial tests (Rodd, 1988) used a knurled surface on the dowels to increase the surface friction, with later testing (Rodd, 1989) using a knurled dowel and epoxy to bond the dowel surface to the timber. Embedment tests were completed using several bolt sizes bonded into softwoods and hardwoods and loaded perpendicular and parallel to the grain. Results showed that resin injected dowels had an increased ultimate strength and stiffness compared to that obtained previously using knurled dowels.

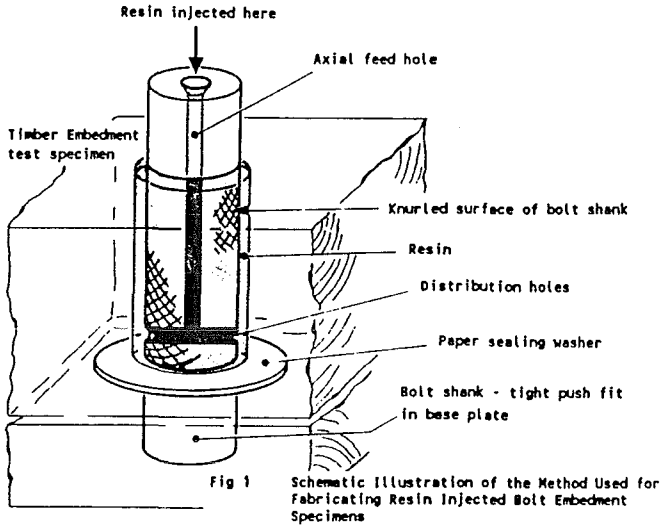

Figure 2.16 The method used to construct resin injected bolt specimens (Rodd, 1989)

Rodd (1991) also investigates the effects on embedment characteristics of a group of resin injected bolts, the density of the laminations in which the bolts are installed, and the direction of bearing. A method is derived using Hankinsons formula to predict the embedment characteristics of bolts at any angle to the grain. The report also describes testing of full-scale moment-resisting connections using glulam, but no results are given.

An extensive testing programme was completed on reinforced laminated timber beams by van Rensburg (1984) to determine the composite action between the steel and the timber. Steel plate sections were placed at the top and bottom of the section in grooves running the length of the member and fixed in place using a phenol resorcinol wood glue. Several different steel geometries were explored. The effects of creep and bond strength between the steel and timber were also investigated.

Gardner (1989, 1991) discusses a new system of reinforcing glued laminated timber using high strength deformed steel reinforcing bars. This system is illustrated in Figure 2.17 and consists of placing large diameter bars at the top and bottom of the section in oversized grooves running the length of the member and fixed in place using high strength epoxy resins. This system improves the strength and stiffness of timber members and reduces long term creep.

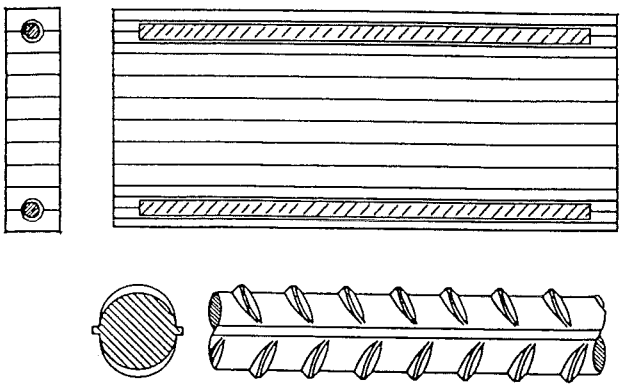

Figure 2.17 Reinforced glued laminated timber system (Gardner, 1989)

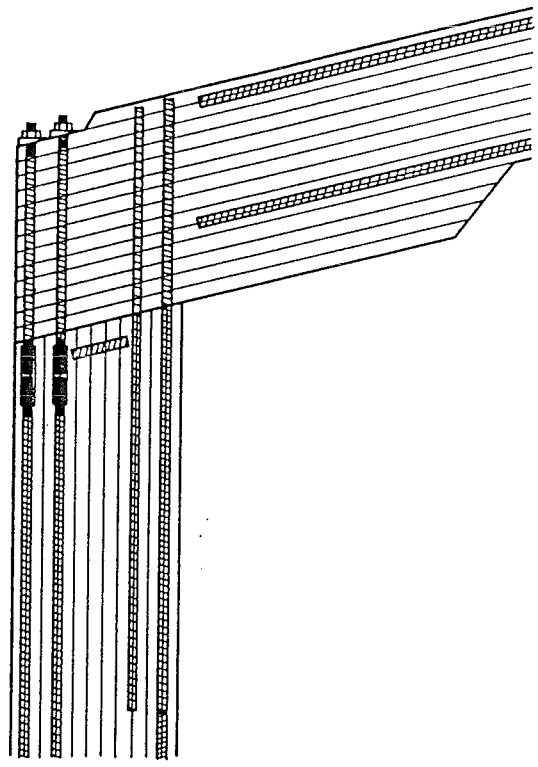

Figure 2.18 Beam-column moment connection (Kauri Timber Company, 1990)

Also mentioned are several applications for connections: member splices using dowels, attaching columns to the foundations, connecting members at the apex, forming beam-column moment connections (see Figure 2.18) and anchoring timber members to steel and concrete using a coupling system.

A design method and safe load tables have been produced for reinforced glued laminated timber by the Kauri Timber Company Limited (Kauri Timber Company, 1990).

Buchanan and Townsend (1990) completed several tests on portal frame knee joints using epoxied steel dowels connecting glue laminated timber members. Three different arrangements of portal frame knee joints were tested: a "square" joint with the rafter running over the top of the column, a "mitred" joint using a diagonal steel plate connecting both the rafter and the column and a "steel knee" joint connecting both the rafter and column using a knee bracket prefabricated from structural steel. A patent application has been made by Hunter Timbers for this new system.

Frost (1990) completed a testing programme using steel dowels epoxied into glulam timber. The process consists of inserting a steel plate into a precut groove, placing steel dowels into the timber and through the steel plate, and injecting epoxy around the dowel. A sketch of the scarf joint is shown in Figure 2.19. These tests considered both loading parallel and perpendicular to the grain and two different dowel geometries. Two epoxies were used; Epar HPN epoxy mortar and Araldite K2005. It was found that the tested joints had superior stiffness to equivalent bolted connections.

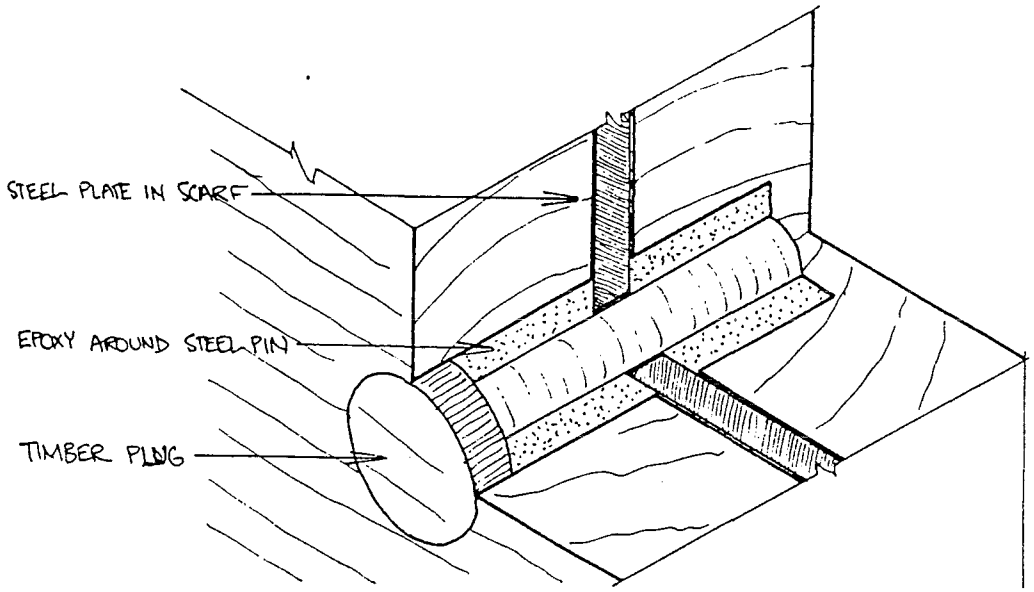

Figure 2.19 The epoxy dowel scarf joint (Frost, 1990)

2.5 EXAMPLES OF EPOXY DOWEL USE IN TIMBER JOINTS

The New Zealand Journal of Timber Construction (1986) reports on a glue laminated timber

space frame roof where the timber elements are connected at the node points by an epoxy injected steel dowel joint.

Buchanan and Fletcher (1989) report on the design and construction of two indoor swimming pools which use epoxied steel dowels for attaching curved glulam portal frames. The portal base connection is shown in Figure 2.20 and uses galvanized threaded steel rods epoxied into holes in the end grain of the timber and the other end grouted into a concrete pedestal. The portal apex connection is displayed in Figure 2.22 also uses epoxied steel rods, but with nuts to pull the connection together. The beam-column connections in the entry hall use threaded steel rods epoxied into the end grain of the beams and pass through the column (see Figure 2.21).

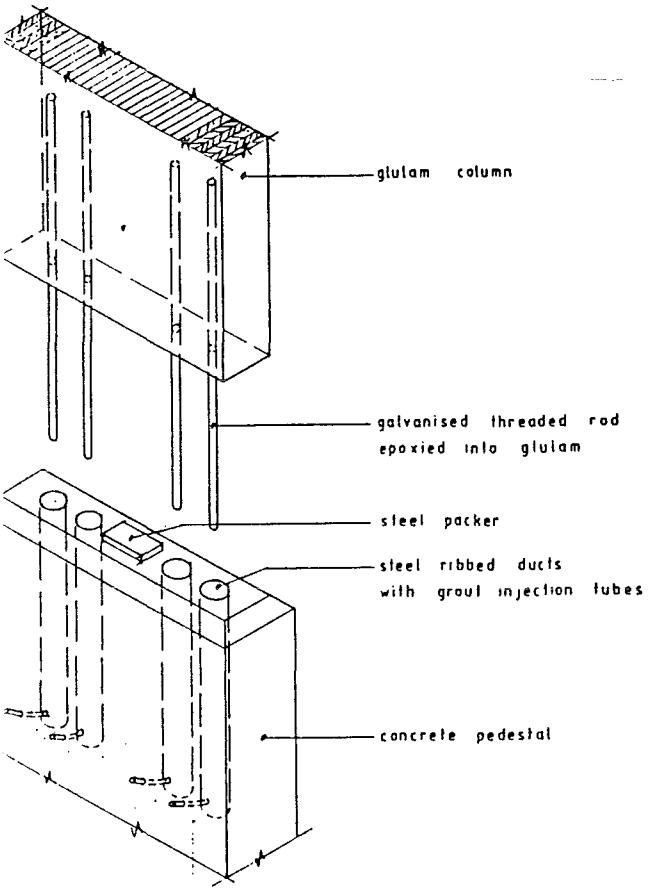

Figure 2.20 Portal base connection (Buchanan and Fletcher, 1989)

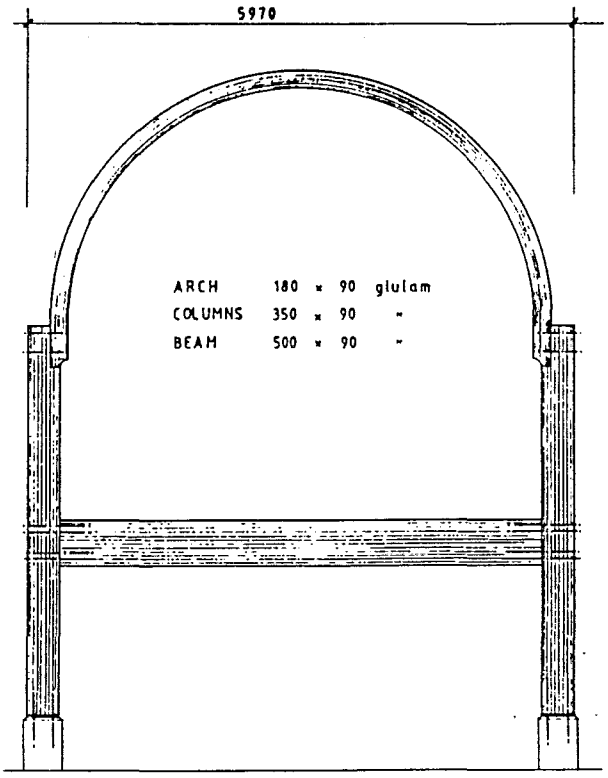

Figure 2.21 Entry hall at Jellie Park (Buchanan and Fletcher, 1989)

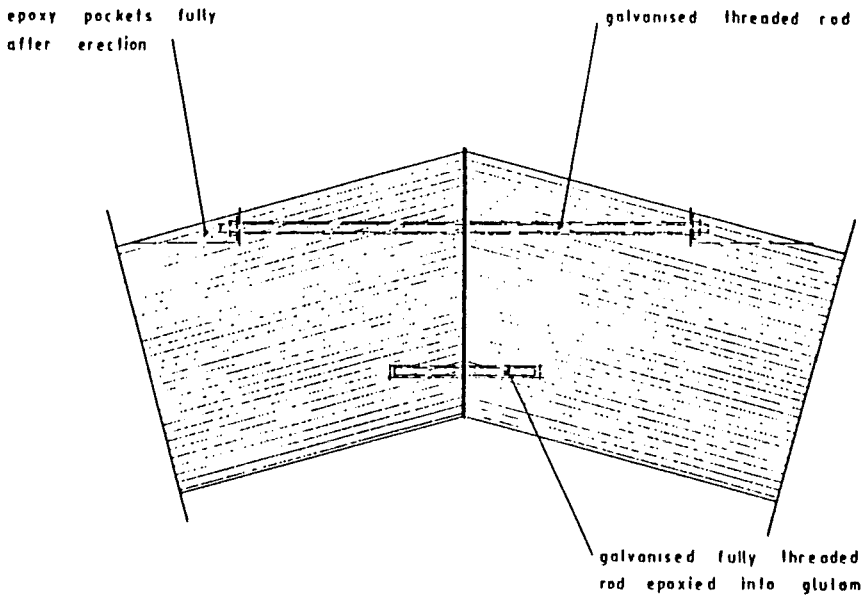

Figure 2.22 Portal apex connection (Buchanan and Fletcher, 1989)

Use of epoxied threaded rods in glulam is documented in several projects using wooden rotors for wind turbines in the United States and Denmark (Nielson, 1988). A new type of bolt was developed that has a hollow at the end to reduce the peak shear stresses in the glue line near the bottom of the bolt. These bolts were made from high strength steel and embedded using a glue line of approximately 1mm.

CHAPTER 3

TEST PROCEDURE

3.1 INTRODUCTION

A recent innovation in New Zealand is the use of steel dowels epoxy bonded into timber. This method comprises of drilling a hole in the timber about 6mm larger than the dowel diameter, centrally placing the bar in the hole and injecting epoxy into a grout hole positioned at one end, until it begins to flow out of an airing hole at the other end. Use of this technique enables steel bars to be placed at the top and bottom of the beams, forming a compression/tension couple which resists the column moment with the shear carried by dowel action. This system has some advantages over presently accepted connection methods: the steel is protected from corrosion, the structural connection is protected from fire by the glulam members and the fastenings are hidden giving an excellent aesthetic appearance.

The testing programme consisted of three types of beam-column connections; four of the first type and two each of the second and third types, giving a total of eight specimens. Each test used a quasi-static cyclic loading with a horizontal load applied at the top of the column, simulating lateral loads on a building due to wind or earthquakes.

The first set of connections, shown in Figure 3.1 (a) and uses a continuous column with beams butting up against it on either side and epoxied dowels embedded in the beams and columns. The second and third types of connection use a steel bracket specially designed so yielding occurs in the beam flange plates or in the web panel. This type of connection is subject to a patent application by Hunter Laminated Ltd (Buchanan and Townsend, 1990). The second set of connections are illustrated in Figure 3.1 (b) and consists of beams and columns bolted to a central steel hub in the joint. As shown in Figure 3.1 (c), the third type of connection consists of a continuous column and two steel brackets, one each side of the column.

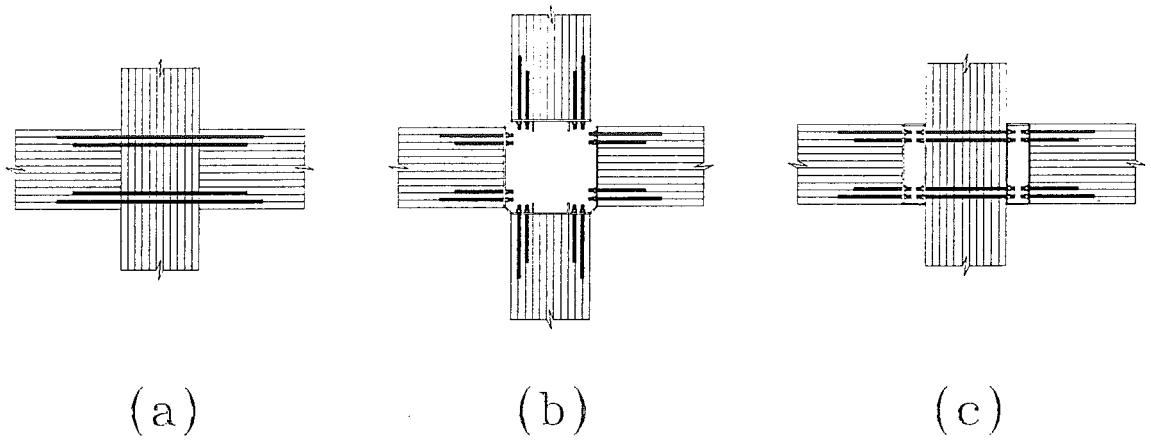

Figure 3.1 The three different types of connection

3.2 MATERIALS

3.2.1 STEEL BARS

Two types of bars were used during testing; mild steel deformed reinforcing bars and high strength threaded rods. The deformed bars were expected to yield, whereas the threaded rods were to remain elastic with the yielding intended to occur elsewhere in the connection. Although deformed bars are more readily available and less expensive than threaded rods, it was found previously that threaded rods performed better than deformed bars in pull-out tests (Townsend, 1990).

The high strength threaded rods were made from 3/4" (19mm) round bar conforming to AISI grade 4140. It is supplied in the heat treated condition, possesses excellent toughness and is readily machineable. A threading machine was used to cut a 3/4" BSW thread onto the bars. Several threaded rods were tested in tension to determine their yield and ultimate strength values. It was found that the bars had a yield strength of 680 MPa and a minimum ultimate strength of 850 MPa.

The mild steel deformed bars had diameters of 16 and 20mm and a nominal yield stress of 300 MPa. Several of these bars were also tested in tension to determine their yield and

ultimate strength values. It was found that the bars gave a yield strength of 320 MPa and a minimum ultimate strength of 452 MPa.

3.2.2 TIMBER

The timber was donated by three manufacturers, Peter Stevens Ltd. of Christchurch, Hunter Laminates Ltd. of Nelson and McIntosh Timber Laminates Ltd of Auckland, under the auspices of the Structural Engineered Timber Manufacturers Association (SETMA). The test units used two sizes of beams; 90 x 495mm and 135 x 495mm and a column with nominal cross sectional dimensions of 180 x 495, most of which was manufactured using 45mm laminates. The glulam was specified as untreated radiata pine, containing timber No.1 framing grade or better with a moisture content between 12 to 16% and no pith in the outer laminations.

The moisture content was checked at arrival and just before each test commenced using two methods; a Protimeter 'Timbermaster' Model D184T and oven drying samples for 24 hours. The average moisture content was found to be 15% at arrival and 12% just before testing. The Modulus of Elasticity was also determined for the timber using a Metriguard Model 239A stress wave timer, giving an average reading of 8203 MPa.

Density of the timber was determined by taking a portion of cross section of timber from several members. The average density of the timber was found to be 499 kg/m^3.

3.2.3 EPOXY

Two types of epoxy were used on the project; a WEST System Z105/Z205 two component epoxy and the Hilti HIT C100 injection technique. Both are high strength, two component epoxies with quick cure times. There are three main differences between the two systems. Firstly the WEST System epoxy was designed for use with wood, whereas the Hilti HIT system was designed originally for use with concrete and rock.

The second difference is in the method of mixing and injecting the epoxy. The WEST system

epoxy has to be manually measured (unless a special dispenser is used which delivers the proper mixing ratios) and stirred together thoroughly. The mixed epoxy is then poured into caulking tubes and injected into the pilot hole. The HIT system epoxy uses a dual-purpose cartridge which not only stores the two components separately, but measures and mixes the two components to the right ratios during the injection process.

The third difference is in the consistency of the epoxy. The WEST system epoxy has the consistency of motor oil and has clear, light-amber colour. The HIT system epoxy has the consistency of peanut butter, the texture of a mortar and has a light-brown colour.

3.2.3.1 WEST SYSTEM Z105/Z205 TWO COMPONENT EPOXY

Adhesive Technologies Ltd of Auckland (part of Gougeon Brothers, Inc.) donated the epoxy for this project. With consultation with the above company, the WEST System Z105/Z205 two component epoxy (Gougeon Brothers, 1988) was selected as the standard epoxy for all the testing as it is a very high strength epoxy with a quick cure time. This epoxy was designed for use with timber and has an optimum hardness, excellent cohesive properties and is also very resistant to water penetration, making it ideally suited for bonding steel rods to timber.

Typical properties for cured Z105/Z205 epoxy are:

Heat distortion temperature	75°C	
Tensile strength, f_t	76 - 83 MPa	(11 - 12,000 psi)
Compressive strength, f_c	69 MPa	(10,000 psi)
Flexural strength, f_b	110 MPa	(16,000 psi)
Modulus of Elasticity, E	2760 MPa	(400,000 psi)

The Z105 resin is a clear, light-amber, low viscosity, 100% reactive, solvent free resin which cures clear over a wide range of temperatures. By using the appropriate powder fillers, the viscosity of this resin can altered from a syrup to a peanut butter consistency. This enables the epoxy to be used for a variety of applications, such as coatings, laminating panels,

filleting, hardware bonding and gap filling. It can be sanded afterwards and even varnished to achieve a natural finish.

There are two types of hardener available for the Z105 resin; the Z205 fast hardener and the Z206 slow hardener. Both hardeners are mixed with the Z105 resin in a five part resin to one part hardener ratio by volume or weight. In most circumstances, the fast hardener is used to produce a rapid cure that develops its physical properties quickly. The Z205 fast hardener consists of a formulated mixture of medium viscosity polyamines and when mixed with the Z105 resin, it has a pot life of 15 to 20 minutes at 20°C and a hard cure time of five to seven hours at 20°C. The maximum strength will not be reached for several days at room temperature, although it can be achieved earlier by curing at elevated temperatures (eg 24 hours at 80°C or 3 hours at 125°C).

The Z206 slow hardener consists of a low viscosity polyamine mixture and when mixed with the Z105 resin, has a pot life of 30 to 40 minutes and hard cures in approximately nine hours. The maximum strength will not be reached for at least a week under normal conditions.

In all of the tests, the epoxy was mixed using resin Z105 and fast hardener Z205.

3.2.3.2 HILTI HIT C100 INJECTION TECHNIQUE

The other epoxy system used was the Hilti HIT C100 injection technique which was donated by Hylton Parker Fasteners of Christchurch, for one set of connection tests using the arrangement shown in Figure 3.1 (c). This epoxy is used for anchor fastening in solid materials like concrete and rock. This epoxy is ideal for use in materials which are continually damp. This epoxy uses a synthetic resin mortar based on a modified epoxy acrylate.

Some typical properties of the HIT C100 injection system:

Shear strength, f_v	150 MPa
Compressive strength, f_c	150 MPa

This adhesive has a working time of 4 minutes at 20°C before it starts to gel and a hard cure time of 45 minutes at 20°C. The maximum strength will not be reached for several days at room temperature

The Hilti HIT C100 injection technique uses a special cartridge which has two compartments for the epoxy and the hardener and a special mixing nozzle. Once the cartridge is placed in the dispenser and the trigger pumped, the two components are dispensed at the right working ratios into the mixing nozzle. Within the mixing nozzle, are several spirals which mix the components thoroughly together as they pass down the nozzle. This mixer provides controlled mixing, ensuring correct performance and quality of epoxy. Since the components are only mixed when being used, there is no wasteage because the capsule can be reused if not finished.

This technique has several advantages; it is very fast to apply, it is clean to handle and easy to use and no mixing is required. Since the adhesive is contained in a compartmentalized capsule, there is no contact with the epoxy during the mixing process.

3.3 PREPARATION OF SPECIMENS

3.3.1 EPOXY PREPARATION

All the WEST system epoxy was mixed manually using a 5:1 by weight resin to hardener ratio. Mixing small quantities by weight is fine but an allowance for specific gravity should be made when mixing "large" quantites. Epoxy was made up in a 300g resin plus 60g of hardener giving a batch of 360g. The two components were mixed thoroughly for several minutes before being poured into cauking tubes and inected into the holes.

Problems were encountered when the epoxy was made in larger batch quantities at warmer temperatures. The resulting reaction was extremely exothermic and melted the mixing pot and caulking tubes and gave a very fast cure (pot life was less than 10 minutes). The solution was to reduce the batch size. Other factors that would have helped would be a combination of:

1. slower hardener
2. lower temperatures
3. inclusion of a silica sand filler to reduce the peak exothermic temperature.

It was also noted that the amount of hardener is critical to the pot life, curing time and the overall performance of the epoxy.

Hilti HIT C100 system required no preparation before injecting epoxy into the holes.

3.3.2 DRILLING AND PLACING THE STEEL DOWELS

The dowel holes were drilled into the timber using a hand held air drill with a wood auger. Two sizes of auger were used; 22mm holes for the D16 bars and 26mm holes for the D20 bars and 3/4" BSW threaded rods. Two 8mm diameter pilot holes were drilled 30mm from both ends of the dowel hole as shown in Figure 3.2; one hole to inject the epoxy, the other allowing the air to escape.

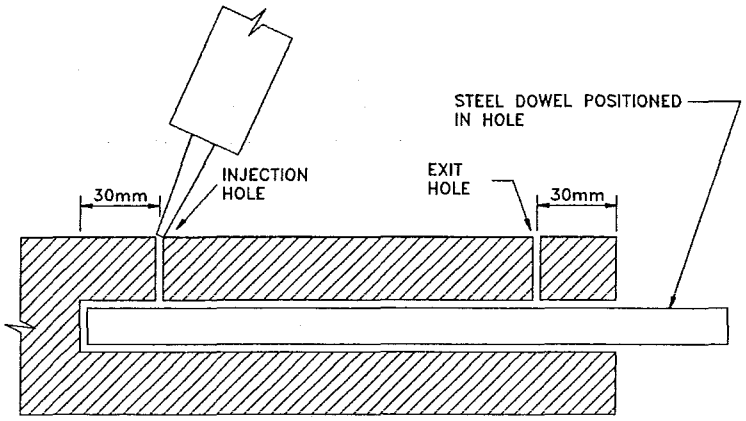

Figure 3.2 Layout of holes in the end grain of the beams

The threaded rods were cleaned of threading oil and grit using Methylethyl Ketone. The deformed bars were firstly thoroughly scrubbed using a wire brush to remove rust and grit and then cleaned with a solvent solution.

Drilling alignment was achieved by using a steel angle guide as a reference to sight along, as shown in the Figure 3.3. All holes were thoroughly cleaned using compressed air.

Figure 3.3 Method used to drill holes

The Epoxy was injected into the pilot hole under gravity, until it began to flow out of the airing hole. The epoxy level in the pilot hole was kept topped until the epoxy began to harden. After some time the epoxy level dropped in the pilot holes. This drop in level is due to the epoxy requiring time to fill all the voids between the wood and the steel and some absorption into the timber. A schematic diagram of the epoxy injection process is shown in Figure 3.4.

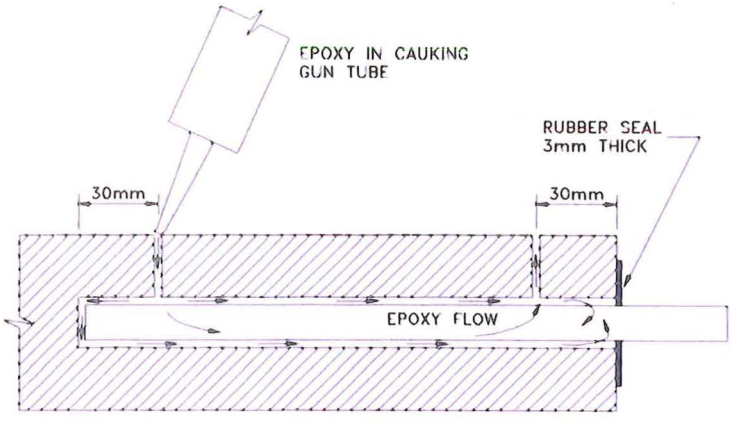

Figure 3.4 Schematic of epoxying operation

3.3.3 ASSEMBLY

The assembly methods used to construct the beam-column connections were different for each type of joint. The construction method requires some precision and skill, especially when drilling through the column as this fixes the position of the beams. A larger hole would provide better tolerances but would weaken the column since the column cross sectional area is reduced. The beam ends need to be square to provide a good surface to butt up against and prevent epoxy leakage.

3.3.3.1 BEAM-COLUMN CONNECTIONS USING EPOXIED STEEL DOWELS ONLY

The dowels were placed and centred in the predrilled holes in the columns and 3mm thick rubber seals were fitted over each bar and pushed hard up against the column face. A template was made from plywood consisting of drilled holes at the right pitch and spacing. The template was aligned with the bars and pushed up against rubber seals and the column face, sealing the ends and preventing epoxy leakage. The column bars were epoxied and allowed to cure overnight before the column was flipped and the bars on the other side epoxied. After 24 hours, the templates were removed.

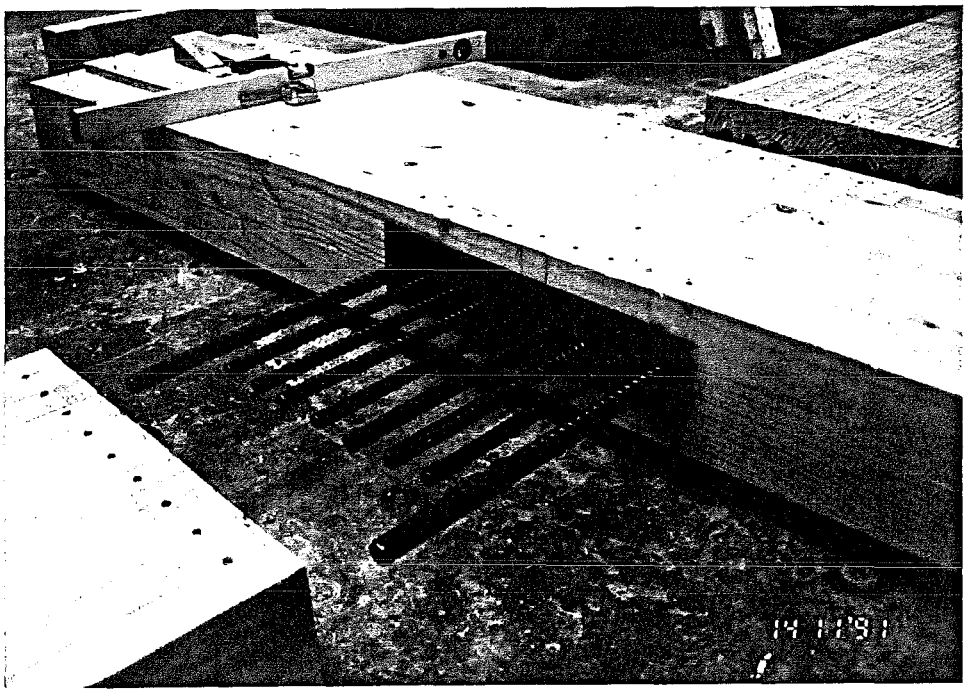

Figure 3.5 Assembling a connection using epoxied steel dowels only

The beams were aligned with the dowels already embedded in the columns (see Figure 3.5). Then the beams were pushed in place against the seals to complete the connection. Clamps were used to keep the beams seating up against the columns, preventing any movement during the epoxy injection process. The beam bars were then epoxied and left to cure overnight before the clamps were removed and the connection rotated to epoxy the bars on the other side. After all the bars were epoxied in place, the connection was left for at least 24 hours at room temperature before being moved to the test rig.

3.3.3.2 BEAM-COLUMN CONNECTIONS USING EPOXIED STEEL DOWELS AND PREFABRICATED STEEL BRACKETS

The threaded rods were placed and centred in the predrilled holes in the both column and beam ends and rubber seals fitted over each rod and pushed hard up against the timber surface (see Figure 3.6). The prefabricated steel bracket was aligned with the bars and pushed up against the end faces of the beams and column, sealing the ends and preventing epoxy leakage.

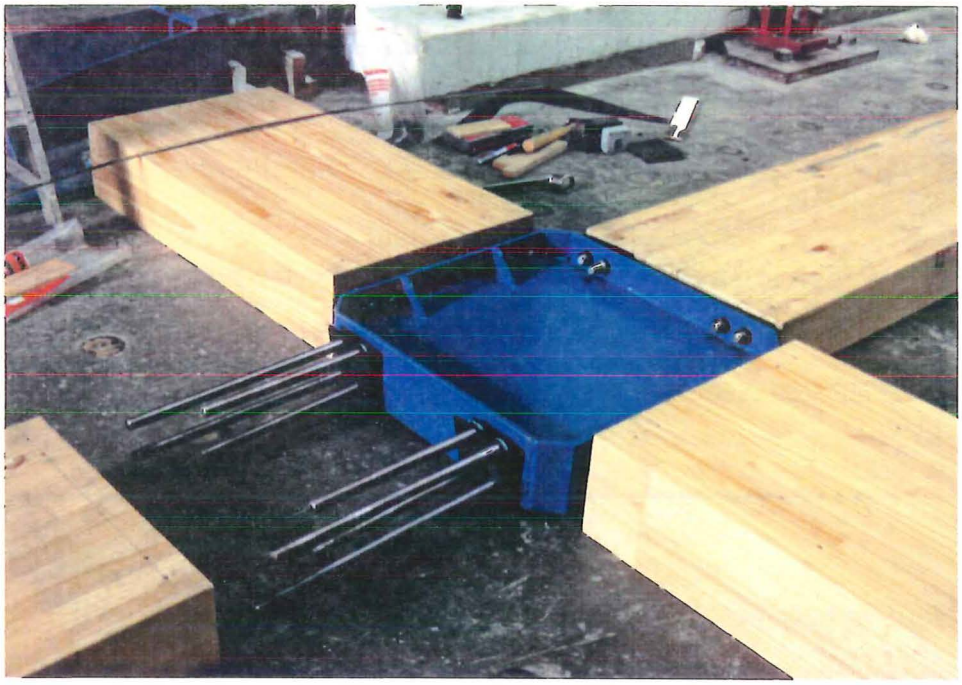

Figure 3.6 Assembling a connection using epoxied steel dowels and prefabricated steel bracket

The column and beam bars were epoxied and allowed to cure overnight before the members were turned and the bars on the reverse face epoxied in place. Hydraulic jacks were used to keep the beams and columns seating up against the steel bracket, preventing any movement during the epoxy injection process or drying stage. After all the bars were epoxied in place, the connection was left for at least 24 hours at room temperature.

3.4 TESTING

The testing programme consisted of three types of cross connections; four of the first type and two each of the second and third types, giving a total of eight specimens. Each test used a quasi-static cyclic loading with the horizontal load applied by a hydraulic jack at the top of the column. The applied load was measured by a load cell positioned above the hydraulic jack; and the shear forces in the beams were measured by strain gauges in the legs of the test rig. The column displacement was measured using a high resolution potentiometer and the distortion of the joint, the horizontal and vertical displacements of the beams relative to the column were measured using clip gauges. The results were recorded directly to a computer at selected intervals by a 104 channel Burr Brown Data Acquisition System, and a continuous plot of the load versus deflection was made on a X-Y recorder.

3.4.1 TESTING PROCEDURE

Two types of testing procedure were employed, depending on the behaviour of the connection; the testing at low load levels was under load-controlled test cycles. If any yielding occurred then the subsequent test cycles were deflection-controlled.

3.4.1.1 LOAD-CONTROLLED TEST CYCLES

The lateral load was applied to the column in one direction and increased until the target load was reached. The load was then applied in the other direction to the same target load. After two cycles at this load level, the load was increased and the process repeated until failure. The loading history chosen is as follows: the jack load level is increased in steps of 20 kN initially, and in 10 kN increments after 60 kN, with two symmetrical loading cycles applied

at each level.

3.4.1.2 DEFLECTION-CONTROLLED TEST CYCLES

The displacement ductility factor is defined as $\mu = \Delta_{max} / \Delta_y$ where Δ_{max} is the maximum displacement and Δ_y is the displacement at yield. In the following tests, the definition of yield displacement was taken as the displacement when yielding first occurs in the structure at the first deviation of the load-deflection plot from a straight line.

The lateral load was applied to the column in one direction and increased until first yield was reached. The load was then applied in the opposite direction until first yield. The yield displacement used to determine the ductility levels during deflection-controlled cycles was taken as the average of the yield displacements over one complete cycle (see Figure 3.7 and eq (3.1), (4.8)).

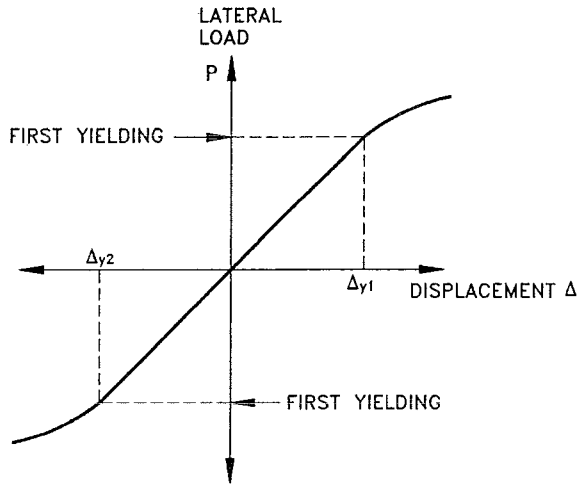

$$\Delta_y = \frac{\Delta_{y1} + \Delta_{y2}}{2} \qquad (3.1)$$

Figure 3.7 Definition of yield displacement

The displacement history used during the testing programme was the standard loading pattern adopted by the University of Canterbury (Park, 1989). The ductility level was increased in steps of 2, with two symmetrical loading cycles applied at each level, giving ductility factors of $\pm$ 2, $\pm$ 4 $\pm$ 6, and $\pm$ 8.

3.4.2 TEST ARRANGEMENT

The test arrangement is shown in Figure 3.8 and consists of a beam-column connection with a column height between pins of 2.8m and a total beam length of 3.81m between pins. Each pin connection consists of two nailon plates welded to a rigid endplate. The timber members are placed between the two nailon plates with nails hammered into the pre-punched holes in the plate.

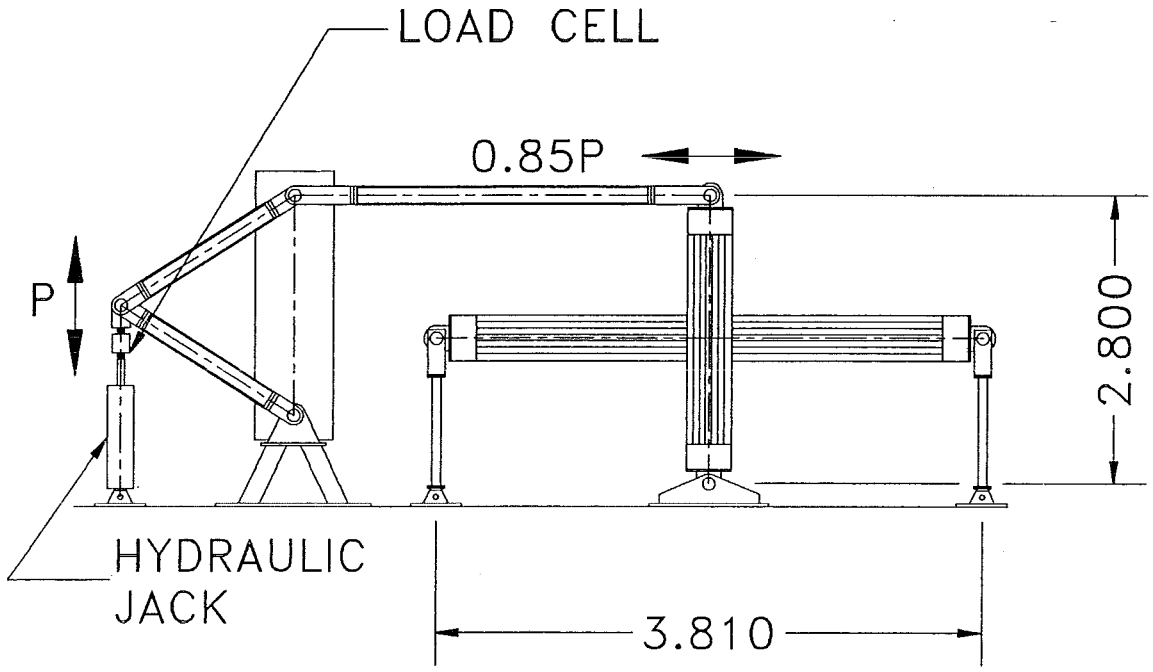

Figure 3.8 The test frame

The lateral load is applied to the column by means of a hydraulic jack and reaction frame. Although the hydraulic jack is mounted vertically, the truss arrangement of the test rig ensures that a horizontal load is applied to the top of the test specimen. The horizontal load is 85% of the jack load measured at the load cell. A lateral restraint was provided at the top of the column to prevent out-of-plane bending of the column.

Both bending moment and shear were transmitted by the beam-column connection. No axial load was applied to the column since higher compressive stresses would increase the load carrying capacity of the timber column.

CHAPTER 4

ANALYSIS OF TEST SPECIMEN

4.1 INTRODUCTION

The following sections outline the methods and computations used to analyze the test results of the beam-column connections. The performance of each connection will based on the several criteria, namely the initial stiffness, the interstorey drift limits, stresses in the members and in the joint region and analysis of the column displacement components.

4.2 INITIAL STIFFNESS OF THE CONNECTION

The initial stiffness K of the timber connection is defined as the stiffness over the first positive half-cycle of the test. This stiffness can be calculated as follows

$$\text{Initial Stiffness, } K = \frac{P}{\Delta_c} \quad \text{(kN/mm)} \tag{4.1}$$

where Δ_c is the column displacement at a lateral load of P.

4.3 INTERSTOREY DRIFT

The interstorey drift is defined as follows

$$\text{Interstorey Drift (\%)} = \frac{\Delta_c}{H} \times 100 \tag{4.2}$$

where H is the storey height which in this case, is the vertical distance between pins. This would be the same as the floor to floor height in an actual building because the pins are assumed to be at the mid-height of the columns.

4.4 CALCULATING THE THEORETICAL FIRST YIELD LOAD AND DISPLACEMENT

The first yield displacement Δ_y is defined as the column displacement at which the connection first yields. Yielding first takes place in the outer-most bars, or in the flange plates nearest the column face. The following method is only applicable for connections using a type (a) arrangement of bars.

By refering to Figure 4.1 and assuming the neutral axis is situated at the centroid of the beam section, the yield moment of the connection can be taken as

$$M_y' = F_{s1}x_1 + F_{s2}x_2 \qquad (4.3)$$

where F_{s1} and F_{s2} are the sum of the bar forces at that level with x_1 and x_2 being the lever arm between the bar groups.

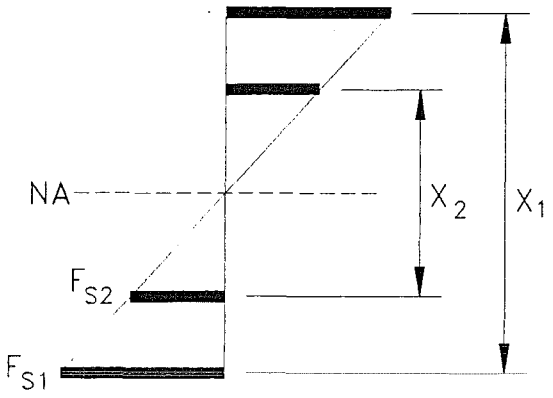

Figure 4.1 Distribution of steel forces in the beam section

Using the geometry given in Figure 4.1, then the force in the inner bars, F_{s2} can be taken as

$$F_{s2} = \frac{x_2}{x_1}F_{s1} \qquad (4.4)$$

substituting (4.4) into (4.3) and assuming $F_{s1} = F_y$, gives

$$M_y' = F_y x_1 + F_y\frac{x_2^2}{x_1} \qquad (4.5)$$

The lateral load P'_y applied at the top of the column at first yield is therefore

$$P_y' = \frac{M_y'}{l_b}\frac{L_b}{L_c} \qquad (4.6)$$

where L_b is the length of the beam to the centre of the column, L_c is the length of the column to the centre of the beams and l_b is the clear distance from the end of the beam to the face of

the column.

The yield displacement at the top of the column is therefore

$$\Delta_y' = \frac{P_y'}{K} \tag{4.7}$$

where K is defined in section 4.3.

4.5 DEFINING THE ACTUAL FIRST YIELD DISPLACEMENT

In the tests, the definition of yield displacement, Δ_y was taken as the displacement when yielding first occurs in the structure at the first deviation of the load-deflection plot from a straight line. The yield displacement, Δ_y is taken as the average of the yield displacements over one complete cycle as shown in equation (4.8).

$$\Delta_y = \frac{\Delta_{y1} + \Delta_{y2}}{2} \tag{4.8}$$

where Δ_{y1} and Δ_{y2} are the yield displacements in the positive and negative directions respectively.

4.6 STRESSES IN THE MEMBERS

The bending stress f_b is determined from the bending moment M in the member and the section modulus of the member cross-section Z. For rectangular sections, the section modulus is

$$Z = \frac{BD^2}{6} \quad (mm^3) \tag{4.9}$$

where D is the depth and B is the breadth of the member. Then the bending stress in the timber member is

$$f_b = \frac{M}{Z} \quad (MPa) \tag{4.10}$$

The maximum shear stresses f_s in the member is determined using the shear force V and the cross sectional area A_v of the member in the direction being considered.

$$f_s = \frac{3V}{2A_v} \quad \text{(MPa)} \tag{4.11}$$

4.7 SHEAR STRESSES IN THE JOINT REGION

The horizontal shear force V_{jh} is found by taking in account the effect of the internal forces acting on the joint core, as illustrated in Figure 4.2. For the beam-column joint, the horizontal shear force is

$$V_{jh} = C + T - V_{col} \tag{4.12}$$

where C and T are the resultant forces in the dowels with V_{col} being the shear force in the column.

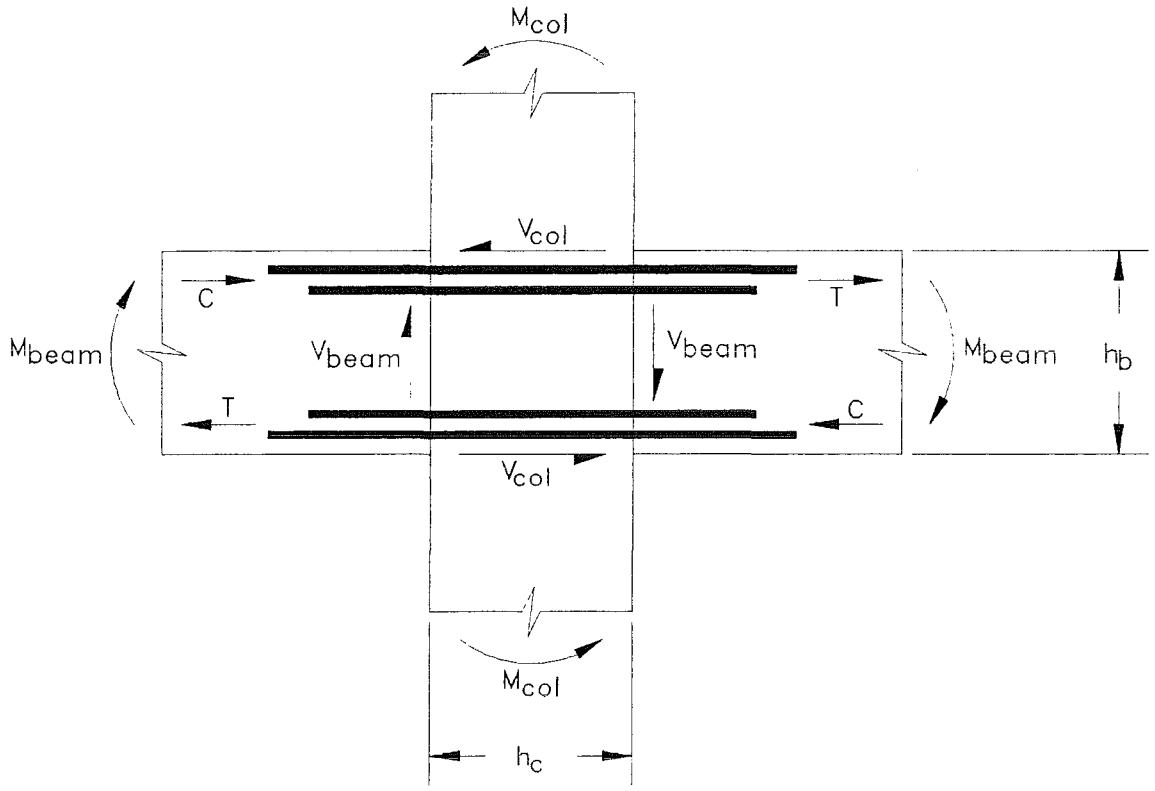

Figure 4.2 Internal actions of beam-column joint

The average shear stress f_{sh} in the horizontal direction is based on the shear area which is the gross cross sectional area of the joint in the direction being considered.

$$f_{sh} = \frac{V_{jh}}{A_{gh}} \tag{4.13}$$

where A_{gh} is the gross area of the joint core in the horizontal direction and defined as $A_{gh} = h_c b_c$ where h_c is the depth of the column and b_c is the column width.

The vertical shear force V_{jv} may also be found by taking in account the effect of the internal forces acting on the joint core. For the beam-column joint shown, the vertical shear force can be approximated as

$$V_{jv} = V_{jh} \frac{h_b}{h_c} \tag{4.14}$$

In this case, $V_{jv} \approx V_{jh}$ since $h_b \approx h_c$ for the specimens, where h_b is the overall depth of the beam and h_c is the overall depth of the column. The average shear stress in the vertical direction f_{sv} is based on the shear area which is the gross cross sectional area of the joint in the direction being considered.

$$f_{sv} = \frac{V_{jv}}{A_{gv}} \tag{4.15}$$

where A_{gv} is the gross area of the joint core in the vertical direction and defined as $A_{gv} = h_b b_c$ where h_b is the depth of the beam and b_c is the column width.

4.8 DISPLACEMENT COMPONENTS

Earthquake actions were simulated by applying horizontal forces at the top of the column. The column displacements and shears were measured using potentiometers, clip gauges and strain gauges. The overall column displacement Δ_c was due to the elastic and inelastic deformations of the members, namely deformations in the beams and columns, shear distortion of the joint core, hinge rotation of beam ends and sliding shear at the beam-column face. The shear distortion in the joint, sliding shear deformations at the beam-column face, hinge rotation and the overall column displacement were measured during the test. All the other components were estimated by calculations based on simple models.

4.8.1 DEFORMATIONS OF THE BEAMS

The deformations of the beams are due to two components; flexure and shear.

$$\Delta_{c,b} = \Delta_{c,b(flexure)} + \Delta_{c,b(shear)} \tag{4.16}$$

The flexural component of beam deformation is shown in Figure 4.3 and can be taken as follows

$$\delta_{b(flexure)} = \frac{V_b L_b^3}{3EI_b} \tag{4.17}$$

where V_b = shear force at the beam end (kN)

L_b = length of the beam to the centre of the column (mm)

I_b = moment of inertia of the beam about the major axis (mm^4)

E = modulus of elasticity of the timber (MPa)

A better approximation is to assume the joint region remains rigid, as shown Figure 4.4. Therefore the flexural deformation of the beams can be taken as

$$\delta_{b(flexure)} = \frac{V_b l_b^3}{3EI_b} \tag{4.18}$$

where l_b = clear distance from the end of the beam to the face of the column (mm)

The shear component of beam deformation is shown in Figure 4.5 and can be estimated by

$$\delta_{b(shear)} = \frac{kV_b l_b}{A_b G} \tag{4.19}$$

where k = Shear distribution factor = 1.5

G = shear modulus which is usually taken as E/15 (MPa)

A_b = cross sectional area of the beam (mm^2)

Considering rigid body rotation of the whole assembly, the beam deflection in terms of column displacement is

$$\Delta_{c,b} = \Delta_{c,b(flexure)} + \Delta_{c,b(shear)} = 2\delta_{b(flexure)}\frac{L_c}{L_b} + 2\delta_{b(shear)}\frac{L_c}{L_b} \tag{4.20}$$

substituting (4.18) and (4.19) into (4.20) gives

$$\Delta_{c,b} = 2\frac{L_c}{L_b}\left[\frac{V_b l_b^3}{3EI_b} + \frac{kV_b l_b}{A_b G}\right] \tag{4.21}$$

4.8.2 DEFORMATIONS OF THE COLUMNS

The deflections of the columns can also be divided into two components; flexural and shear deformations.

$$\Delta_{c,c} = \Delta_{c,c(flexure)} + \Delta_{c,c(shear)} \tag{4.22}$$

The flexural component of column deformation is shown in Figure 4.3 and can be estimated by

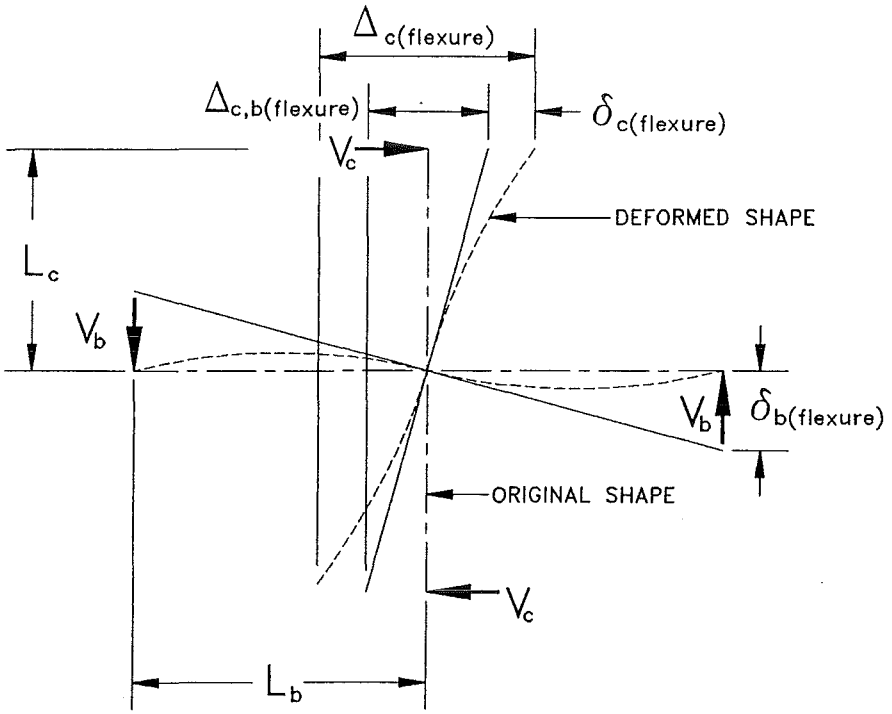

Figure 4.3 Member deformations due to flexure

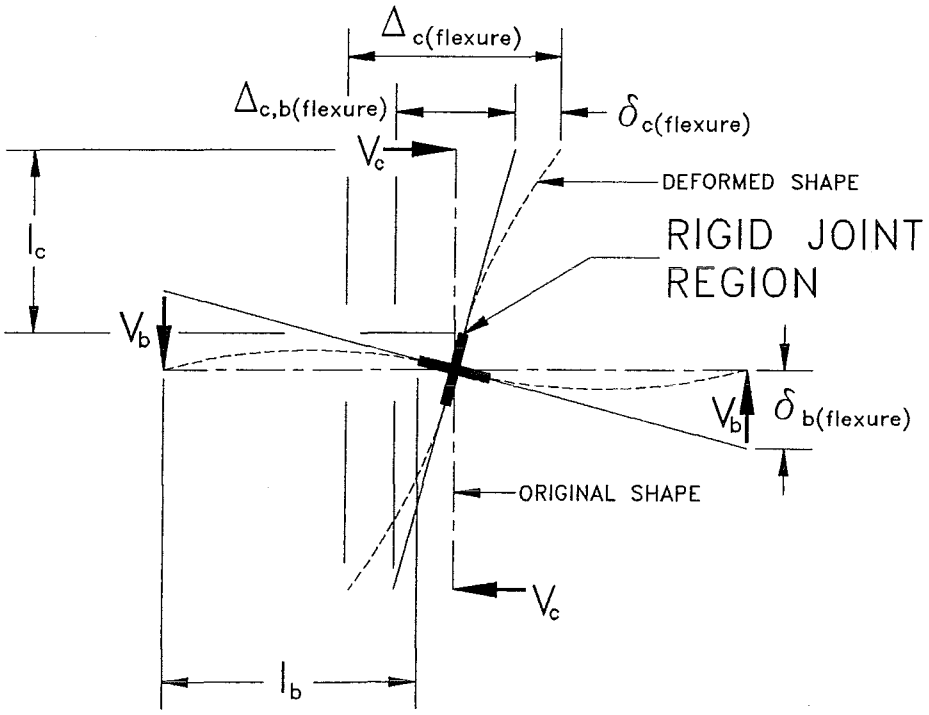

Figure 4.4 Member deformations due to flexure, assuming a rigid joint region

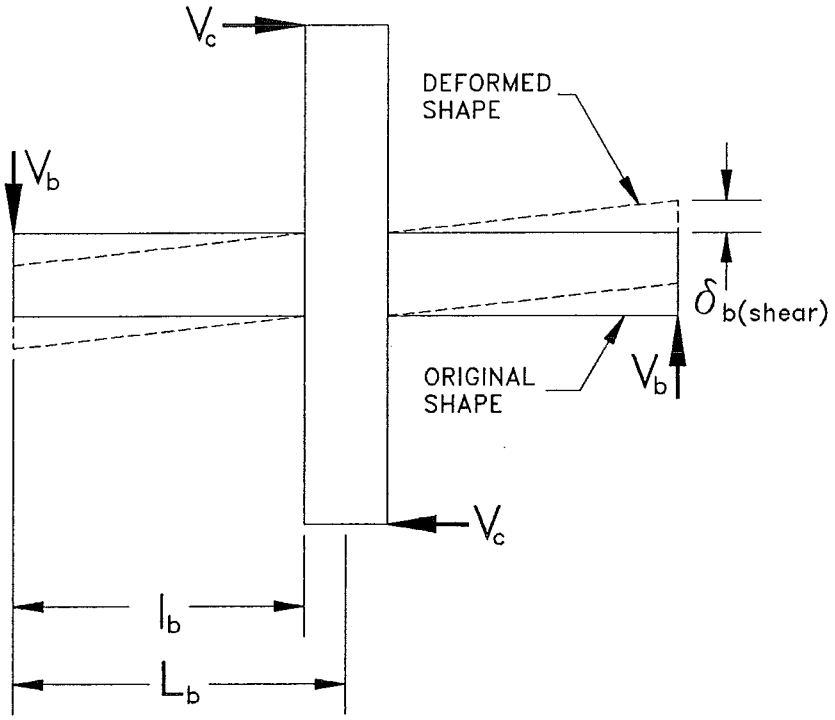

Figure 4.5 Shear component of beam deformations

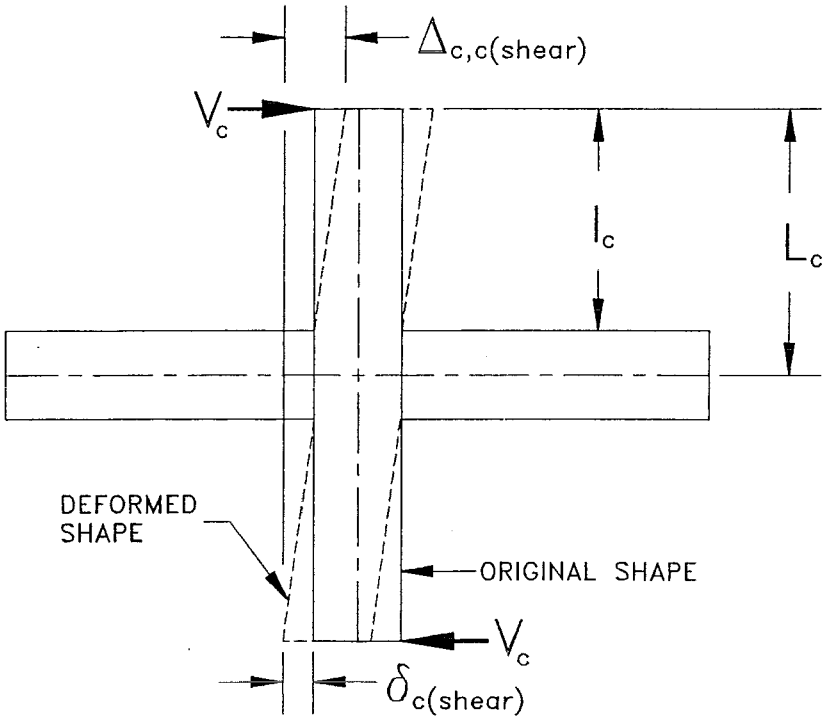

Figure 4.6 Shear component of column deformations

$$\delta_{c(flexure)} = \frac{V_c L_c^3}{3EI_c} \tag{4.23}$$

where V_c = shear force at the column end (kN)

L_c = length of the column to the centre of the beams (mm)

I_c = moment of inertia of the column about the major axis (mm^4)

A better model is to assume the joint region remains rigid, as illustrated in Figure 4.4, hence the flexural deformation of the column assuming a rigid joint core is

$$\delta_{c(flexure)} = \frac{V_c l_c^3}{3EI_c} \tag{4.24}$$

where l_c = clear distance from the top of the column to the top of the beams (mm)

The shear component of column deformation is shown in Figure 4.6 and can be estimated by

$$\delta_{c(shear)} = \frac{kV_c l_c}{A_c G} \tag{4.25}$$

The column deflection can then be estimated as

$$\Delta_{c,c} = \Delta_{c,c(flexure)} + \Delta_{c,c(shear)} = 2\delta_{c(flexure)} + 2\delta_{c(shear)} \tag{4.26}$$

Substituting (4.24) and (4.25) into (4.26) assuming a rigid joint region gives

$$\Delta_{c,c} = 2\left[\frac{V_c l_c^3}{3EI_c} + \frac{kV_c l_c}{A_c G}\right] \tag{4.27}$$

4.8.3 DEFORMATIONS DUE TO HINGE ROTATION OF COLUMN AND BEAMS

Clip gauges were placed vertically at the top and bottom edges of the joint region to measure

the top and bottom vertical displacements of the columns where the measured displacements δ_1 and δ_2 are shown in Figure 4.7.

The end rotation of the column ϕ_c is

$$\phi_c = \frac{\delta_1 + \delta_2}{e} \quad \text{(radians)} \qquad (4.28)$$

where e is the horizontal distance between the vertical gauges as shown in Figure 4.7.

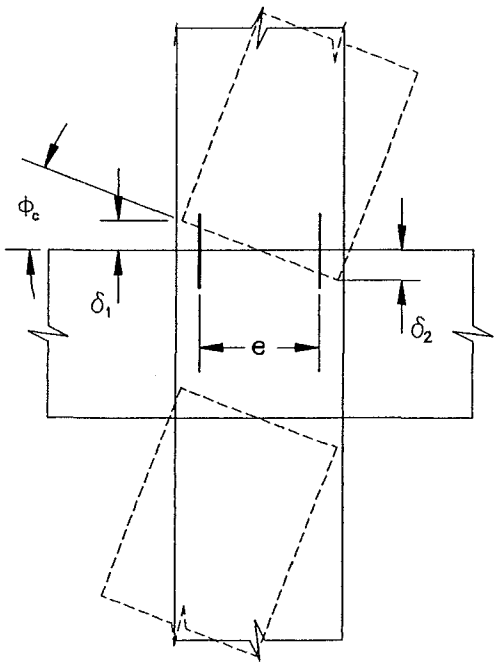

Figure 4.7 Deformation due to hinge rotation of the column

With reference to Figure 4.9, the overall deformation due to hinge rotation of the column can be taken as

$$\Delta_{c,r(column)} = 2\phi_c l_c \qquad (4.29)$$

This mode of deformation only occurs in the two tests using the steel joint core.

Horizontal clip gauges were placed at the top and bottom edges of the beams at the beam-column face to measure the top and bottom horizontal displacements of the beams where the measured displacements δ_3 and δ_4 are shown in Figure 4.8.

The end rotation of the beams ϕ_b is

$$\phi_b = \frac{\delta_3 + \delta_4}{g} \quad \text{(radians)} \qquad (4.30)$$

where g is the vertical distance between the horizontal gauges as shown in Figure 4.8.

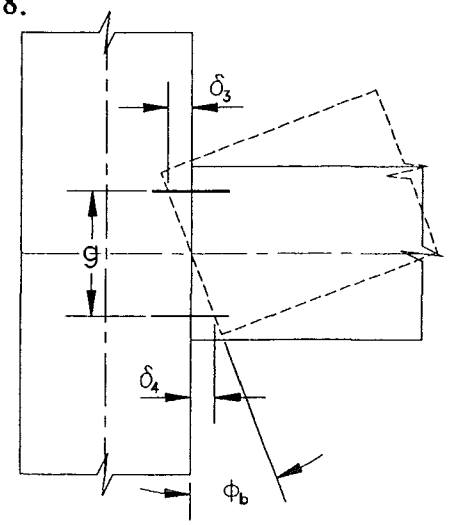

Figure 4.8 Deformation due to hinge rotation of the beams

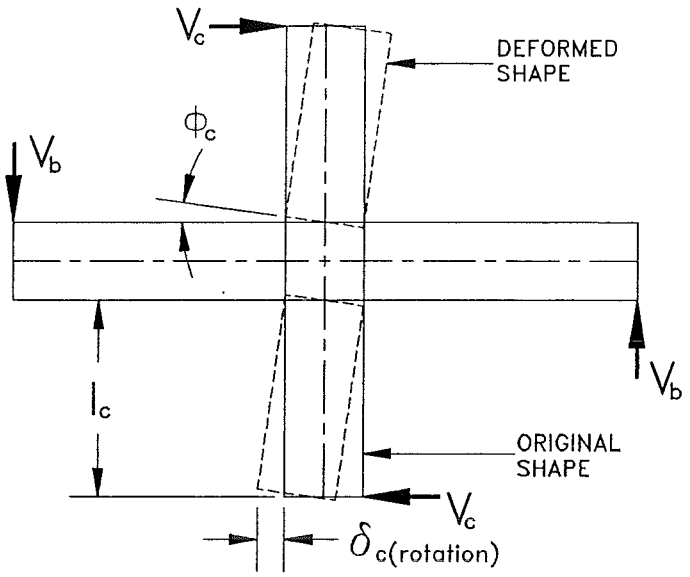

Figure 4.9 Deformations due to hinge rotation of the column

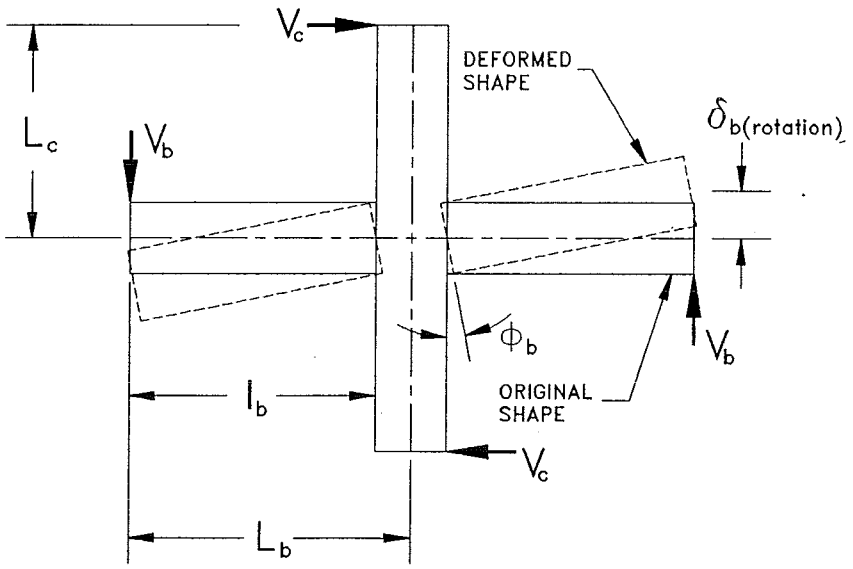

Figure 4.10 Deformations due to hinge rotation of the beams

With reference to Figure 4.10, the overall deformation due to hinge rotation of the beams can be taken as

$$\Delta_{c,r(beam)} = 2\phi_b l_b \frac{L_c}{L_b} \tag{4.31}$$

The column deflection due to hinge rotation of both the beams and column is

$$\Delta_{c,r} = \Delta_{c,r(column)} + \Delta_{c,r(beam)} \tag{4.32}$$

Substituting (4.29) and (4.31) into (4.32) gives

$$\Delta_{c,r} = 2\phi_c l_c + 2\phi_b l_b \frac{L_c}{L_b} \tag{4.33}$$

4.8.4 DEFORMATIONS DUE TO SLIDING SHEAR AT BEAM-COLUMN FACE

The deformation of the column relative to the joint due to sliding shear, $\delta_{c(sliding\ shear)}$ was measured using clip gauges at each beam-column face. Using the geometry of the frame as shown in Figure 4.11, then the deformation due to sliding shear of the columns can be computed as follows

$$\Delta_{c,s(column)} = 2\,\delta_{c(sliding\ shear)} \tag{4.34}$$

This mode of deformation only occurs in the two tests using the steel joint core.

If the deformation of the beams relative to the joint due to sliding shear $\delta_{b(sliding\ shear)}$ was measured, and using the geometry of the frame as shown in Figure 4.12, then the deformation due to sliding shear of the beams can also be computed as follows

$$\Delta_{c,s(beam)} = 2\frac{L_c}{L_b}\delta_{b(sliding\ shear)} \tag{4.35}$$

The column deflection due to sliding shear of both the beams and column is

$$\Delta_{c,s} = \Delta_{c,s(column)} + \Delta_{c,s(beam)} \tag{4.36}$$

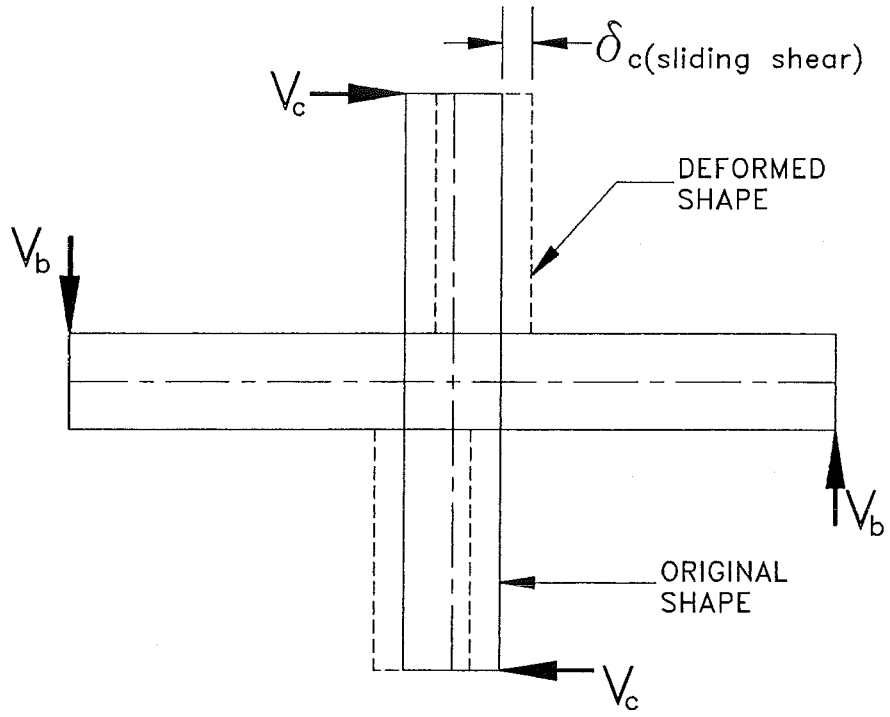

Figure 4.11 Deformations due to sliding shear of the column

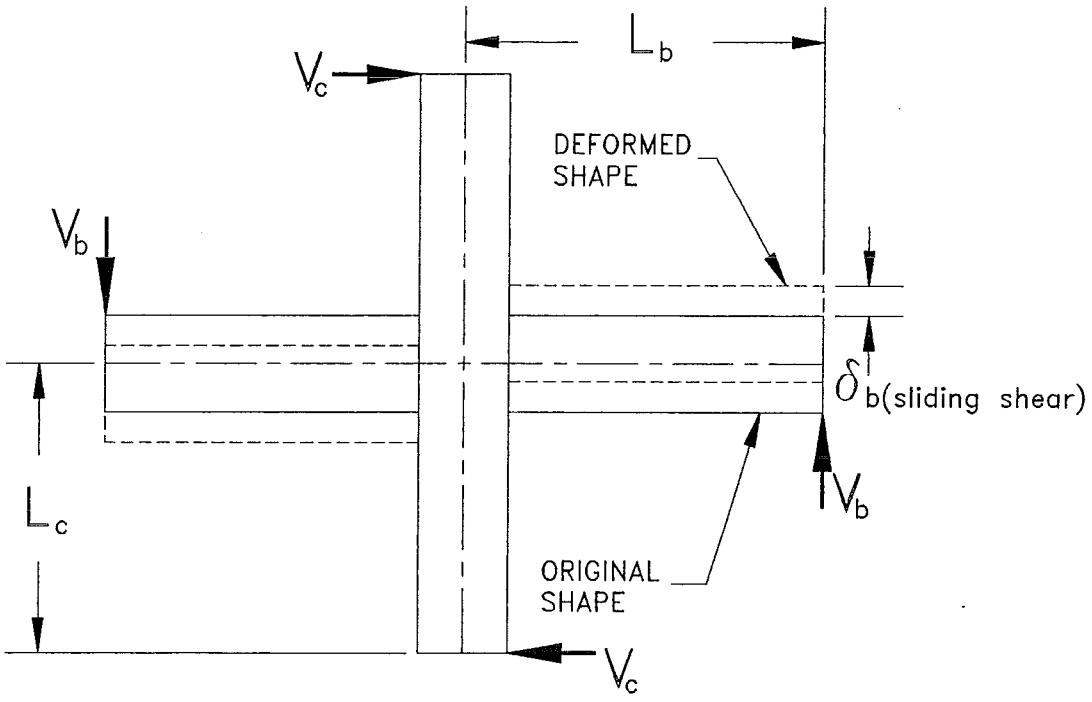

Figure 4.12 Deformations due to sliding shear of the beams at the beam-column face

substituting (4.34) and (4.35) into (4.36) gives

$$\Delta_{c,s} = 2\delta_{c(\text{sliding shear})} + 2\frac{L_c}{L_b}\delta_{b(\text{sliding shear})} \tag{4.37}$$

4.8.5 DEFORMATIONS DUE TO SHEAR DISTORTION OF JOINT REGION

Clip gauges along the the diagonals of the joint region of each unit, enabled the joint core distortion to be measured. From the geometry shown in Figure 4.13, the total joint shear strain γ is as follows

$$\gamma = \gamma_1 + \gamma_2 = \frac{\delta_6 - \delta_5}{2d}\left[\tan\theta + \frac{1}{\tan\theta}\right] \tag{4.38}$$

where the measured displacements δ_5 and δ_6 are taken as positive when the diagonal length d extends and negative when it shortens and θ is the angle of inclination between the diagonal and the horizontal.

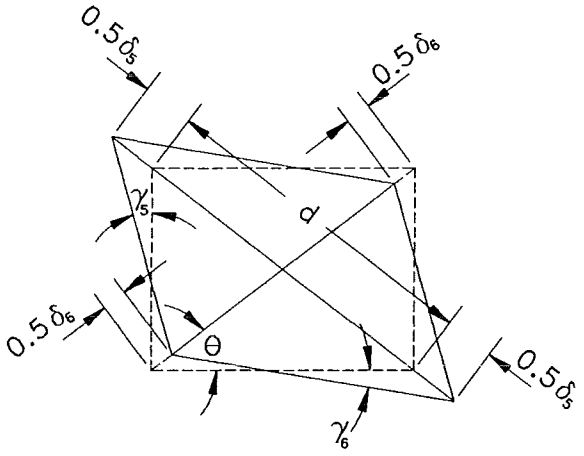

Figure 4.13 Shear distortion of joint panel

The displacement $\Delta_{c,j}$ due to the joint strain γ is shown in Figure 4.14 and can be shown to be

$$\Delta_{c,j} = \gamma\left[2l_c - h_c\frac{L_c}{L_b}\right] \tag{4.39}$$

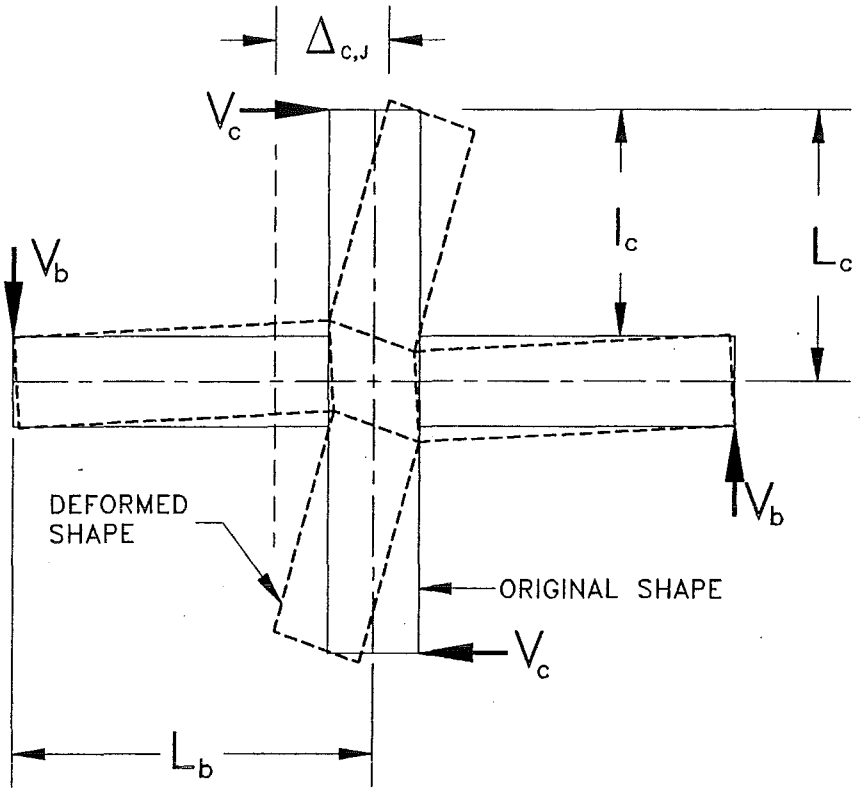

Figure 4.14 Deformations due to the shear distortion of the joint region

4.8.6 TOTAL DEFORMATIONS

All the components mentioned above can now be summed up to find the overall column deflection, Δ_c where

$$\Delta_c = \Delta_{c,b} + \Delta_{c,c} + \Delta_{c,r} + \Delta_{c,s} + \Delta_{c,j} \qquad (4.40)$$

The overall column deflection can now be determined at all the loading stages and compared with the measured column deflection.

CHAPTER 5

TEST RESULTS

5.1 EXPERIMENTAL RESULTS

Three different types of beam-column connections were tested; four of the first type and two each of the second and third types, giving a total of eight specimens.

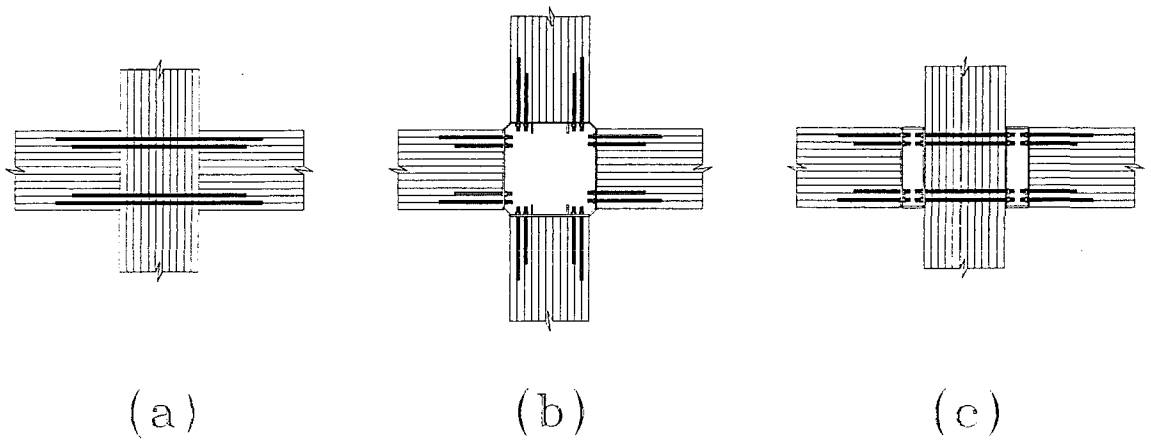

Figure 5.1 The different types of connections that were tested

Connection type A is shown in Figure 5.1 (a) and uses a continuous column with beams butting up against it on either side and epoxied dowels embedded in the beams and columns. The second and third types of connection use a steel bracket specially designed so yielding occurs in the beam flange plates or in the web panel. A type B connection is illustrated in Figure 5.1 (b) and consists of beams and columns bolted to a central steel hub in the joint. As shown in Figure 5.1 (c), the type C joint consists of a continuous column and two steel brackets, one each side of the column.

5.2 JOINT TYPE A

The first four tests consisted of beam-column connections using epoxied steel dowels passing

through the beams and the column. By changing the dowel type and the geometry of the steel dowels, the behaviour of the connection could be changed from elastic to ductile behaviour.

To reduce the number of different deflection components shown on the graphs, the flexural and shear deformations have been summed together for the columns and beams and put into two categories; beam and column deformations. The contributions of the flexural and shear deformations to the total beam deformation can be taken as 67% for flexure and 33% for shear respectively. Half the total column deformation was due to flexural deformations and half to shear deformations.

5.2.1 UNIT 1

The arrangement of reinforcing bars for Unit 1 is shown in Figure 5.2. Reinforcement consists of eight 3/4" BSW high strength threaded rods that were epoxied into 26mm holes drilled into the outer laminations at both the top and bottom of the glulam beams and passing through the column.

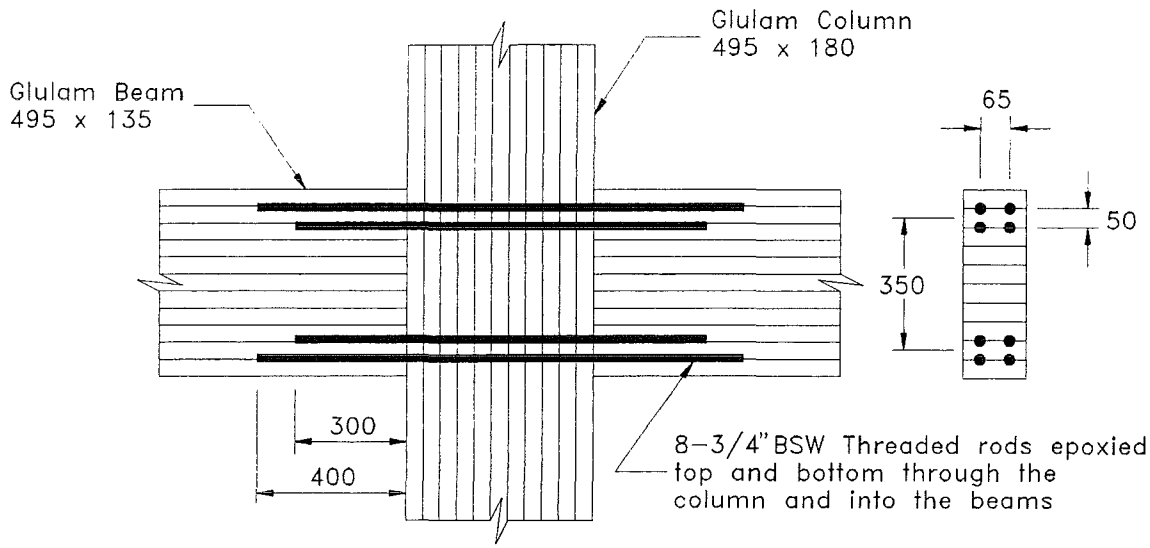

Figure 5.2 Arrangement of bars for unit 1

5.2.1.1 DESCRIPTION OF FAILURE MODE

The first crack was a local tension failure in the first laminate around the bars on south-west top face of the beam-column junction. Immediately after the first crack, at a moment of 86.3 kNm, a shear crack formed diagonally across the joint region. The average shear stress in the joint core was 5.0 MPa with a bending stress of 12.3 MPa. As the lateral load increased to the target load in negative direction, the shear crack continued open and propagate across the joint core. The maximum load in the negative direction was reached.

The specimen was then unloaded and loaded back up in the opposite direction. As the load increased in the positive direction, another diagonal crack appeared in the joint region at a similar load level as the first, but inclined in the opposite direction to the first crack. The average shear stress in the joint core was 4.4 MPa with a bending stress of 10.9 MPa. A flexural crack formed at the south-west bottom face of the column in the outer laminates and proceeded to spread horizontally across the joint region at the level of the lower reinforcement. The average shear stress in the joint core was 4.8 MPa with a bending stress of 11.8 MPa.

The specimen was then unloaded and loaded back up in the opposite direction to final failure. As the load increased, the first diagonal cracks within the joint opened up. Flexural cracks formed at the north-east top and bottom faces of the column in the outer laminates at the level of the reinforcement. The average shear stress in the joint core was 4.2 MPa with a bending stress of 10.5 MPa. When the moment reached 85.1 kNm, the column failed suddenly in brittle manner. The maximum stresses reached in the connection were: 13.1 MPa bending stress in the column with an average shear stress of 5.3 MPa in the joint core. In the beams, the bending stress was 14.7 MPa with a shear stress of 0.9 MPa.

A photograph of the overall connection at the end of the test is shown in Figure 5.3. The failure pattern in the joint core is shown in Figure 5.4.

Figure 5.3 Overall view of Unit 1 at the end of test

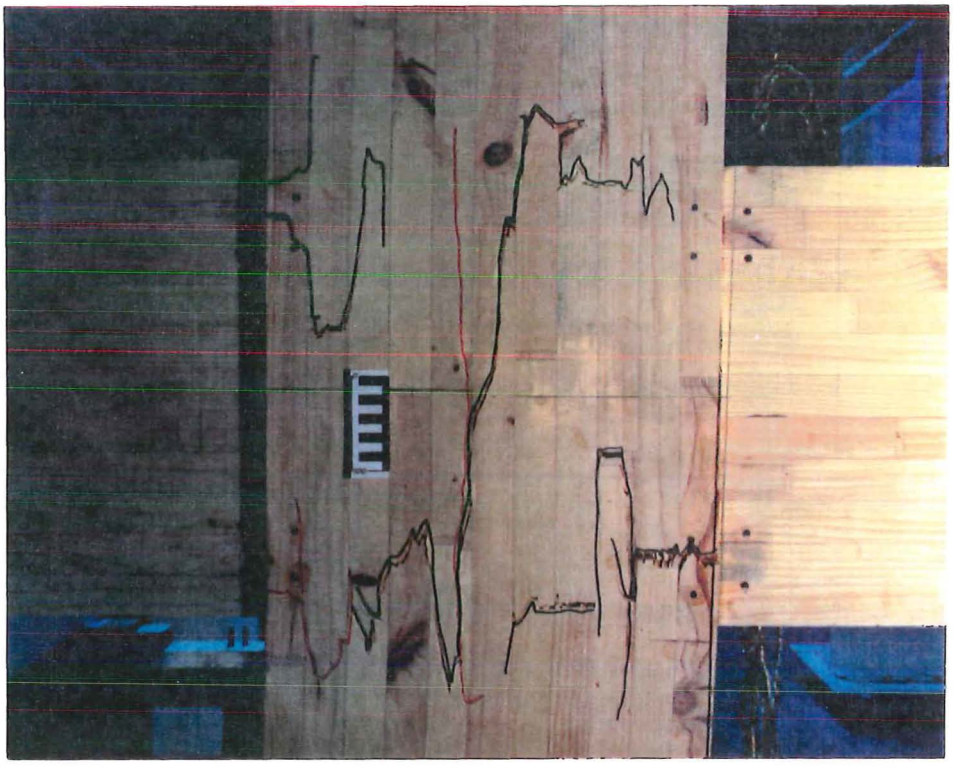

Figure 5.4 View of the joint region of Unit 1 at the end of the test

5.2.1.2 RESULTS

The initial stiffness for Unit 1 was 1.41 kN/mm. The load-deflection plot for Unit 1 is shown in Figure 5.5 and displays linear behaviour up to formation of the first crack. The fat loops are due to cracking in joint core by shear and flexure, causing permanent offsets of the curves. The plot of the load versus the shear distortion of the joint core as a component of column deflection is shown in Figure 5.6. This graph clearly shows the effect that the diagonal shear cracking has on the joint core.

The calculated components are shown in Figure 5.7. This graph shows two main points; that sliding shear is neglible and joint distortion is a major contributor of deflection, especially near failure.

A comparison of the calculated and measured components of column deflections is shown in Figure 5.8. This graph shows that the calculated components have been overestimated. Since the difference between the calculated and measured components increases linearly with load increasing, the assumed values for the modulus of elasticity may be too low.

5.2.1.3 DISCUSSION

The permissible shear and bending stresses permitted by NZS 3603:1981- Timber Design Code for No.1 framing glulam timber is 2.70 MPa and 15.9 MPa respectively (the basic shear and bending stresses are 1.8 MPa and 10.6 MPa, both multiplied by the short term duration of load factor, $K_1 = 1.5$).

Table 5.1 Minimum stresses in member at first cracking of Unit 1

Failure Mode	Shear Stress (MPa)	Flexural Stress (MPa)
Shear cracks in joint core	4.4	10.9
Flexural cracks in joint core	4.2	10.5

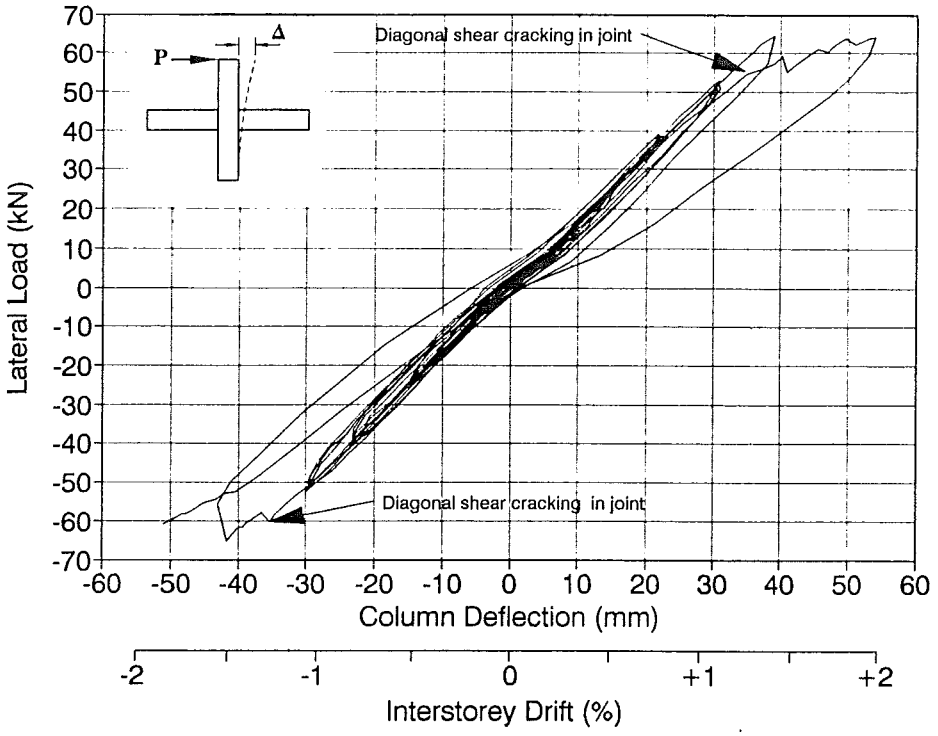

Figure 5.5 Load-deflection plot for Unit 1

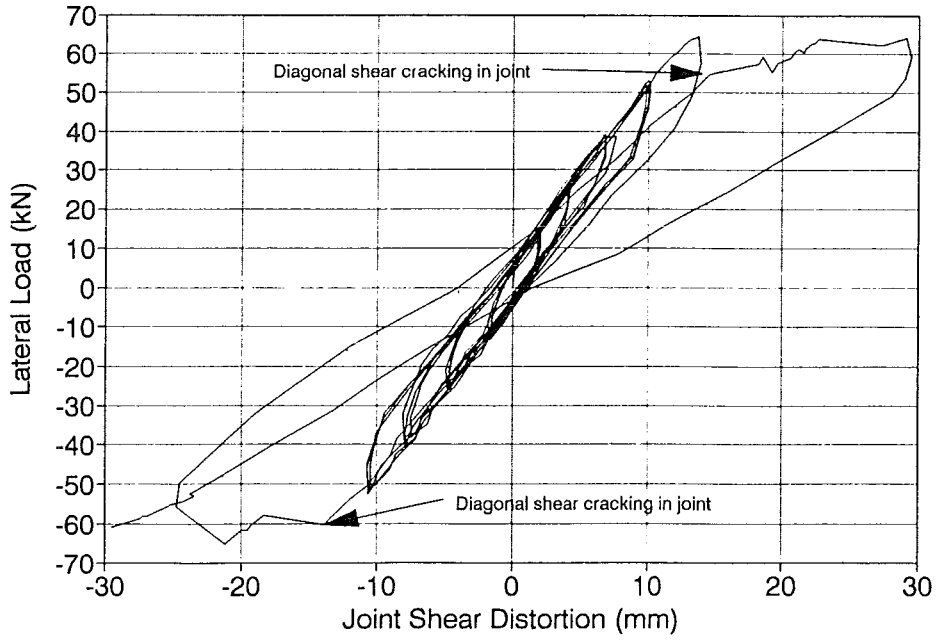

Figure 5.6 Load-joint shear distortion plot for Unit 1

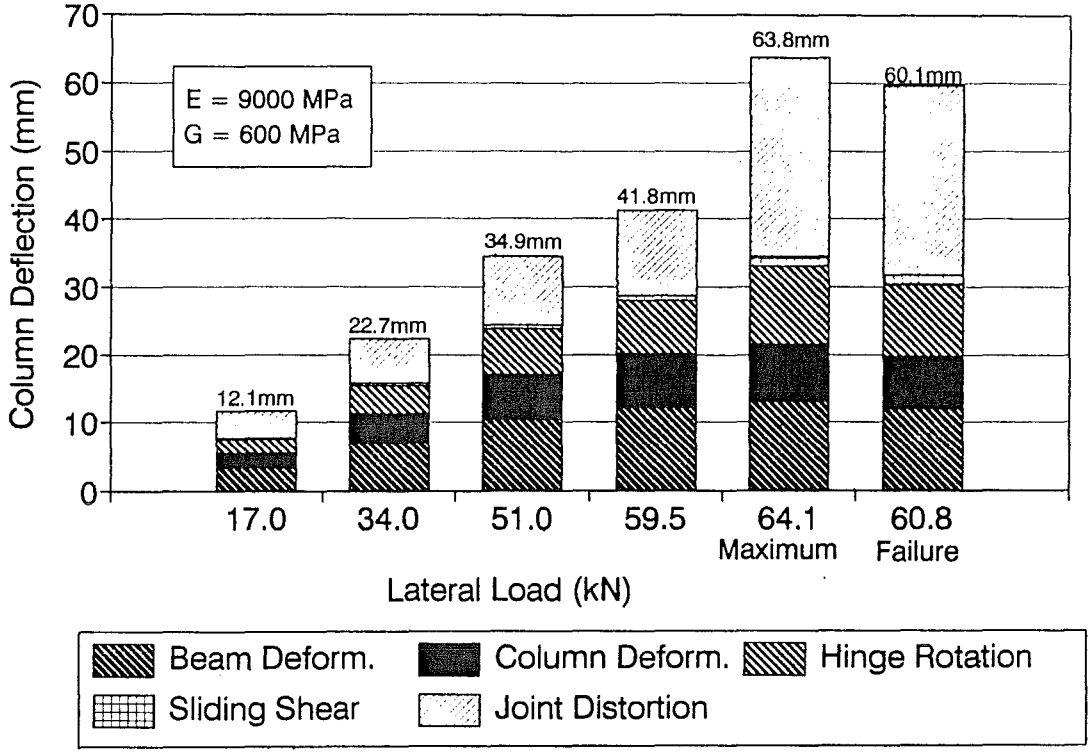

Figure 5.7 Calculated components of column deflection for Unit 1

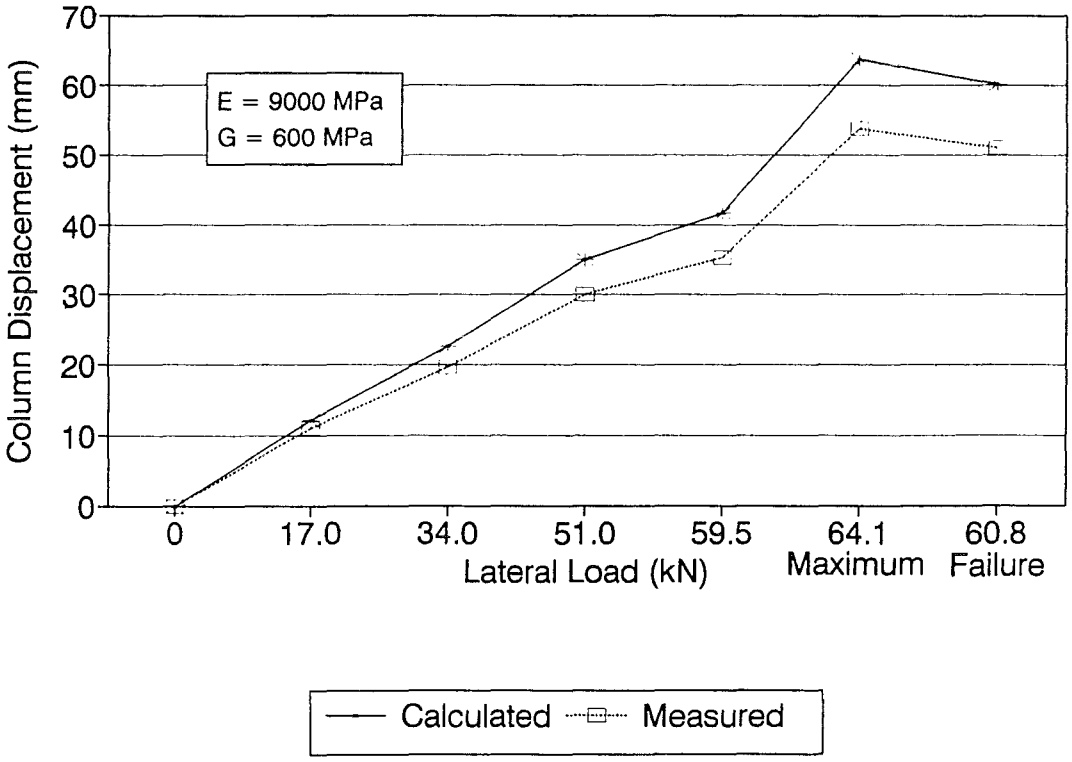

Figure 5.8 Comparision of calculated and measured column deflections for Unit 1

By refering to Table 5.1 which shows the stresses at first cracking of the joint region, the shear stress are well within the permisible design criteria, but the flexural stresses are not. This suggests that the combination of high shear and moderate flexural stresses in the joint core is critical and code values for this case may be unconservative.

5.2.2 UNIT 2

The arrangement of reinforcing bars for Unit 2 is shown in Figure 5.9. Reinforcement consists of eight D16 mild steel deformed bars that were epoxied into 22mm holes drilled into the outer laminations at both the top and bottom of the glulam beams and passing through the column.

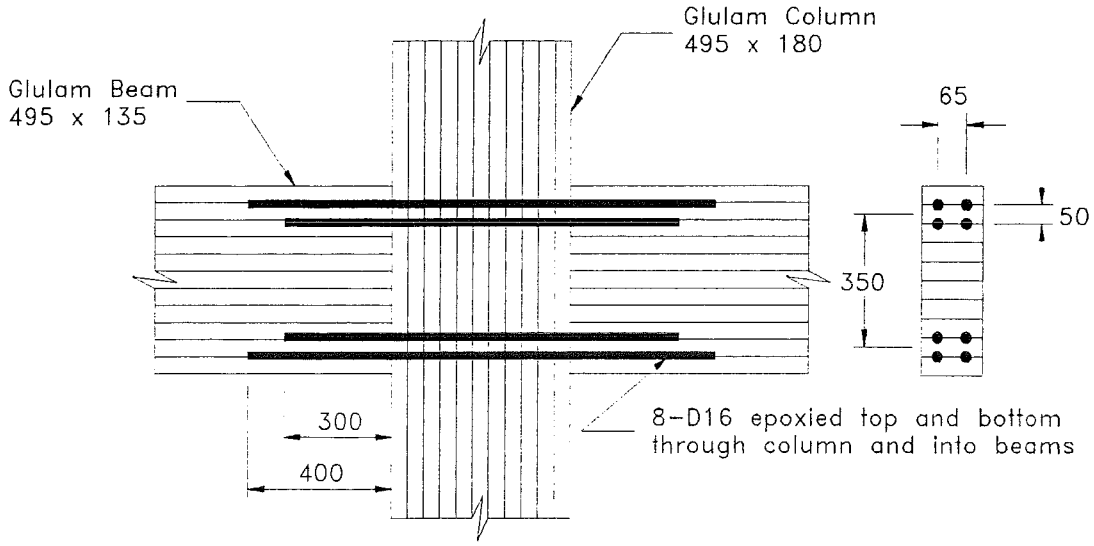

Figure 5.9 Arrangement of bars for Unit 2

5.2.2.1 DESCRIPTION OF FAILURE MODE

The first crack was a tension failure in the laminates around the bars in the south beam. This crack appears to have started at a finger joint that was close to the end of the dowel positioned in the outer laminate. At the time the south beam cracked, the lateral load had just reached the target load in negative direction, giving a moment of 88.5 kNm, giving shear stresses in the beams and joint core of 1.0 MPa and 5.1 MPa respectively. The flexural stresses in the

column and beams were 12.8 MPa and 13.9 MPa respectively.

The specimen was then unloaded and loaded back up in the opposite direction. As the load increased in the positive direction, another crack appeared, this time in the top steel of north beam. This crack was due to wood splitting parallel to the grain, travelling along the top inner bar line. The shear stresses in the beams, column and joint core of 1.12 MPa, 1.18 MPa and 5.5 MPa respectively. The flexural stresses in the column and beams were 13.8 MPa and 15.0 MPa respectively. As the target load was reached, it was decided that another half cycle should be completed, so the specimen was then unloaded and loaded back up in the opposite direction to final failure.

As the load increased, the first crack in the south beam began to propogate parallel to grain, travelling along the inner bar line. At the same time, a crack formed in north beam at the level of the lower inner bar and proceeded to travel along a poor glue line between wood laminations. At a moment of 95.1 kNm, both beams failed in a sudden brittle manner.

The maximum stresses reached in the connection were: 15.1 MPa bending stress in the column with an average shear stress of 6.1 MPa in the joint core. In the beams, the bending stress was 16.4 MPa with a shear stress of 1.23 MPa.

A photograph of the overall connection at the end of the test is shown in Figure 5.10. The failure pattern in the joint core is shown in Figure 5.11.

5.2.2.2 RESULTS

The initial stiffness for Unit 2 was 1.54 kN/mm. The load-deflection plot for Unit 2 is shown in Figure 5.12 and displays linear behaviour up first yield of the deformed bars. The plot of the load versus the shear distortion of the joint core as a component of column deflection is shown in Figure 5.13. This graph shows that the joint core behaved linearly up to failure.

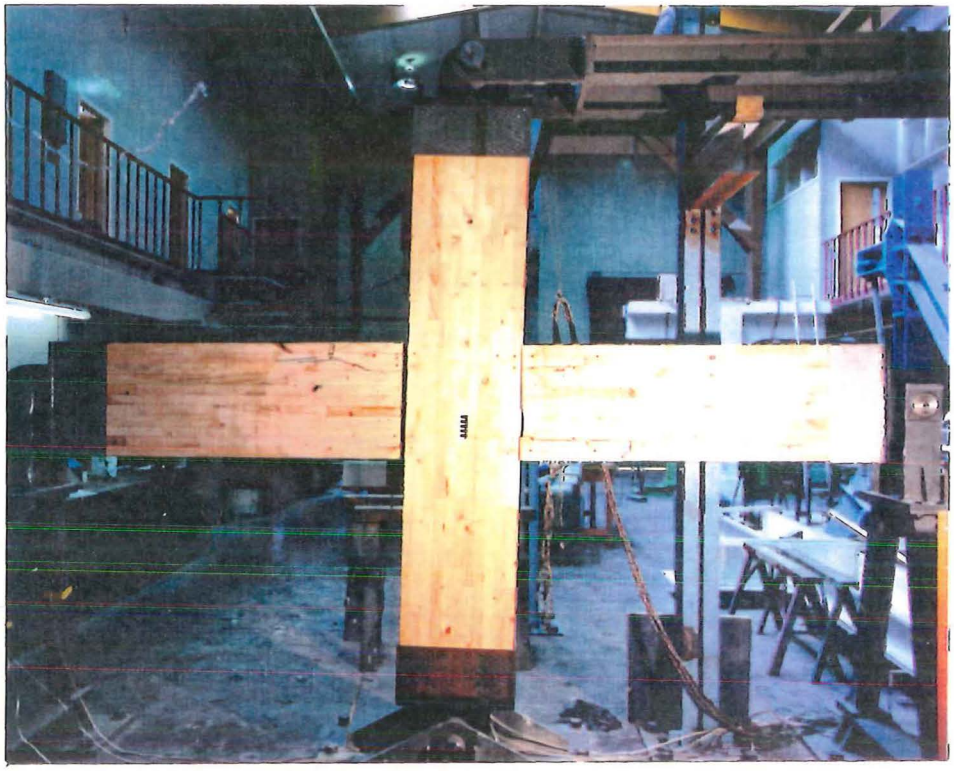

Figure 5.10 Overall view of Unit 2 at the end of test

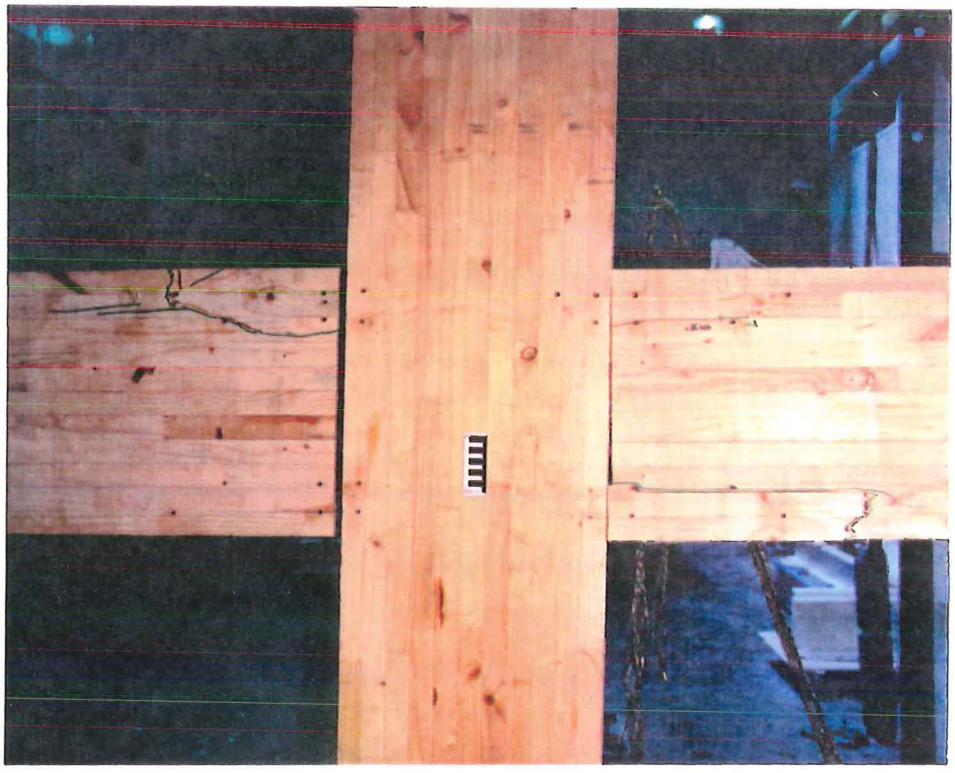

Figure 5.11 View of the joint region of Unit 2 at the end of the test

The calculated components are shown in Figure 5.14. This graph shows three main points; that sliding shear component remains neglible, joint distortion is a smaller component and the hinge rotation of the beams increased due to yielding of the bars.

A comparison of the calculated and measured components of column deflections is shown in Figure 5.15. This graph shows that the calculated components have been overestimated. Since the difference between the calculated and measured components increases linearly with load increasing, the assumed values for the modulus of elasticity may be too low.

5.2.2.3 DISCUSSION

The permissible shear and bending stresses permitted by NZS 3603:1981- Timber Design Code for No.1 framing glulam timber is 2.70 MPa and 15.9 MPa respectively (the basic shear and bending stresses are 1.8 MPa and 10.6 MPa, both multiplied by the short term duration of load factor, $K_1 = 1.5$).

Table 5.2 Minimum stresses in member at first cracking of Unit 2

Failure Mode	Shear Stress (MPa)	Flexural Stress (MPa)
Flexural cracks in beam	1.0	13.9

By refering to Table 5.2 which shows the stresses at first cracking of the beam, the shear and flexural stresses are not within the permisible design criteria. This suggests that the combination of moderate shear and flexural stresses in the beam ends failure may be causing failure in the beams.

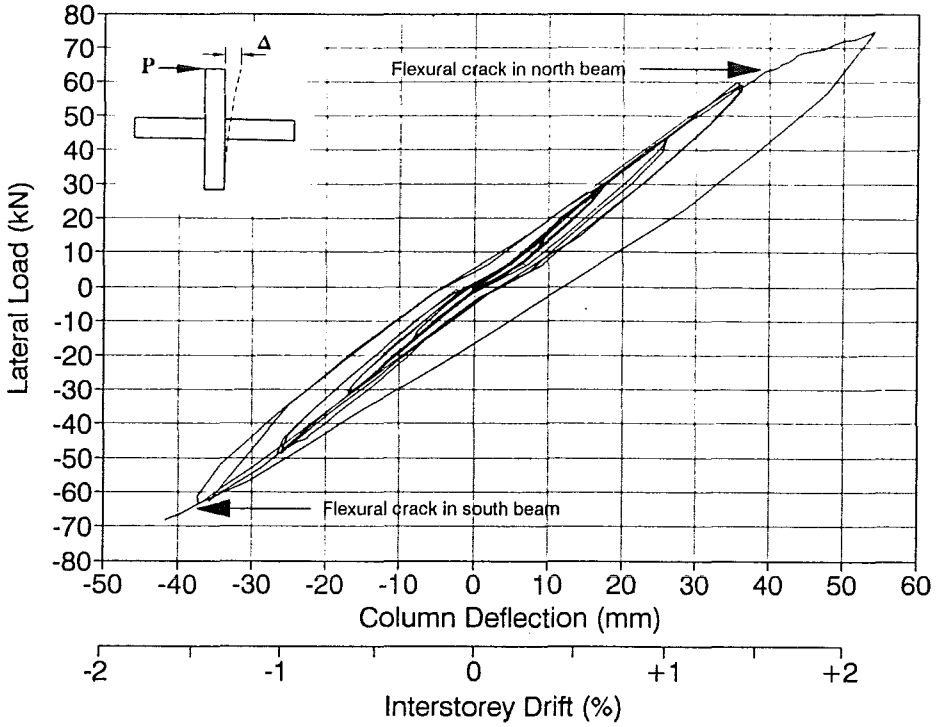

Figure 5.12 Load-deflection plot for Unit 2

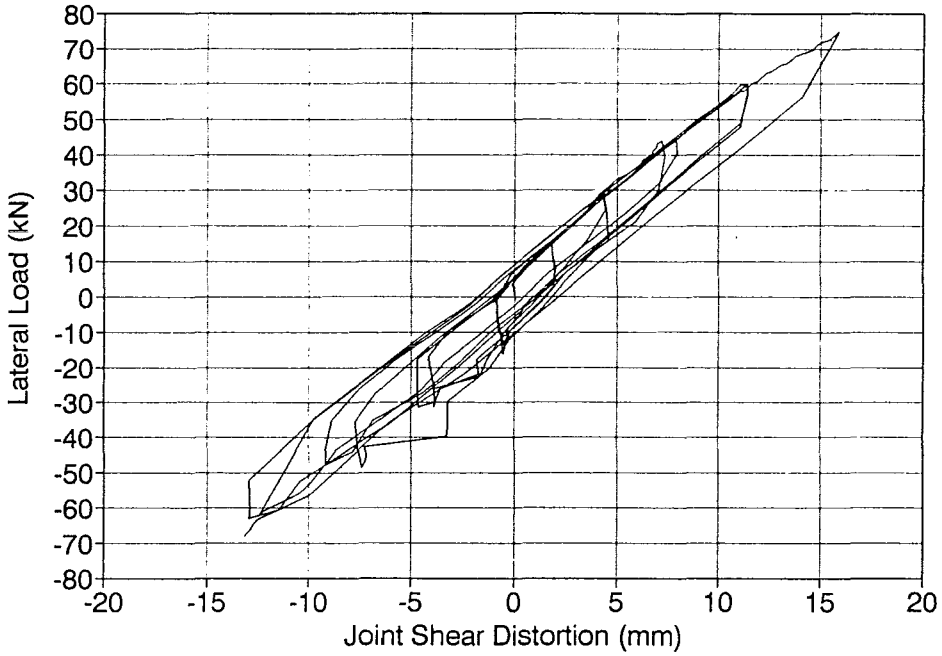

Figure 5.13 Load-joint shear distortion plot for Unit 2

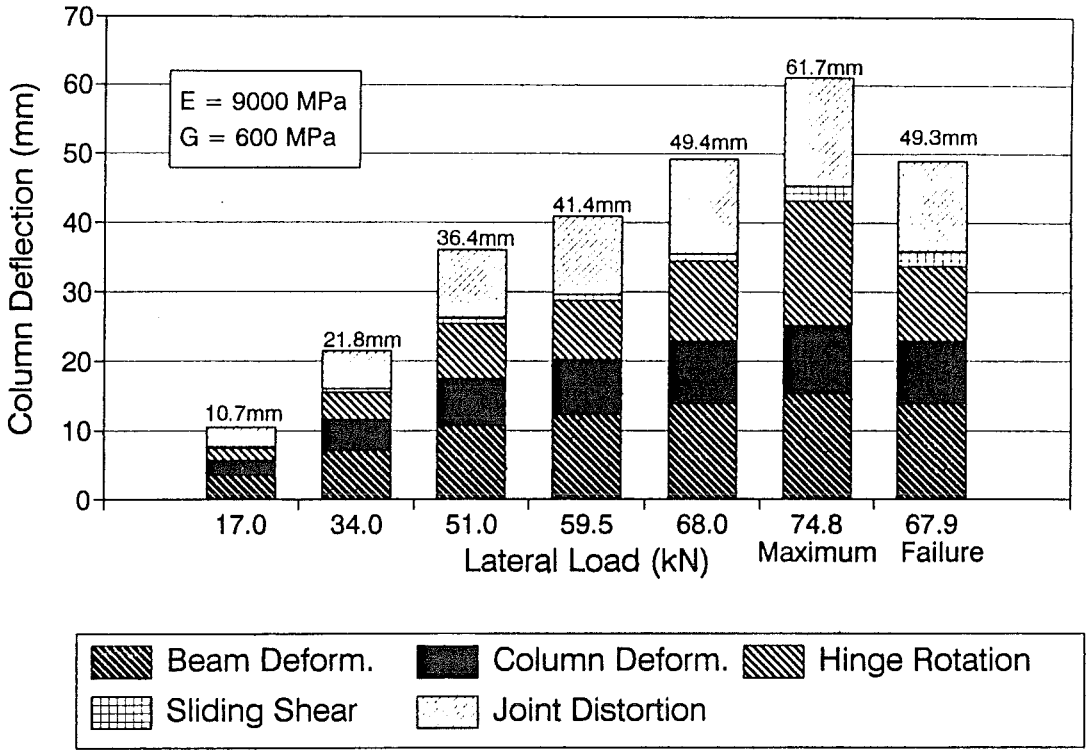

Figure 5.14 Calculated components of column deflection for Unit 2

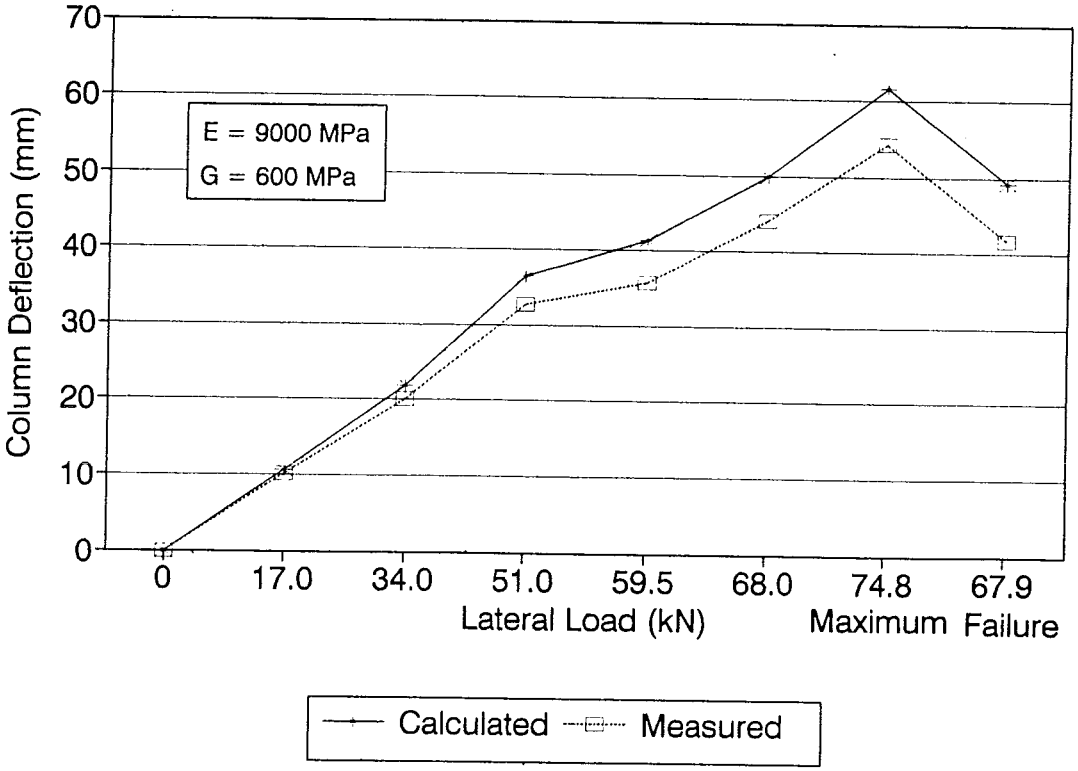

Figure 5.15 Comparision of calculated and measured column deflections for Unit 2

5.2.3 UNIT 3

The arrangement of reinforcing bars for Unit 3 is shown in Figure 5.16. Reinforcement consisted of nine mild steel deformed bars placed throughout the section; two D20 bars epoxied into 26mm holes in the outer laminations and seven D16 bars epoxied into 22mm holes in the inner laminations.

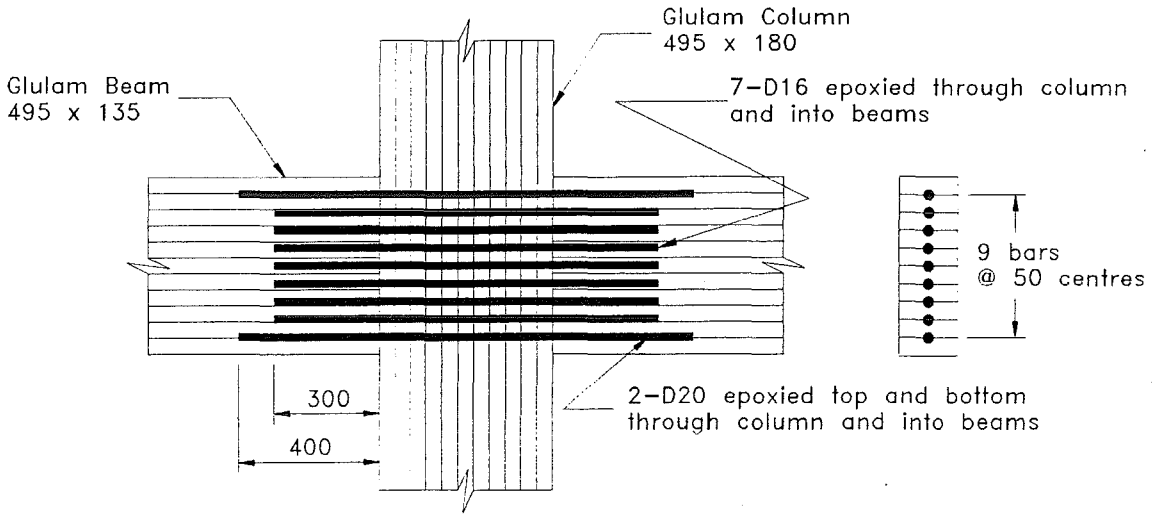

Figure 5.16 Arrangement of bars for Unit 3

5.2.3.1 DESCRIPTION OF FAILURE MODE

The first crack was a diagonal shear crack across the joint region at a moment of 84.0 kNm. The bending stress in the column was 11.8 MPa with average shear stress in the joint core was 6.5 MPa. As the shear crack propogated, a local flexural crack started in the column at a finger joint in the outer lamination, positioned near the lower bars. Another flexural crack formed at the south-west top face of the column joint region in the outer laminates and proceeded to spread horizontally across the joint region at the level of the outer reinforcement. When the moment reached 68.8 kNm, the column failed suddenly in brittle manner.

The maximum stresses reached in the connection were: 13.6 MPa bending stress in the column with an average shear stress of 7.4 MPa in the joint core. In the beams, the bending stress was 16.8 MPa with a shear stress of 1.14 MPa.

A photograph of the overall connection at the end of the test is shown in Figure 5.17. The failure pattern in the joint core is shown in Figure 5.18.

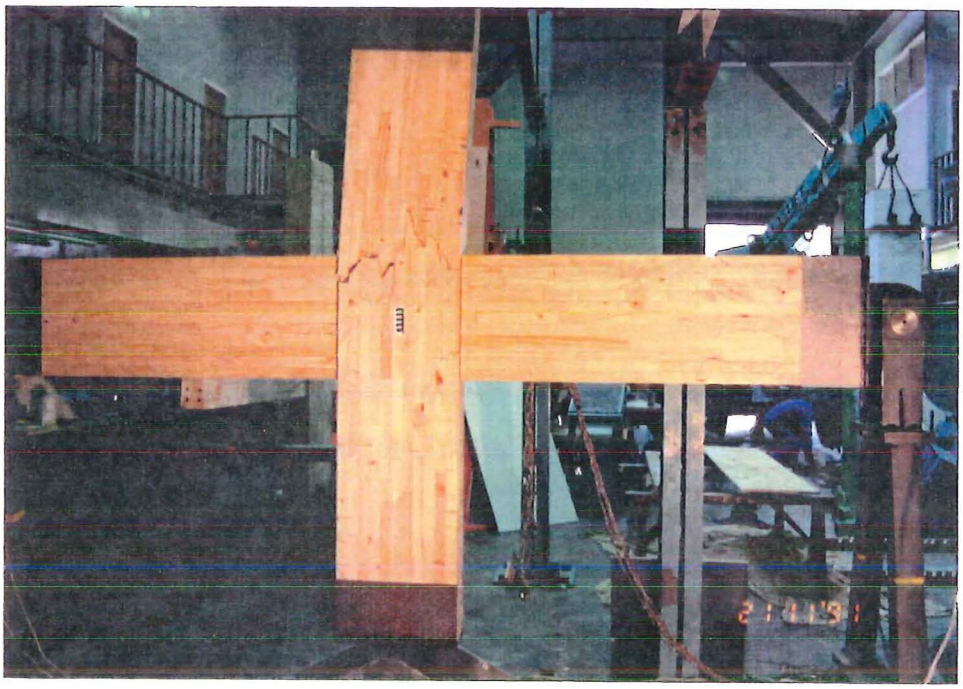

Figure 5.17 Overall view of Unit 3 at the end of test

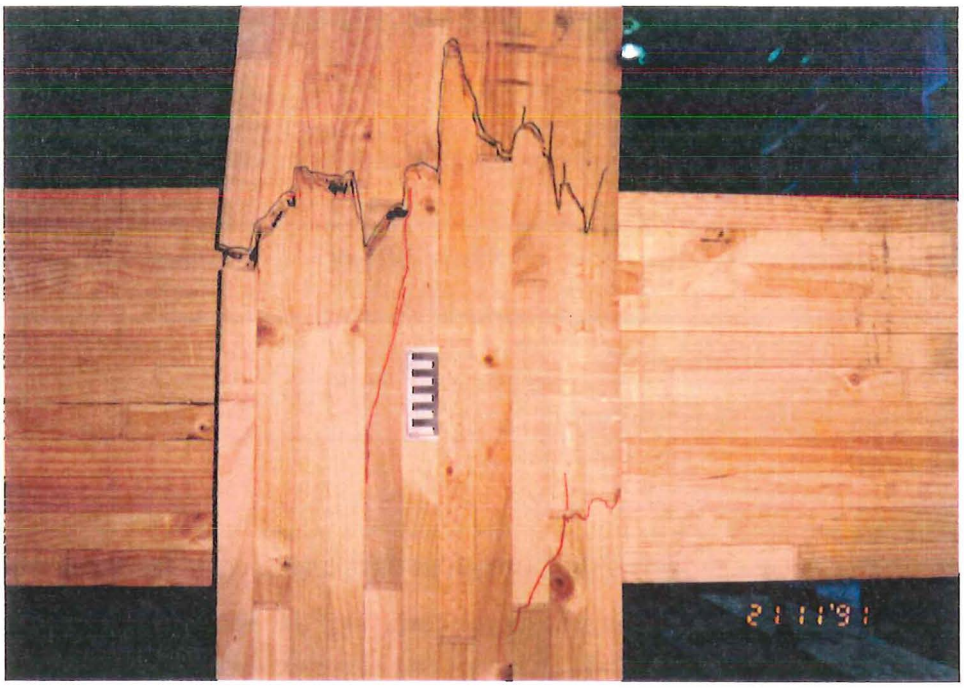

Figure 5.18 View of the joint region of Unit 3 at the end of the test

5.2.3.2 RESULTS

The initial stiffness for Unit 3 was 1.44 kN/mm. The load-deflection plot for Unit 3 is shown in Figure 5.19 and displays linear behaviour up first yield of the deformed bars. The plot of the load versus the shear distortion of the joint core as a component of column deflection is shown in Figure 5.20. This graph shows that the joint core behaved linearly up to failure.

The calculated components are shown in Figure 5.21. This graph shows three main points; that sliding shear component is neglible, joint distortion is a smaller component than in the previous two tests and hinge rotation of the beams has increased due to yielding of the bars.

A comparison of the calculated and measured components of column deflections is shown in Figure 5.22. This graph shows that the calculated and measured deflections are in good agreement.

5.2.3.3 DISCUSSION

The permissible shear and bending stresses permitted by NZS 3603:1981 - Timber Design Code for No.1 framing glulam timber is 2.70 MPa and 15.9 MPa respectively (the basic shear and bending stresses are 1.8 MPa and 10.6 MPa, both multiplied by the short term duration of load factor, $K_1 = 1.5$).

Table 5.3 Minimum stresses in member at first cracking of Unit 3

Failure Mode	Shear Stress (MPa)	Flexural Stress (MPa)
Shear cracks in joint core	6.5	11.8
Flexural cracks in joint core	6.5	11.8

By refering to Table 5.3 which shows the stresses at first cracking of the joint region, the shear stress is well within the permisible design criteria, but the flexural stress is not.

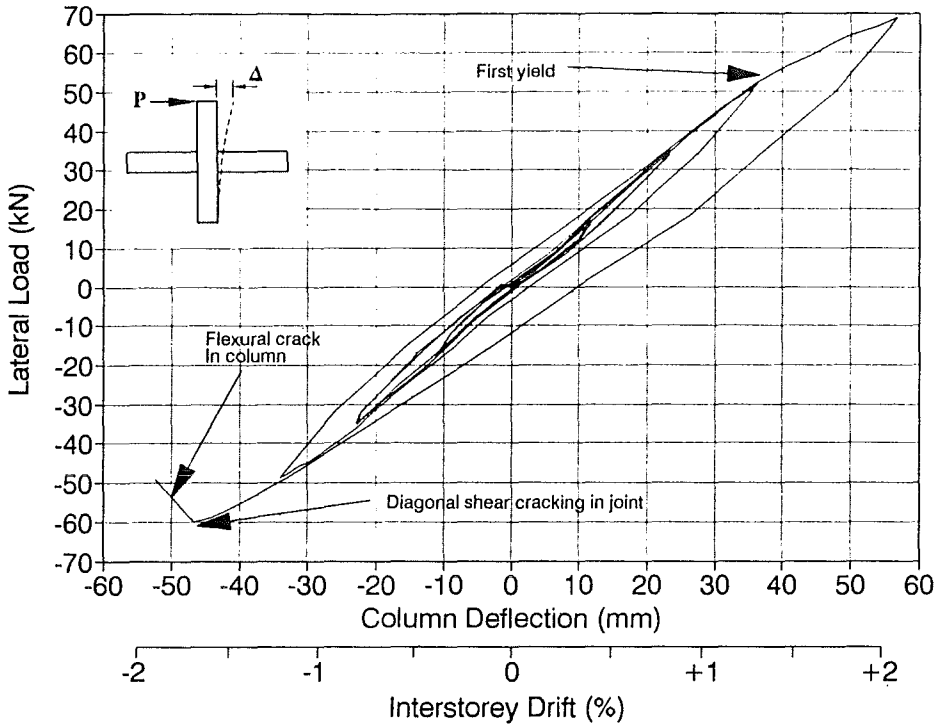

Figure 5.19 Load-deflection plot for Unit 3

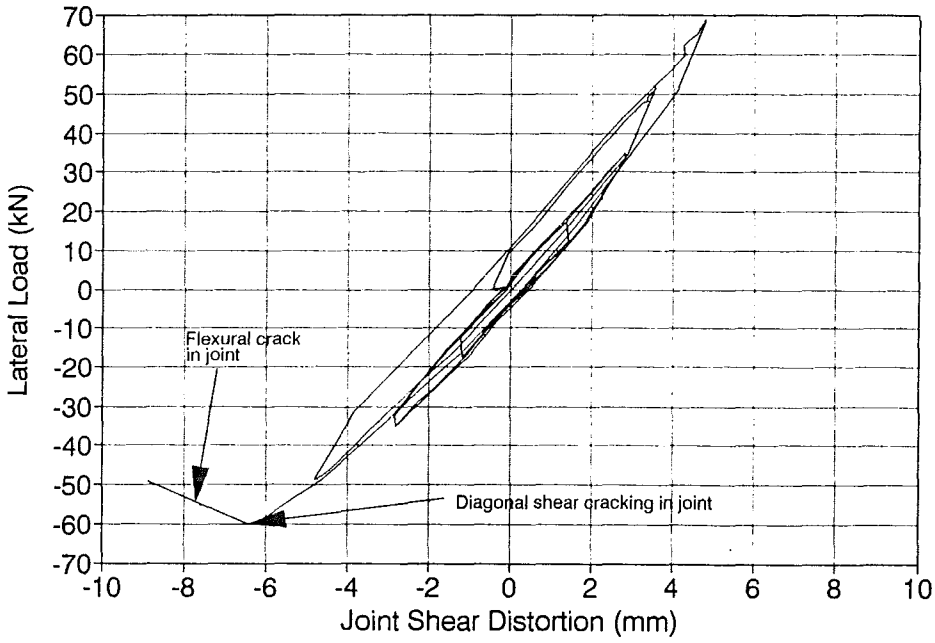

Figure 5.20 Load-joint shear distortion plot for Unit 3

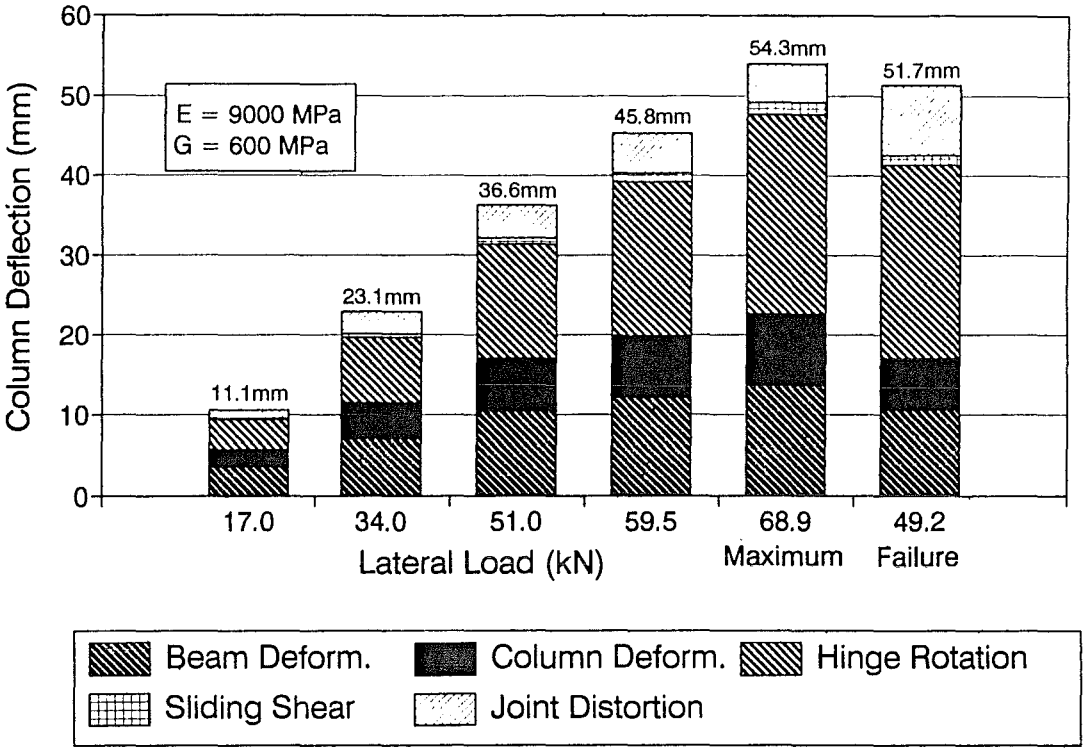

Figure 5.21 Calculated components of column deflection for Unit 3

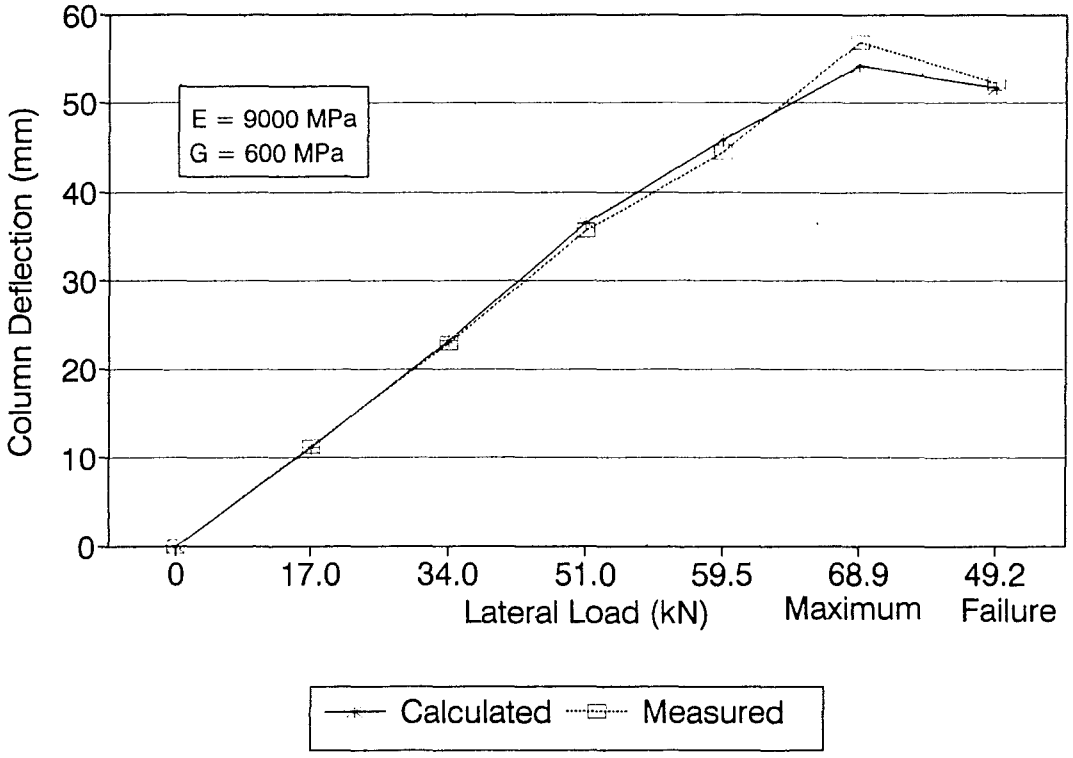

Figure 5.22 Comparision of calculated and measured column deflections for Unit 3

This suggests that the combination of high shear and moderate flexural stresses in the joint core could be important and code values for this case may be unconservative.

After examining the failed region of the joint, it was concluded that the quality of the timber within the joint was poor; not only was pith was visible in the outer laminations but there were too many finger joints. The standard for the manufacture of glue laminated timber (NZS 3606:1981) does not permit pith in the outer laminations of No.1 framing grade glulam timber.

5.2.4 UNIT 8

The arrangement of reinforcing bars for Unit 8 is shown in Figure 5.23. Reinforcement consisted of five D16 mild steel deformed bars epoxied into 22mm holes placed throughout the section. Four bars were placed in the outer laminations; two bars at the top and two at the bottom of the section and a single bar placed at the centroid of the beam section. Each bar was debonded over 40mm (20mm into the column and 20mm into the beam) using insulation tape. This was done to increase the length of the bar over which yielding took place.

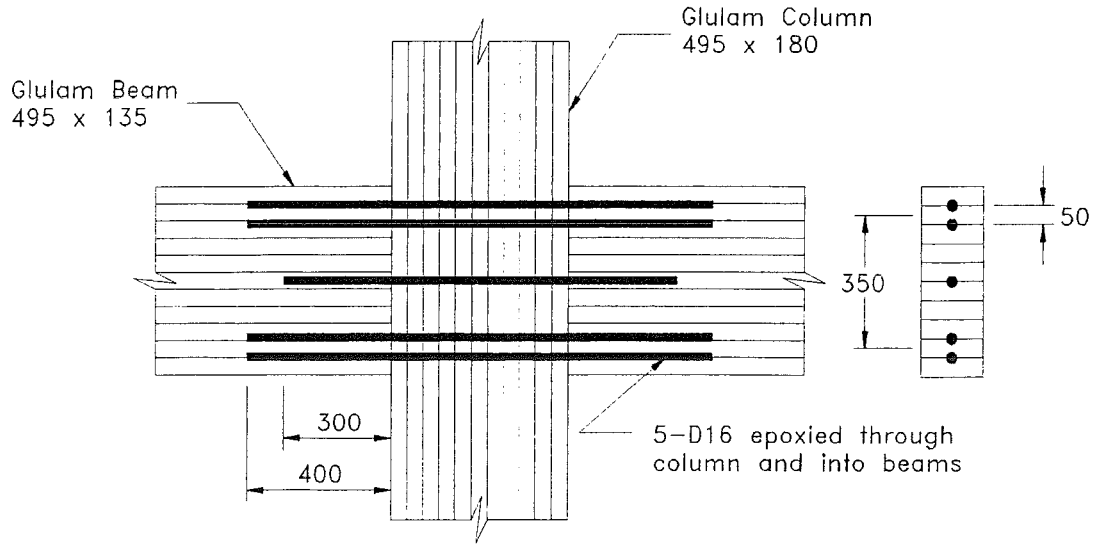

Figure 5.23 Arrangement of bars for Unit 8

5.2.4.1 DESCRIPTION OF FAILURE MODE

Initial wood failure began as a horizontal crack that started at the end of the south beam, at the same position as the inner bar. At the time the south beam cracked, the lateral load had almost reached a displacement ductility factor of +5, giving a moment of 76.1 kNm with the shear stresses in the column, beams and joint core being 0.9 MPa, 0.9 MPa and 4.2 MPa respectively. The flexural stresses in the column and beams were 10.1 MPa and 12.0 MPa respectively.

The specimen was then unloaded and cycled until a ductility level of -6. As the load increased, the crack continued to split the wood parallel to the grain. Once the crack had travelled the full beam length, the test was ended.

The maximum stresses reached in the connection were: 11.0 MPa bending stress in the column with an average shear stress of 4.6 MPa in the joint core. In the beams, the bending stress was 13.1 MPa with a shear stress of 1.0 MPa.

A photograph of the overall connection at the end of the test is shown in Figure 5.24. The failure pattern in the joint core is shown in Figure 5.25.

5.2.4.2 RESULTS

The initial stiffness for Unit 8 was 1.48 kN/mm. The load-deflection plot for Unit 8 is shown in Figure 5.26 and displays linear behaviour up first yield of the deformed bars. Excellent ductile behaviour the achieved up to a displacement ductility factor of ± 6 when the test was stopped due to beam cracking. The plot of the load versus the shear distortion of the joint core as a component of column deflection is shown in Figure 5.27. This graph shows relatively fat loops, indicating that bar yielding penetrated into the joint core.

The calculated components are shown in Figure 5.28 and Figure 5.29. Note that the asterisk indicates that the deflections were estimated at this point because the gauges measuring the displacements went off-scale.

Figure 5.24 Overall view of Unit 8 at the end of test

Figure 5.25 View of the joint region of Unit 8 at the end of the test

These graphs show three main points; the sliding shear component was large, shear distortion of the joint was small and the hinge rotation of the beams increased greatly due to yielding of the bars.

A comparison of the calculated and measured components of column deflections is shown in Figure 5.30. This graph shows that the calculated components have been underestimated for the ductility levels, but have good agreement during the elastic load levels.

5.2.4.3 DISCUSSION

The permissible shear and bending stresses permitted by NZS 3603:1981- Timber Design Code for No.1 framing glulam timber is 2.70 MPa and 15.9 MPa respectively (the basic shear and bending stresses are 1.8 MPa and 10.6 MPa, both multiplied by the short term duration of load factor, $K_1 = 1.5$).

Table 5.4 Minimum stresses in member at first cracking of Unit 8

Failure Mode	Shear Stress (MPa)	Flexural Stress (MPa)
Flexural cracks in beam	0.9	12.0

By refering to Table 5.4 which shows the stresses at first cracking of the beam, the shear and flexural stresses are not within the permisible design criteria. This suggests that the combination of moderate shear and flexural stresses in the beam ends may have overstressed the timber, resulting in failure.

After removing the wood covering the epoxied bars, it was discovered that the bar at which the crack formed, had very poor glue coverage. Poor bonding of the bar into the timber would have resulted in stress concentrations which probably caused premature failure in the timber.

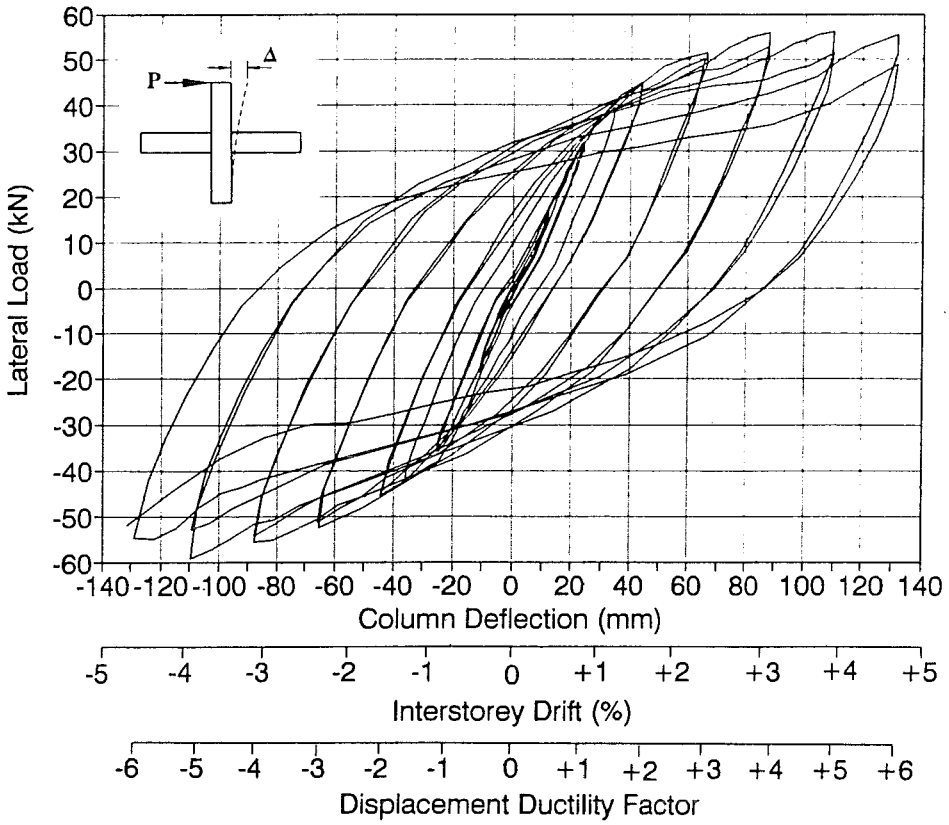

Figure 5.26 Load-deflection plot for Unit 8

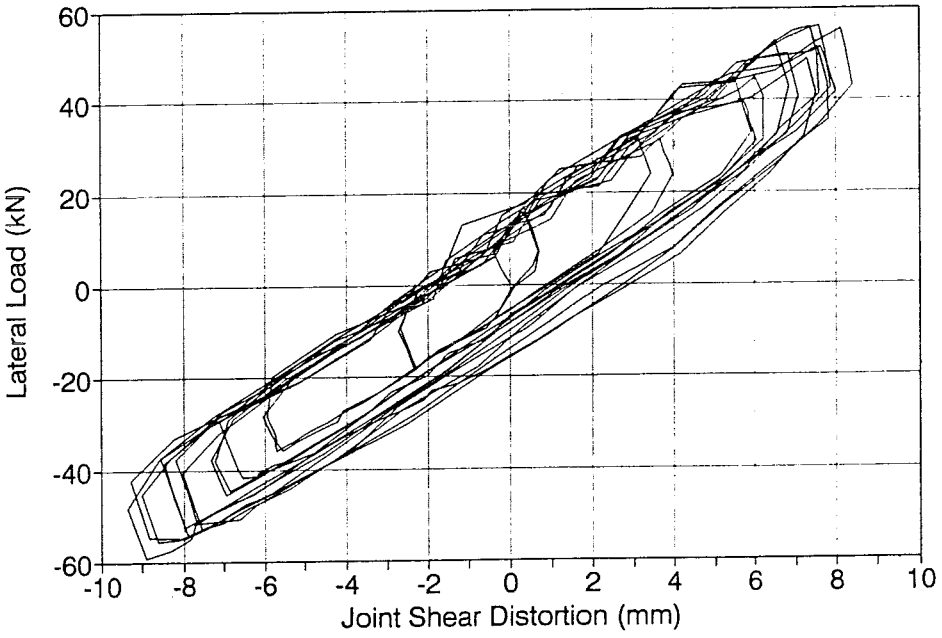

Figure 5.27 Load-joint shear distortion plot for Unit 8

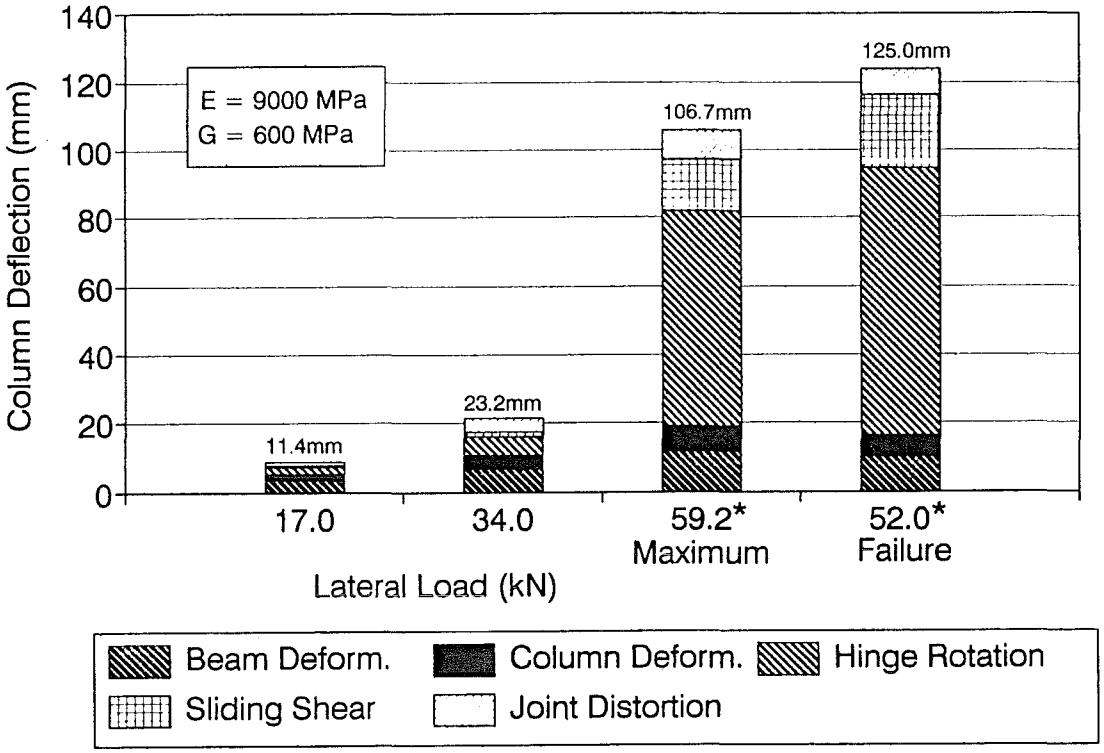

Figure 5.28 Calculated components of column deflection for Unit 8

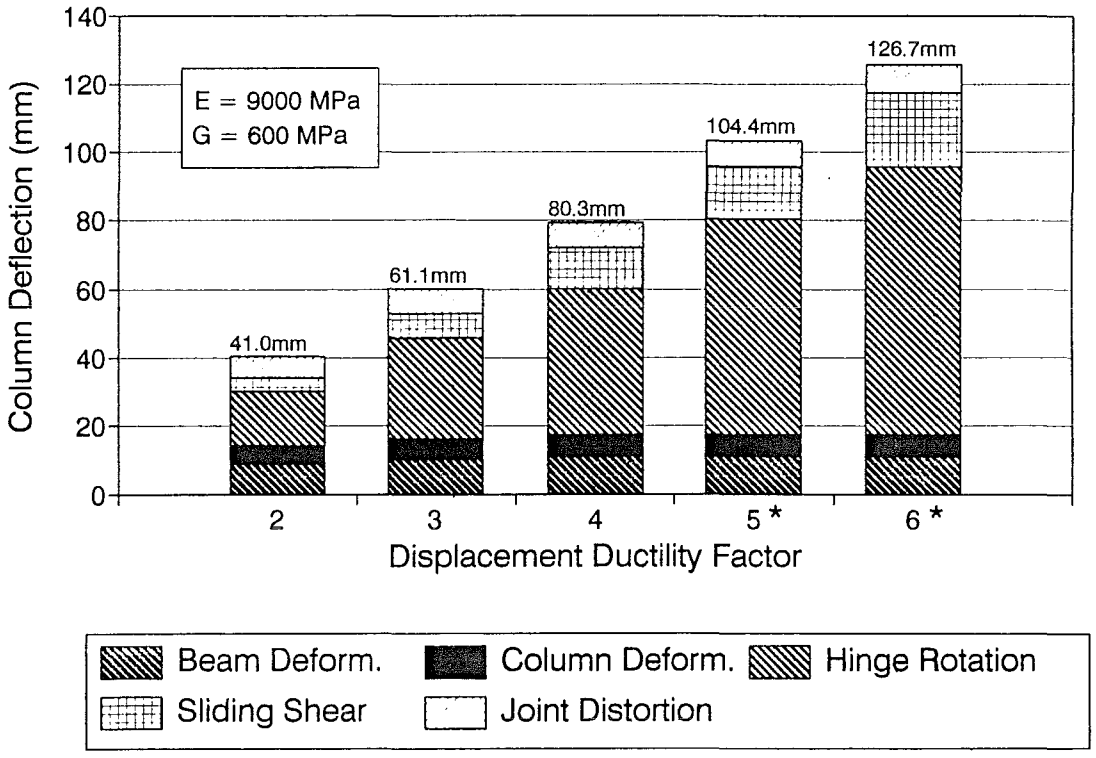

Figure 5.29 Calculated components of column deflection at ductility increments for Unit 8

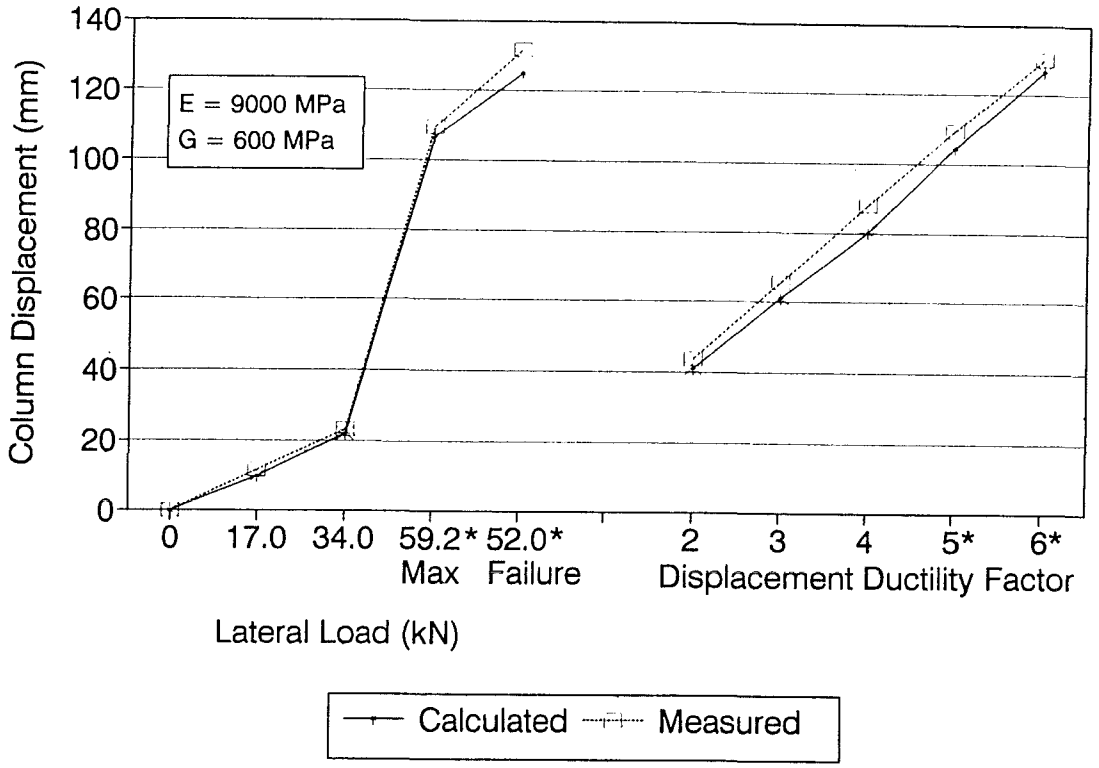

Figure 5.30 Comparision of calculated and measured column deflections for Unit 8

5.2.5 SUMMARY AND DISCUSSION OF RESULTS FOR TYPE A JOINTS

All of the connections were loaded to failure. Failure in every case was a wood failure in either the beams by flexure (Units 2 and 8) or in the joint region by flexure and shear (Units 1 and 3). No pullout of the epoxied steel bars occurred. Generally the stresses in the wood when the first crack appears, were below the code permissible values for No.1 framing grade radiata pine glue laminated timber. These low stresses are probably due to the very complex distribution of shear and bending stresses around the reinforcing bars. Poor bonding of the steel into the timber probably caused the wood failure in Unit 8.

A summary of the failure loads and stresses are shown in Table 5.5.

In all cases, the timber quality is of vital importance to the performance of the joint. Finger joints in the outer laminations of the timber should not be near the epoxied bars. Poor timber quality within the joint region probably caused early failure of Unit 3.

As shown in Table 5.5, the initial stiffnesses for the connections were all approximately the same.

Table 5.5 Summary of failure loads and stresses for joint type A

			UNIT 1	UNIT 2	UNIT 3	UNIT 8
Initial Stiffness		kN/mm	1.41	1.54	1.44	1.48
Failure Loads	**Lateral**	kN	60.8	67.9	49.2	52.0
	Moment	kNm	85.1	95.1	68.8	72.8
Flexural Stresses at failure	**Beam**	MPa	13.64	14.93	10.98	11.50
	Column		12.20	13.70	9.67	9.68
Shear Stresses at failure	**Beam**	MPa	1.01	1.13	0.81	0.86
	Column		1.05	1.17	0.84	0.87
	Joint		4.89	5.49	5.29	4.05
Maximum Column Deflection		mm	53.9	54.3	56.9	131.6
Maximum Interstorey Drift		%	1.93	1.94	2.03	4.70
Timber Failure Mode			Column Flexure & Joint Shear	Beam Flexure	Column Flexure & Joint Shear	Beam Flexure

Three different types of behaviour were seen: elastic, very limited ductility and ductile response. Unit 1 essentially behaved elastically up to failure, Units 2 and 3 showed some ductility (up to a ductility of 1.5) and Unit 8 exhibited excellent ductile behaviour (up to a ductility of 6).

The graphs showing the calculated components of column deflection display several interesting trends. The joint shear distortion was larger for Units 1 and 2 (which had all the bars at the top and bottom of the section) than Units 3 and 8 (which had steel spread down the section). This trend implies that bars spread down the section increased the shear stiffness of the joint, but did not increase the shear strength of the timber within the joint region.

Sliding shear of the beams was generally small; it slightly increased when the bars started to yield. This increase is due to "softening" of the bars during yielding, making them less effective at transferring shear by dowel action. In Unit 8, the sliding shear component was significant. The reason for the larger sliding shear deformations in Unit 8 could be attributed to two items:

- considerably more yielding of the bars than in previous tests
- a change in the way the bars transfer shear across the joint

The only difference between Unit 8 and previous units was that the reinforcing bars were debonded over a distance of 20mm each side of the beam-column face. By debonding the bars, the mechanism of transfering shear across the beam-column interface changed from shear to flexure of the reinforcement. In the early tests, the shear force acted over a small distance, whereas for Unit 8, the shear force acted over a much larger distance, causing flexure of the reinforcing bars. The two mechanisms are shown in Figure 5.31.

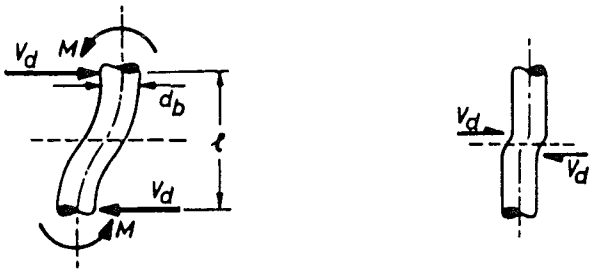

(a) Flexure (b) Shear

Figure 5.31 Mechanism of dowel action across a shear interface (Park and Paulay, 1975)

Park and Paulay (1975) give equations for the dowel strength across a shear plane, where the associated shear force V_d is expressed in terms of the yield strength of the bar. For dowel action by flexure, the shear force is

$$V_d = \frac{4d_b}{3\pi}\frac{A_s f_y}{1} = 0.17A_s f_y \qquad (5.1)$$

and for shear across the bars

$$V_d = \frac{A_s f_y}{\sqrt{3}} = 0.58A_s f_y \qquad (5.2)$$

where d_b = bar diameter = 16mm

1 = debonded length of bar = 80mm

From (5.1) and (5.2) it can be seen that transferring shear across the beam-column interface by shear in the bars is more effective than by flexure of the bars.

The amount of hinge rotation increased as the amount of yielding increased.

The yield load and displacement were predicted reasonably accurately by the method used in section 4.4. A summary of the calculations is shown in Table 5.6.

Table 5.6 Summary of calculated and predicted yield loads and deflections

		UNIT 2	UNIT 3	UNIT 8
Theoretical yield load, P'_y	kN	66.0	53.0	33.0
Theoretical yield deflection, Δ'_y	mm	43.0	36.7	22.7
Measured yield load, P_y	kN	61.0	54.5	31.5
Measured yield deflection, Δ_y	mm	36.0	36.5	22.0
Maximum Ductility, μ		1.5	1.6	6

5.3 JOINT TYPE B

Two tests were completed using a prefabricated structural steel hub and epoxied steel dowels embedded in the ends of the beams and columns. These tests were almost identical, the only difference was the plate thickness of the beam flanges in the steel hub. Unit 4 used heavy flange plates, resulting in elastic behaviour. The next test used a lighter beam flange to obtain ductile behaviour by inelastic buckling of the flanges.

To reduce the number of different deflection components shown on the graphs, the flexural and shear deformations have been summed together for the columns and beams and put into two categories; beam and column deformations. The contributions of the flexural and shear deformations to the total beam deformation can be taken as 65% for flexure and 35% for shear respectively. The contributions of the flexural and shear deformations to the total column deformation can be taken as 46% for flexure and 54% for shear respectively.

The arrangement of reinforcing bars for Units 4 and 5 are shown in Figure 5.32. Reinforcement consists of thirty-two 3/4" BSW high strength threaded rods epoxied into 26mm holes drilled into the outer laminations at both the top and bottom of the glulam beams and columns.

Details of the structural steel hub are shown in Figure 5.33. The thicknesses of the web and flange plates for Units 4 and 5 are shown in Table 5.7.

Table 5.7 Dimensions of steel hub

	Unit 4	Unit 5
T (mm)	10	10
t (mm)	10	8

The column flanges were intentionally made stronger (to prevent yielding) than the beam flanges by welding transverse stiffeners to the flanges. This ensures a strong-column weak beam arrangement. It is undesirable to have yielding of the column flanges as a column sidesway mechanism may form. All yielding was detailed to occur in the beam flanges.

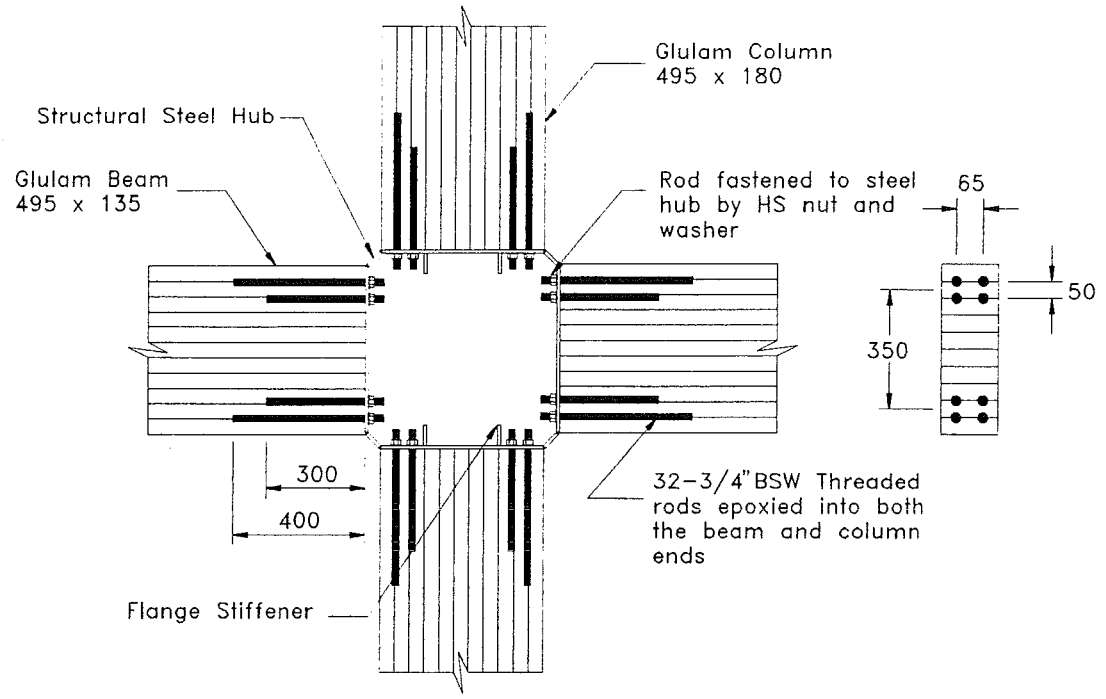

Figure 5.32 Arrangement of bars for Units 4 and 5

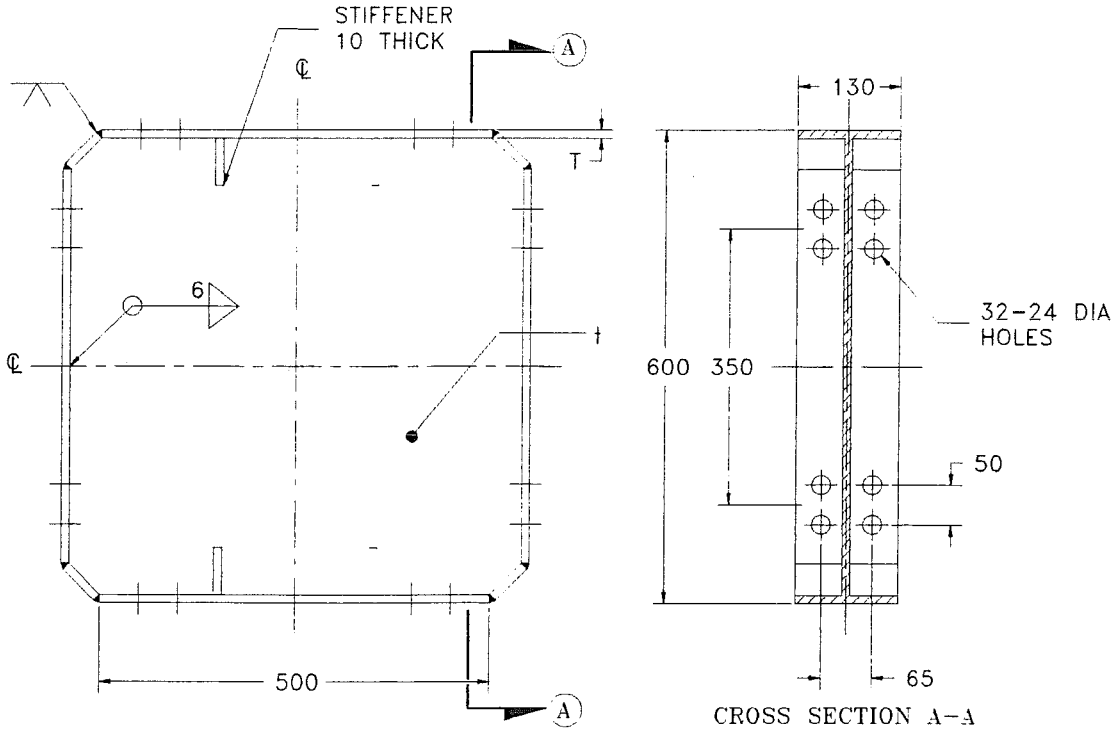

Figure 5.33 Detail of Structural Steel Hub

5.3.1 UNIT 4

5.3.1.1 DESCRIPTION OF FAILURE MODE

Initial wood failure began as a vertical crack that started at the top of the lower column, at the north inner bar. At the time the lower column cracked, the unit was being unloaded back to zero load, after reaching the target load in the negative direction. The shear stresses in the columns and beams were 1.1 MPa and 1.1 MPa respectively with flexural stresses in the column and beams being 9.1 MPa and 13.5 MPa respectively.

The specimen was then unloaded back to zero load and reloaded in the positive direction. As the lateral load increased, another crack formed in the lower column at the south inner bar. When the crack developed, the shear stresses in the columns and beams were 1.2 MPa and 1.2 MPa respectively with flexural stresses in the column and beams being 10.1 MPa and 14.9 MPa respectively. As the load increased to the target load, the crack continued to split the wood parallel to the grain.

The specimen was then unloaded back to zero load and reloaded in the negative direction. As the lateral load increased, the first crack continued to split the wood parallel to the grain. At a moment of 70.8 kNm, the lower column failed by flexure due to a wood failure around the tension bars.

The maximum stresses reached in the connection were: 10.9 MPa bending stress in the column with a shear stress of 1.3 MPa. In the beams, the bending stress was 16.1 MPa with a shear stress of 1.3 MPa.

A photograph of the overall connection at the end of the test is shown in Figure 5.34. The failure mode of the lower column is shown in Figure 5.35.

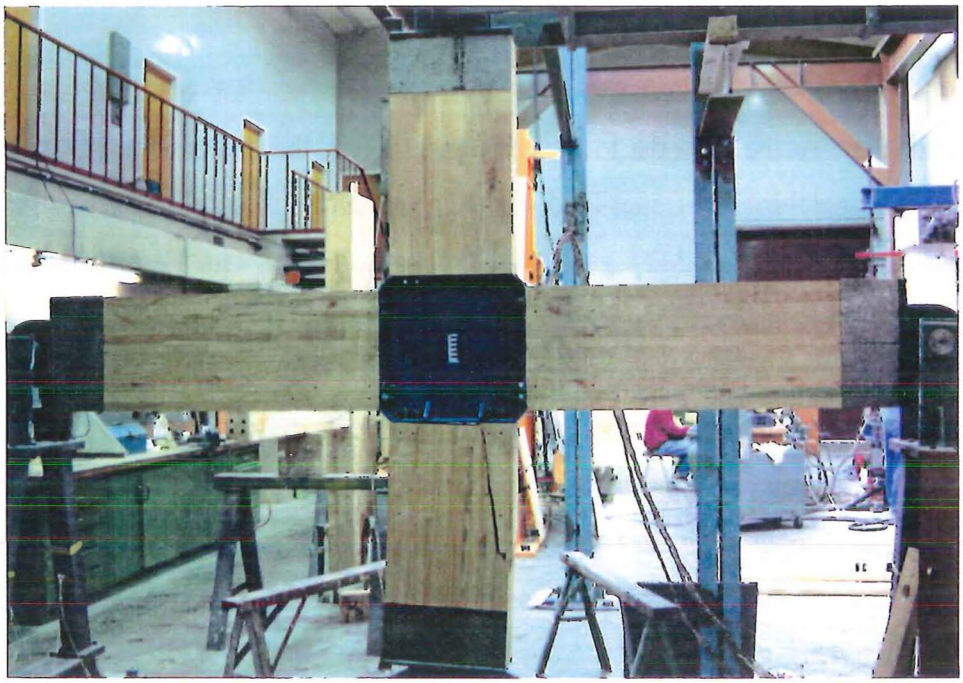

Figure 5.34 Overall view of Unit 4 at the end of test

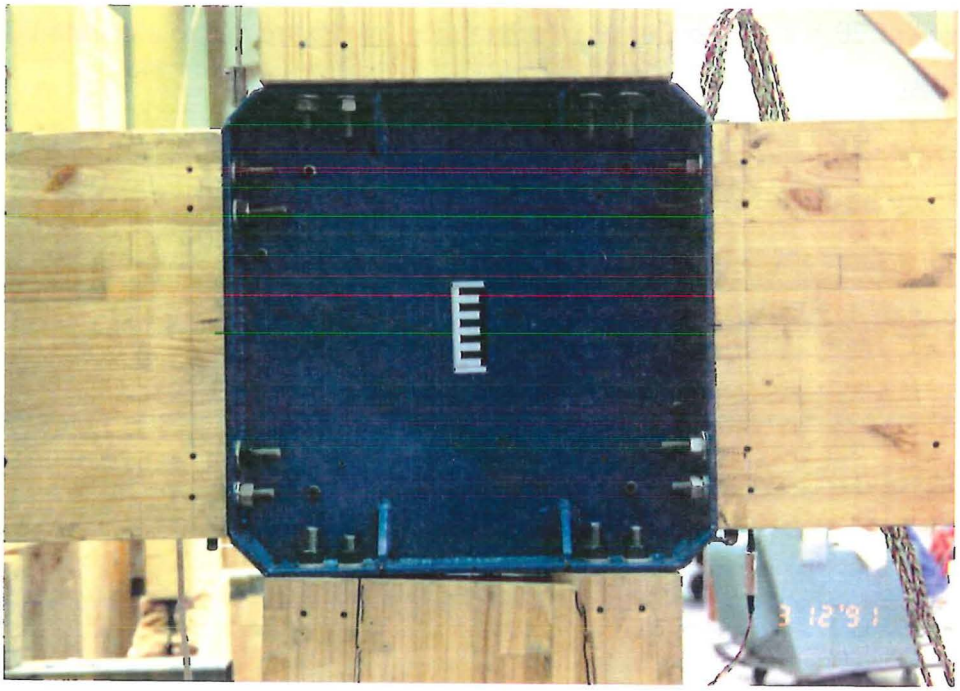

Figure 5.35 View of the joint region of Unit 4 at the end of the test

5.3.1.2 RESULTS

The initial stiffness of Unit 4 was 2.67 kN/mm. The load-deflection plot for Unit 4 is shown in Figure 5.36 and displays linear behaviour up to the wood failure in the lower column.

The calculated components of column deflection are shown in Figure 5.37. Note that the column sliding shear component had to be estimated, since no gauges were placed to measure the sliding shear at the column-joint face. The graph shows the total sliding shear component due to both the columns and beams. These graphs show several points; the sliding shear component was generally small, the hinge rotation of the beams and columns was large, the beam and column deformations were substantial and there was no component of column deflection due shear distortion of the joint.

A comparison of the calculated and measured components of column deflections is shown in Figure 5.38. This graph shows that the calculated column deflection was higher than the measured deflection.

5.3.1.3 DISCUSSION

By referring to Table 5.8 which shows the stresses at first cracking of the column, the shear and flexural stresses are not within the permissible design criteria. This suggests that the combination of moderate shear and flexural stresses in the column may have overstressed the timber, resulting in failure.

Table 5.8 Minimum stresses in member at first cracking of Unit 4

Failure Mode	Shear Stress (MPa)	Flexural Stress (MPa)
Flexural cracks in lower column	1.1	9.1

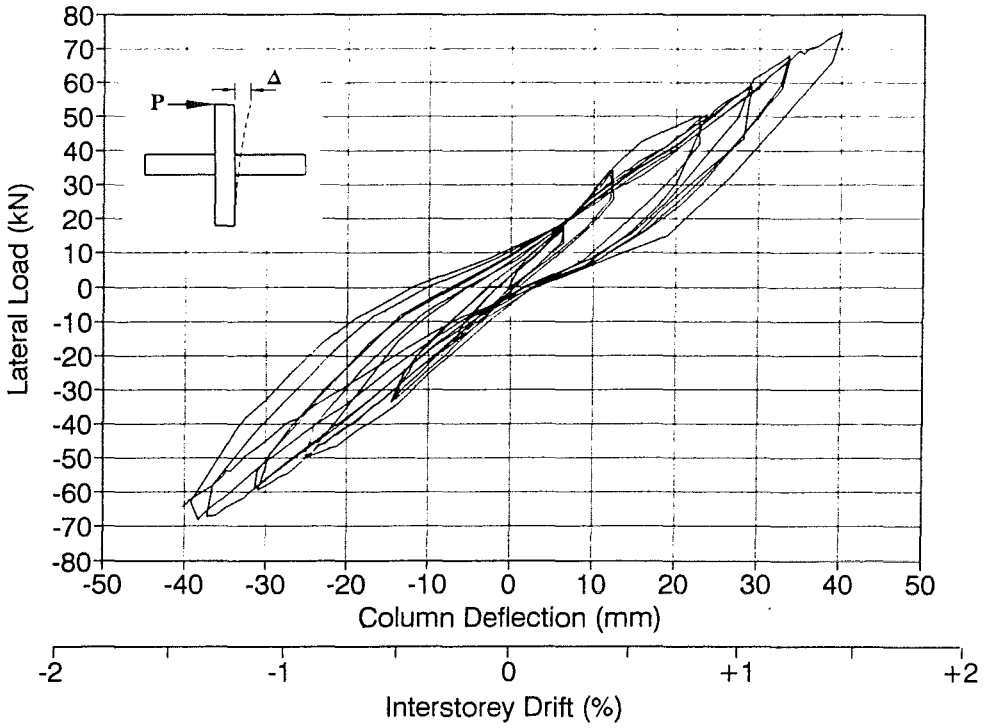

Figure 5.36 Load-deflection plot for Unit 4

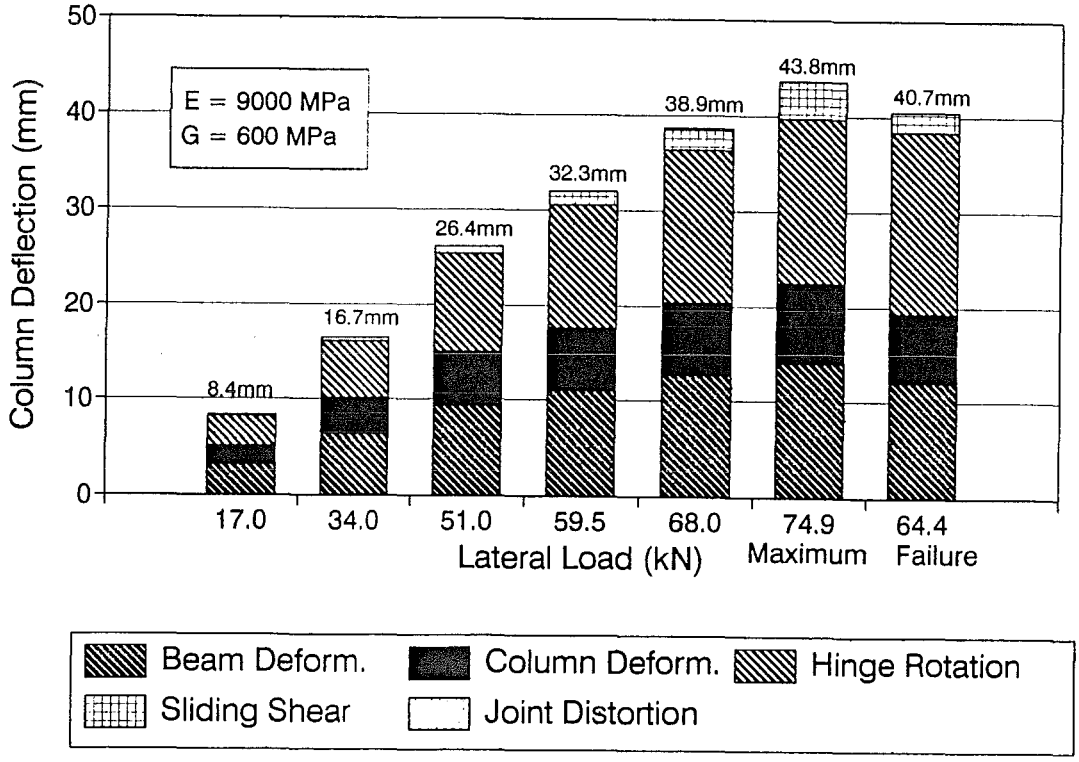

Figure 5.37 Calculated components of column deflection for Unit 4

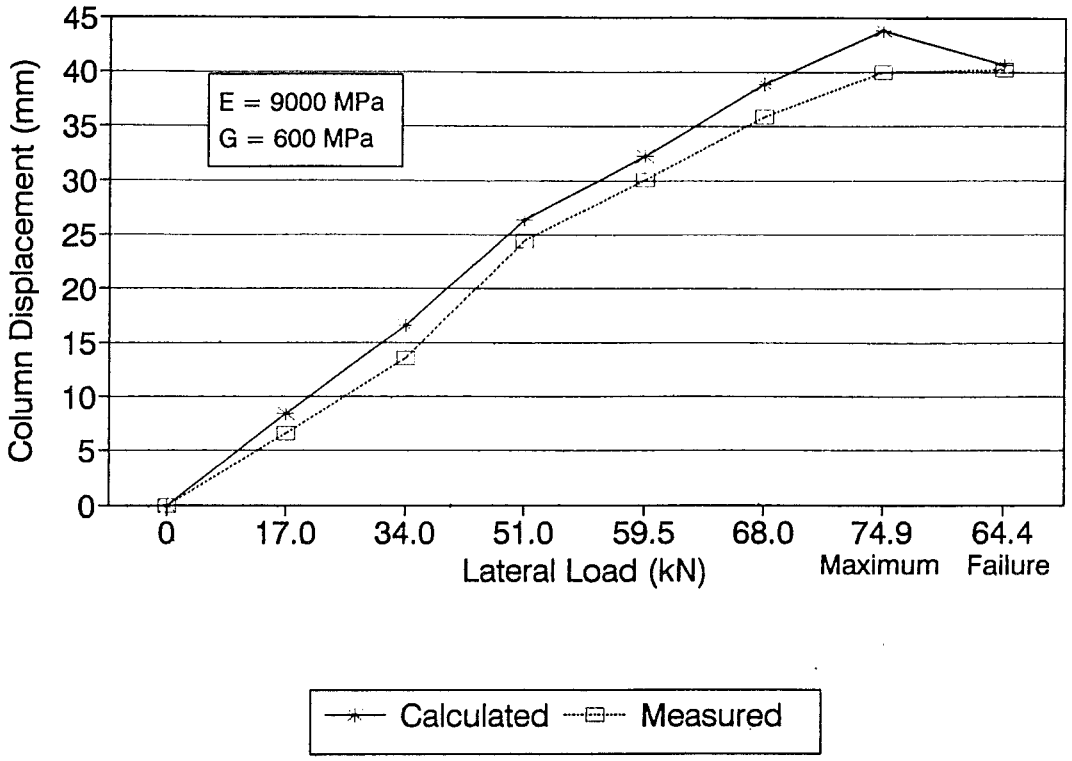

Figure 5.38 Comparision of calculated and measured column deflections for Unit 4

5.3.2 UNIT 5

5.3.2.1 DESCRIPTION OF FAILURE MODE

Initial wood failure began as a vertical crack that started at the top of the lower column, at the south inner bar. At the time the lower column cracked, the unit had just reached the target load in the positive direction. The shear stresses in the columns and beams were 1.1 MPa and 1.1 MPa respectively with flexural stresses in the column and beams being 9.6 MPa and 14.2 MPa respectively.

The specimen was then unloaded back to zero load and reloaded in the negative direction. As the lateral load increased, another crack formed in the lower column at the north inner bar. When the crack developed, the shear stresses in the columns and beams were 1.2 MPa and 1.2 MPa respectively with flexural stresses in the column and beams being 10.6 MPa and 15.6 MPa respectively. As the load increased to the target load, the crack continued to split the wood parallel to the grain.

Several more cycles were completed at higher load levels; each time the cracks continued to split the wood parallel to the grain. As the lateral load increased on the negative direction, the second crack continued to split the wood parallel to the grain. When the crack had travelled the full length of the lower column, the test was ended.

The maximum stresses reached in the connection were: 11.8 MPa bending stress in the column with a shear stress of 1.4 MPa. In the beams, the bending stress was 17.5 MPa with a shear stress of 1.4 MPa.

A photograph of the overall connection at the end of the test is shown in Figure 5.39. The failure mode of the lower column is shown in Figure 5.40.

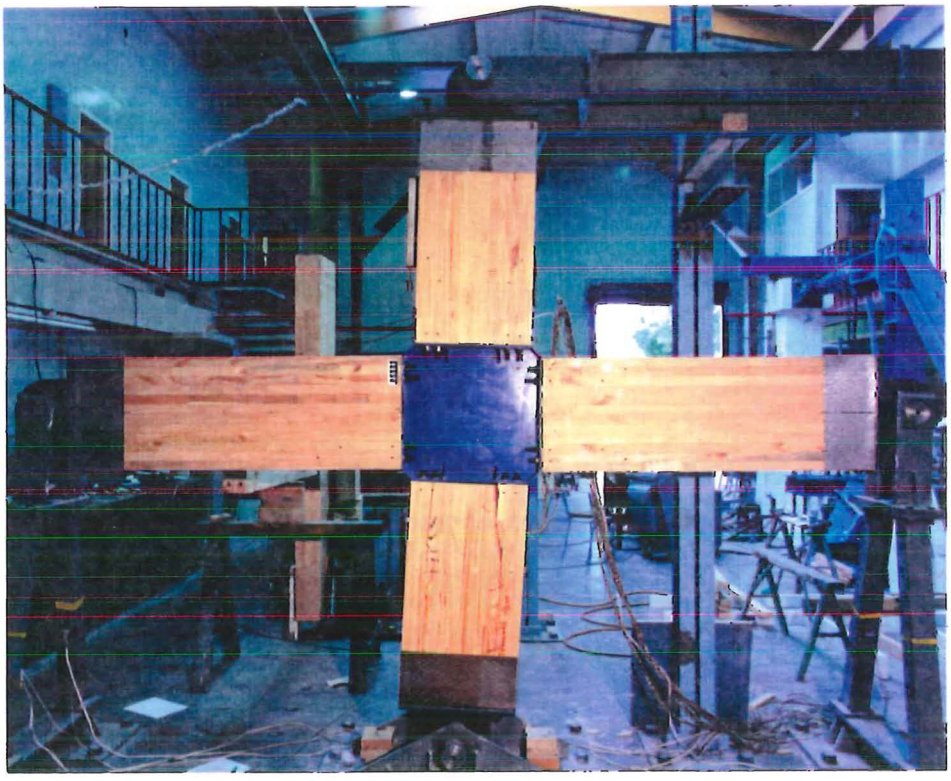

Figure 5.39 Overall view of Unit 5 at the end of test

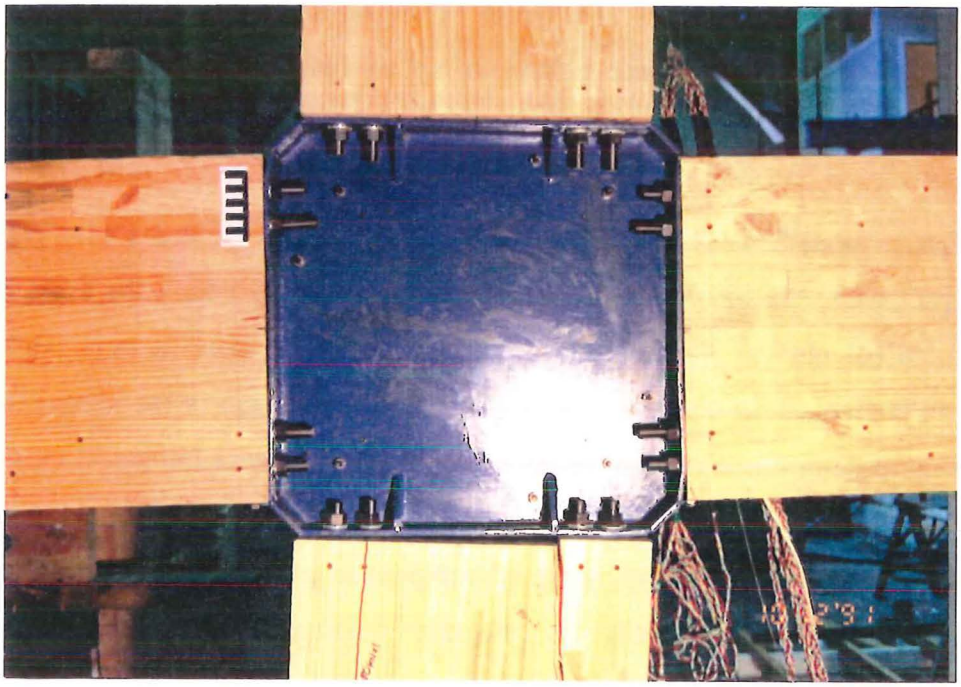

Figure 5.40 View of the joint region of Unit 5 at the end of the test

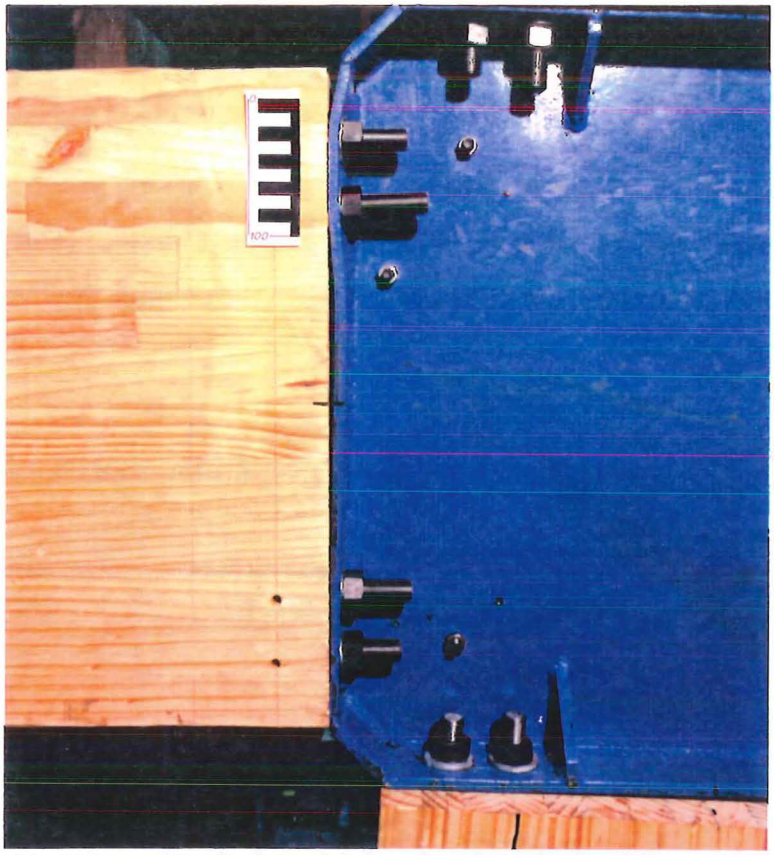

Figure 5.41 View of Unit 5 steel joint showing the buckling of the beam flanges

5.3.2.2 RESULTS

The initial stiffness of unit 5 was 2.11 kN/mm. The load-deflection plot for Unit 5 is shown in Figure 5.42 and displays linear behaviour up to first yielding of the flange plates. Thereafter, several pinched hysteresis loops can be seen.

The calculated components of column deflection are shown in Figure 5.44. These graphs show several trends; the sliding shear component was generally small, the hinge rotation of the beams and columns was large, the beam and column deformations were substantial and there was no component of column deflection due shear distortion of the joint. There was a significant increase in hinge rotation of the beams and columns at failure.

A comparison of the calculated and measured components of column deflections is shown in Figure 5.43. This graph shows that the calculated column deflection was higher than the measured deflection.

5.3.2.3 DISCUSSION

By referring to Table 5.9 which shows the stresses at first cracking of the beam, the shear and flexural stresses are not within the permissible design criteria. This suggests that the combination of moderate shear and flexural stresses in the column may have overstressed the timber, resulting in failure.

Table 5.9 Minimum stresses in member at first cracking of Unit 5

Failure Mode	Shear Stress (MPa)	Flexural Stress (MPa)
Flexural cracks in lower column	1.1	9.6

The behaviour of the connection changed when the high strength washers were replaced with mild steel washers. The high strength washers locally increased the stiffness of the flange

plates around the bolt holes, increasing the yield strength of the plate. This made the beam flanges too strong; the timber failed before the flanges could reach the yield load.

For most of the test, high strength washers were used, hence the connection showed elastic behaviour up to first cracking of the timber. After the first crack, the steel washers were changed. Consequently, the flanges started to yield in tension around the bolt groups, resulting in ductile behaviour.

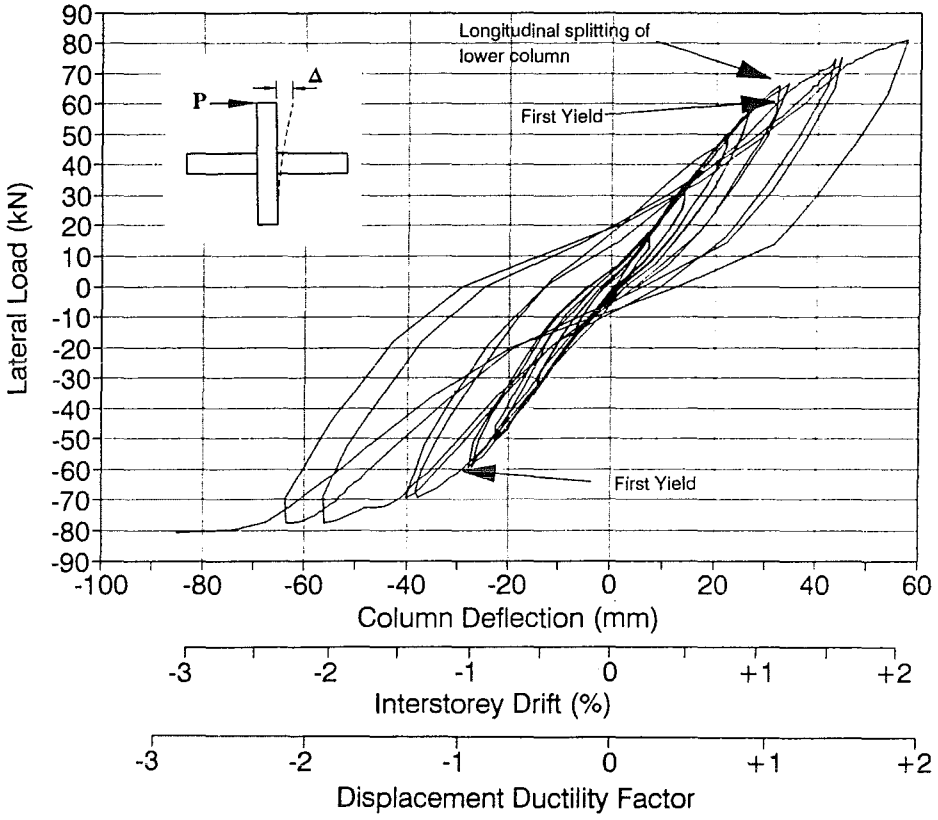

Figure 5.42 Load-deflection plot for Unit 5

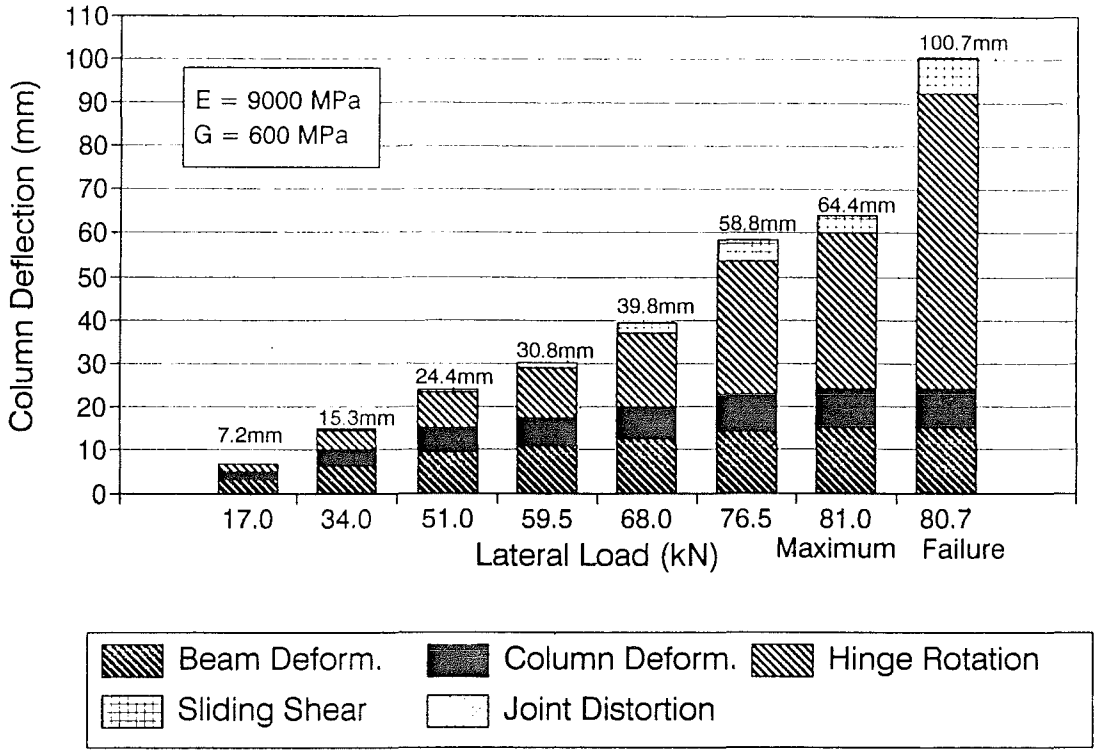

Figure 5.43 Calculated components of column deflection for Unit 5

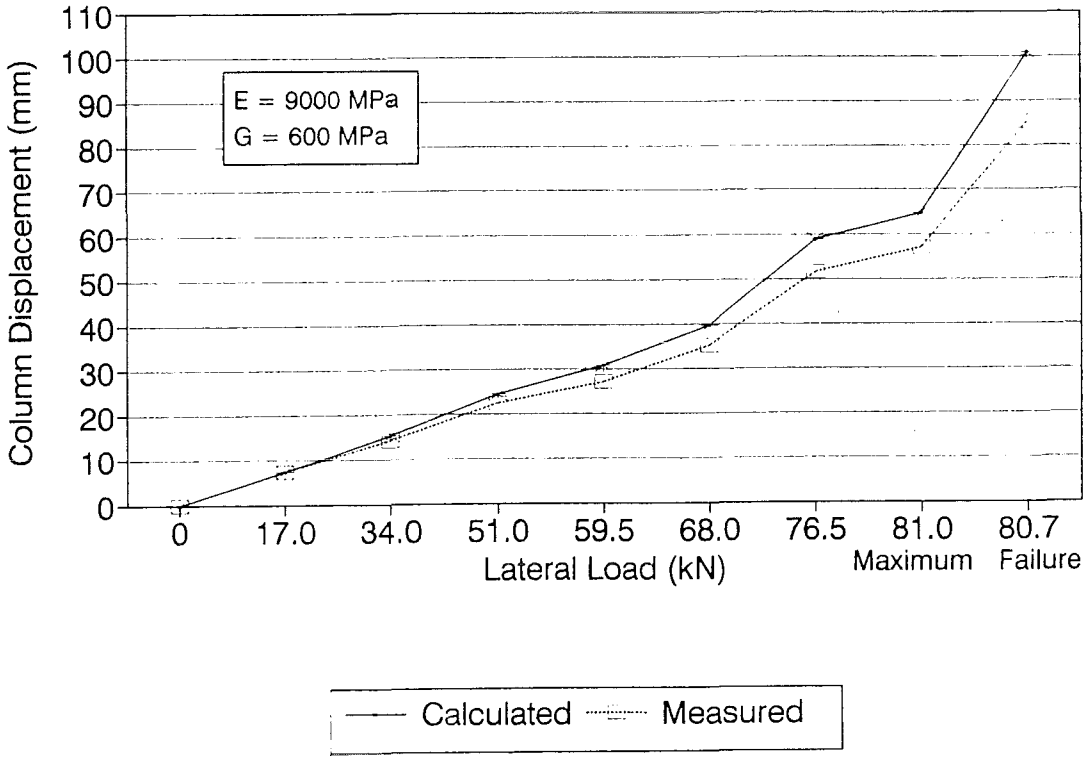

Figure 5.44 Comparision of calculated and measured column deflections for Unit 5

5.3.3 SUMMARY AND DISCUSSION OF RESULTS FOR TYPE B JOINTS

Both of the connections were loaded to failure. Failure in both cases consisted of longitudinal splitting of the wood along the grain of the lower column. No pullout of the epoxied steel bars from the timber occurred. In Unit 4, the bars and the surrounding wood were pulled out. Generally the stresses in the wood when the first crack appears, were below the code permissible values for No.1 framing grade radiata pine glue laminated timber. These low timber stresses were probably due the effect of sliding shear on the bolt groups, and/or to the complex stress distribution around the bars.

A summary of failure loads and stresses are shown in Table 5.10.

As shown in Table 5.10, the initial stiffness of the two connections varied; Unit 4 was much stiffer than Unit 5. This variation is probably due to the thickness of the beam flanges to which the timber members were attached; Unit 4 had 10mm thick beam flanges and Unit 5 had 8mm thick beam flanges.

Two different types of behaviour were seen: elastic and limited ductile behaviour. Unit 4 behaved elastically up to failure and Unit 5 showed limited ductility (up to a displacement ductility of 2).

The behaviour of the connection changed when the high strength washers were replaced with mild steel washers. The high strength washers locally increased the stiffness of the flange plates around the bolt holes, increasing the yield strength of the plate. This made the beam flanges too strong; the timber failed before the flanges could reach the yield load.

Unit 5 may have given a better result if the washers had been changed before the formation of the first crack.

The graphs showing the calculated components of column deflection displayed similar trends. There was no component of column deflection due to shear distortion of the joint; the steel web was very rigid. The beam and column deformations were similar for both cases and so

was the sliding shear component. The hinge deformations were of similar sizes up to first yield in Unit 5. Thereafter for Unit 5, the hinge deformations became larger than for Unit 4.

Table 5.10 Summary of failure loads and stresses for joint type B

			UNIT 4	UNIT 5
Initial Stiffness		kN/mm	2.67	2.11
Failure Loads	**Lateral**	kN	64.4	80.7
	Moment	kNm	70.8	88.8
Flexural Stresses at failure	**Beam**	MPa	13.9	17.4
	Column		9.4	11.8
Shear Stresses at failure	**Beam**	MPa	1.1	1.4
	Column		1.1	1.3
Column Deflection at failure		mm	40.2	85.2
Interstorey Drift at failure		%	1.44	3.04
Failure Mode			Column flexure	Column flexure

The combination of flexure, shear and sliding of the columns may have caused the splitting failures seen in both connections. In both tests, the column was sliding 4mm with respect to the steel joint. If the column shear is transferred using dowel action of the bars, each bar acts as a cantilever bearing into the wood, and anchored by a compression strut. In figure Figure 5.45, all the bars transfer the shear equally. The compression region is much larger, therefore lower stresses result in the timber and no failure occurs.

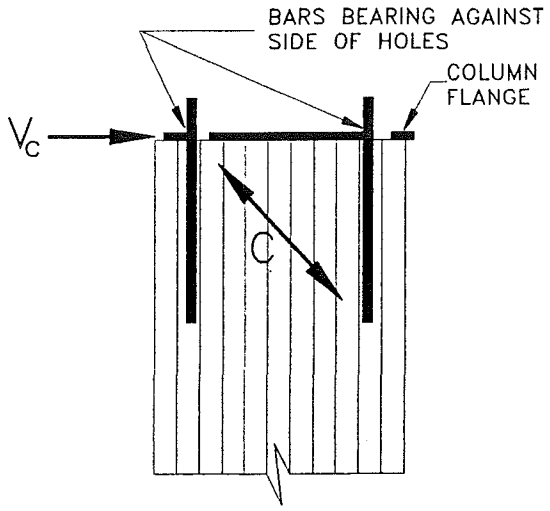

Figure 5.45 Bars bearing on all the bolt holes

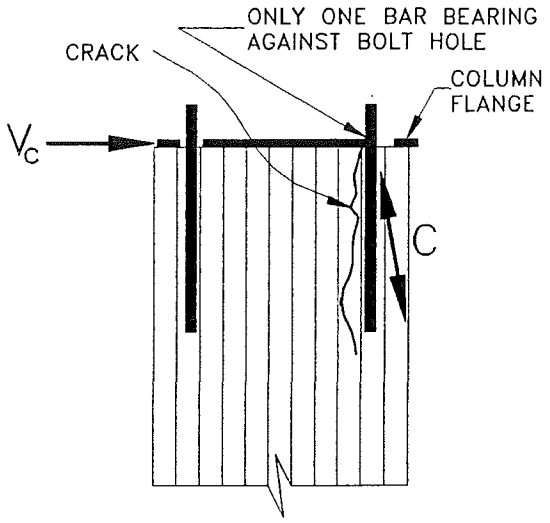

Figure 5.46 The worst case - only a few bars are bearing against the bolt holes

In the worst case, only a few bars may be bearing up against the holes in the steel plate hence the shear will be transferred by only those few bars. If those bars are situated at end of the timber, as shown in Figure 5.46, a compression strut forms between the bars and the edge of the timber. This compression strut is ineffective since there is nothing to resist it, hence the timber in tension attempts to transfer the load. As timber is much weaker in tension than compression, the timber fails and a longitudinal crack forms along the bar.

To prevent splitting of the timber along the grain for epoxied bolts subjected to lateral load, Riberholt (1988b) recommends that a plywood sleeve be glued to the end grain of the timber. Otherwise (5.3) must be satisfied.

$$F < \frac{2}{3} b_e t f_v \qquad (5.3)$$

Where F is the lateral force on a bolt group, b_e is the distance from the loaded edge to the furthest bolt, t is the thickness of the member and f_v is the permissible shear strength of the timber.

5.4 JOINT TYPE C

Two tests were completed using epoxied steel dowels embedded in the ends of the beams and through the columns. These tests had the same overall geometry, the only difference was in the side bracket plates. Unit 6 used a thin flange to get ductile behaviour by inelastic buckling of the flanges. Unit 7 used a thin web and rigid end plates to obtain ductile shear yielding of the web.

To reduce the number of different deflection components shown on the graphs, the flexural and shear deformations have been summed together for the columns and beams and put into two categories; beam and column deformations. The contributions of the flexural and shear deformations to the total beam deformation can be taken as 62% for flexure and 38% for shear respectively. The contributions of the flexural and shear deformations to the total column deformation can be taken as 48% for flexure and 52% for shear respectively.

The arrangement of reinforcing bars for Units 6 and 7 are shown in Figure 5.48. Reinforcement consists of twenty-four 3/4" BSW high strength threaded rods epoxied into 26mm holes drilled into the outer laminations at both the top and bottom of the glulam beam ends.

Details of the structural steel side brackets are shown in Figure 5.47. The thicknesses of the web and flange plates are shown in Table 5.11.

A capacity design approach was used to design the connection. For Unit 6, the web was deliberately made stronger (to prevent web yielding) than the beam flanges. The timber members were also designed to be stronger than the beam flanges. All yielding was detailed to occur in the flanges of the side bracket.

For Unit 7, the web was the weak element and not the flanges. The beam flanges were made stronger than the web. As with Unit 6, the timber members were designed to be stronger than the web. Since the shear forces acting on the steel web were small, a very thin web plate was needed to achieve shear yielding. Very thin plates are prone to buckling before the yield load

is reached in the section. To prevent this, several lateral restraints in the form of 50 x 50 x 3 angles were welded to the web. Welding the thin plate to the flanges caused distortion of the web.

Table 5.11 Dimensions of side brackets

	Unit 6	Unit 7
D (mm)	24	22
T (mm)	6	10
t (mm)	10	1

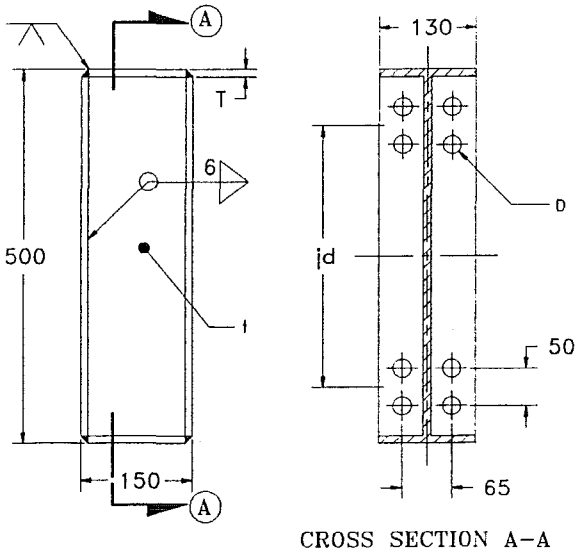

Figure 5.47 Detail of structural steel side bracket

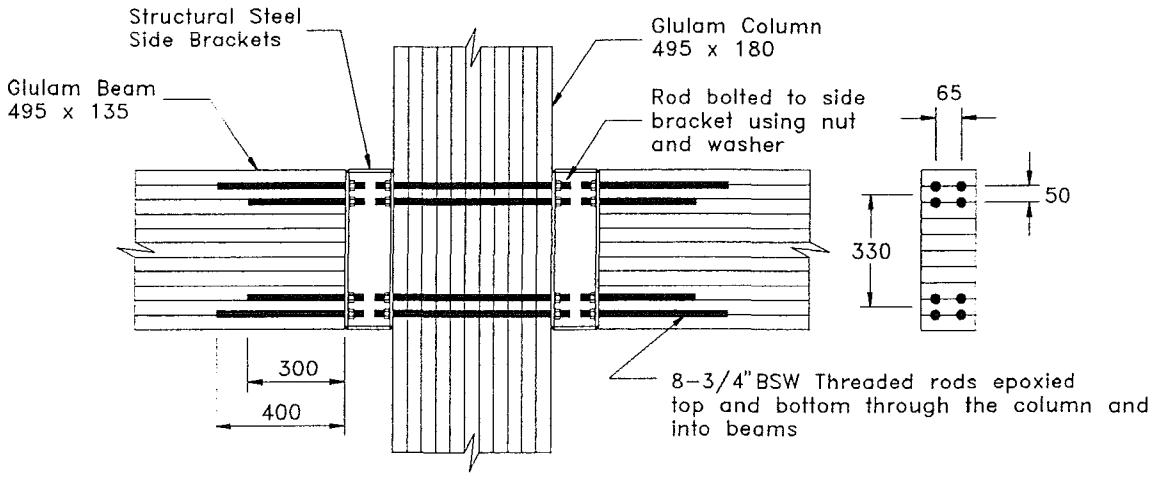

Figure 5.48 Arrangement of steel side brackets and bars for Units 6 & 7

5.4.1 UNIT 6

5.4.1.1 DESCRIPTION OF FAILURE MODE

Failure in this test was a steel failure and not a timber member failure. After the beam flanges yielded around the bolt groups, the specimen was subjected to increasing displacements, giving displacement ductilities of 2, 4, 6 and 8. As the ductility increased, the amount of yielding in the flanges increased, resulting in extensive flange deflections (up to 16mm) at a constant load. At a ductility of 4, the flanges were yielding in both compression and tension with some timber crushing happening where the side brackets were being pushed into the column. At a ductility of 6, the welds connecting the flanges to the web began to deteriorate. Several welds failed at the web-flange junction, just below the bolt group. The weld failures were not catastrophic. After a ductility of 8 was reached, the test was ended.

A photograph of the overall connection at the end of the test is shown in Figure 5.49. Details of the side brackets at the end of test are shown in Figure 5.50 and a close up of the damage to the flanges around the bolt group is shown in Figure 5.51.

5.4.1.2 RESULTS

The initial stiffness for Unit 6 was 1.41 kN/mm. The load-deflection plot for Unit 6 is shown in Figure 5.52 and displays linear behaviour up to first yield of the flange plates. Excellent ductile behaviour is achieved up to a displacement ductility of $\pm$ 8. The hysteresis loops are relatively fat, although they have a "pinched" shape. This shape is due the clearances of the bolt holes and the side plates crushing the timber in the column. The plot of the load versus the joint shear distortion as a component of column deflection is shown in Figure 5.53. This graph shows linear behaviour up to the end of the test.

The calculated components of column deflection are shown in Figure 5.54 and Figure 5.55. Note that the asterisk in Figure 5.54 and Figure 5.56 indicates that the hinge rotation of the beams was estimated since the gauges measuring this deformation went offscale.

Figure 5.49 Overall view of Unit 6 at the end of test

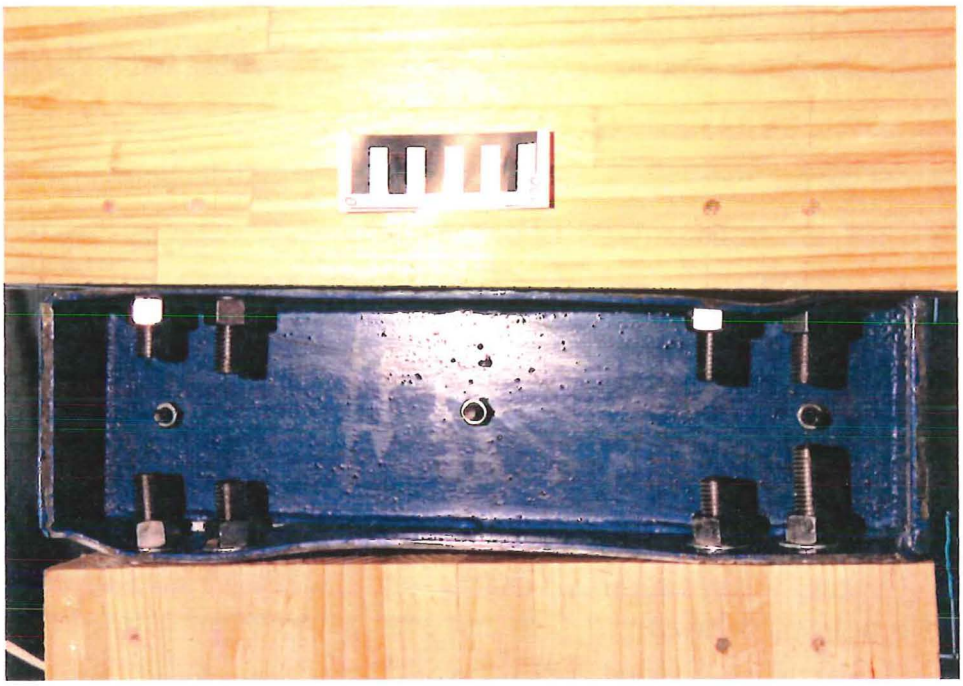

Figure 5.50 View of the joint region of Unit 6 at the end of the test

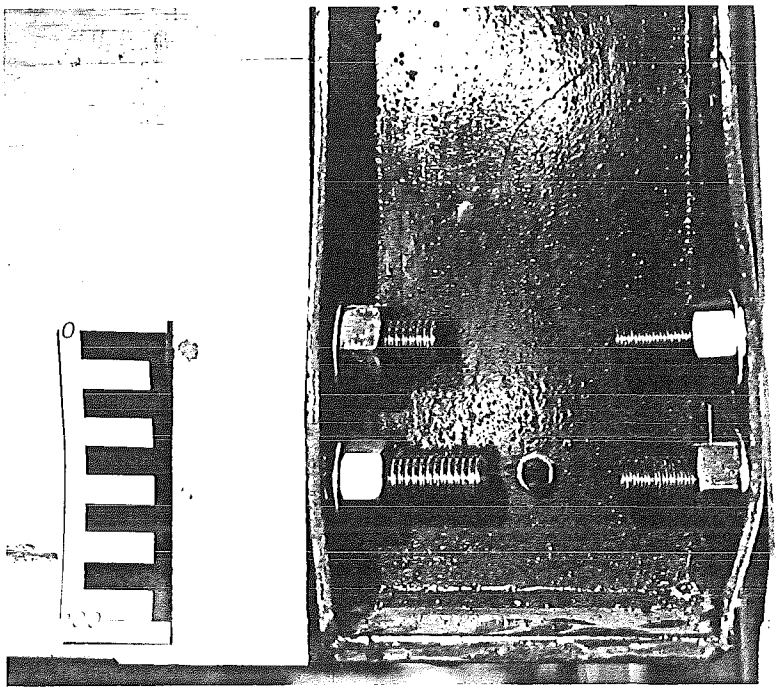

Figure 5.51 View of Unit 6 joint region showing the buckling of the beam flanges

These graphs show two main trends: the deformations due to joint distortion, bean column deformations and sliding shear are all about the same size; the deformations al mentioned are small compared to the deformations due to hinge rotation of the beams the deformations due hinge rotation increase linearly as the ductility factor increases.

A comparison of the calculated and measured components of column deflections is sho Figure 5.56. This graph shows that the calculated components are in good agreement the overall measured deflection, except at a ductility of 8, where the calculated deform underestimate the actual deflection. This inaccuracy was probably due to the estimation for the hinge rotation at this level.

5.4.1.3 DISCUSSION

This type of connection behaved very well and exhibited excellent ductile behaviour capacity design procedure could be used for this type of connection. No wood fa occurred as the stresses within the joint region never reached a critical level.

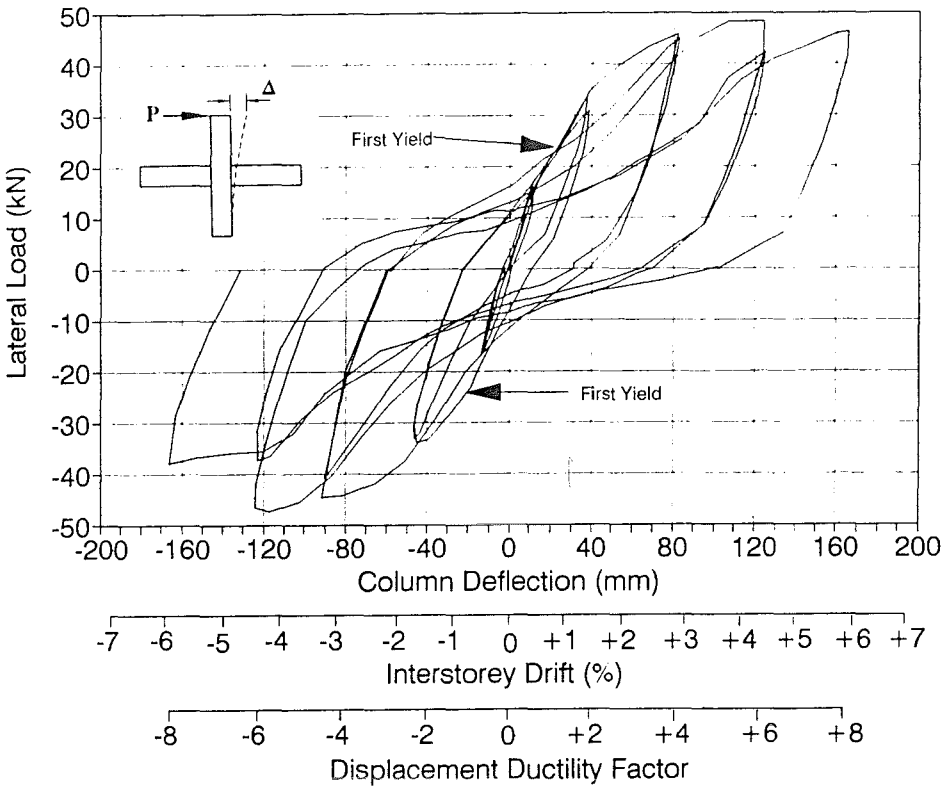

Figure 5.52 Load-deflection plot for Unit 6

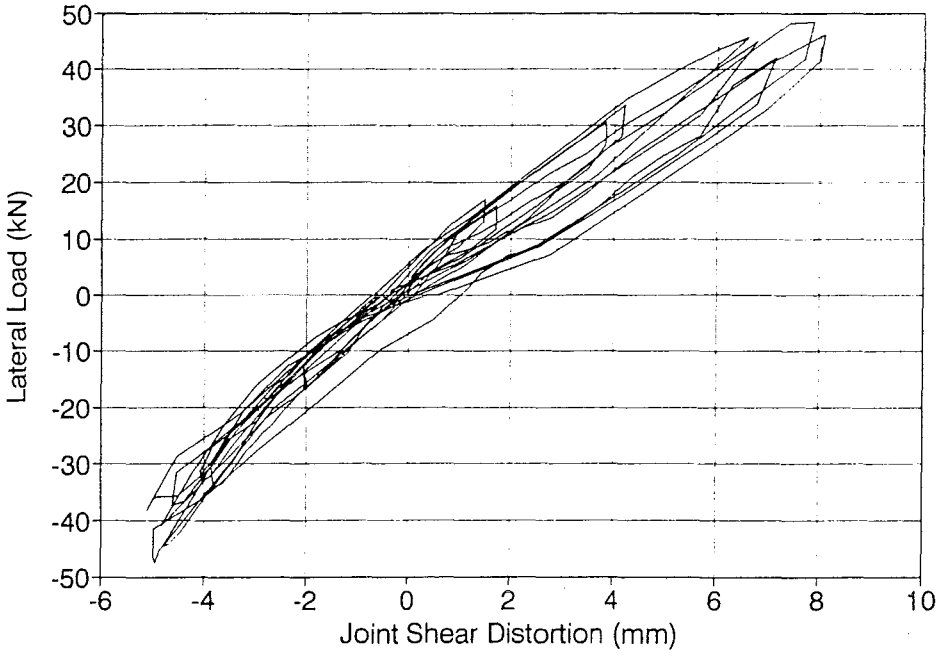

Figure 5.53 Load-joint shear distortion plot for Unit 6

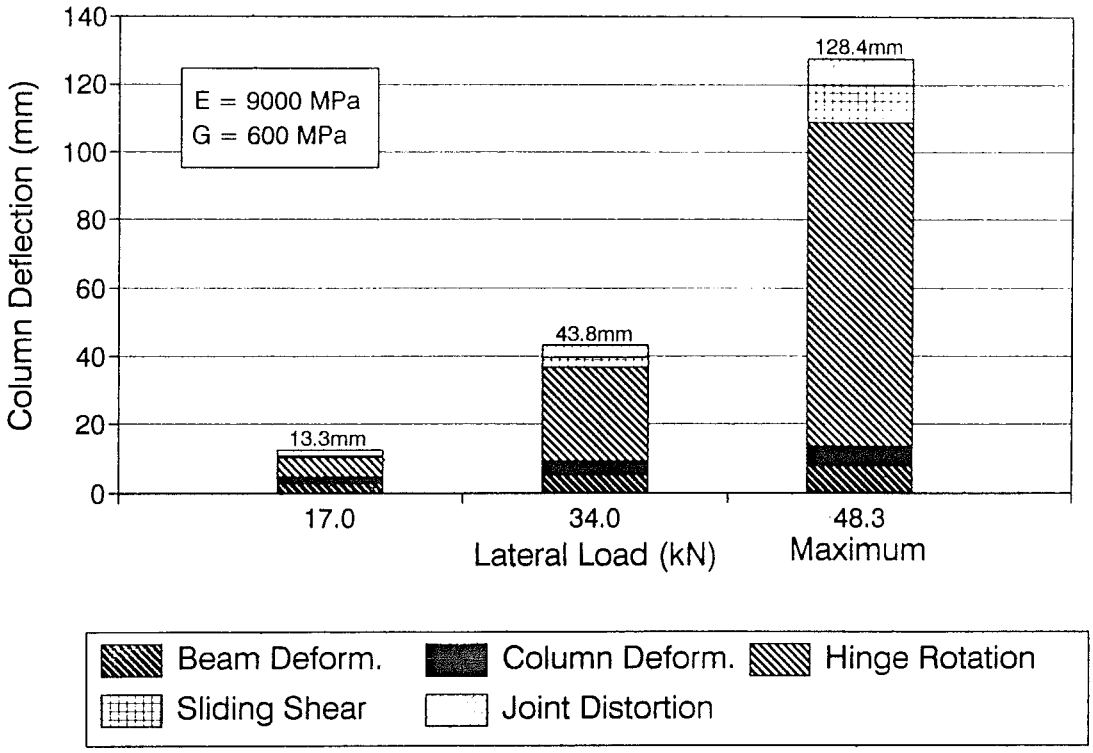

Figure 5.54 Calculated components of column deflection for Unit 6

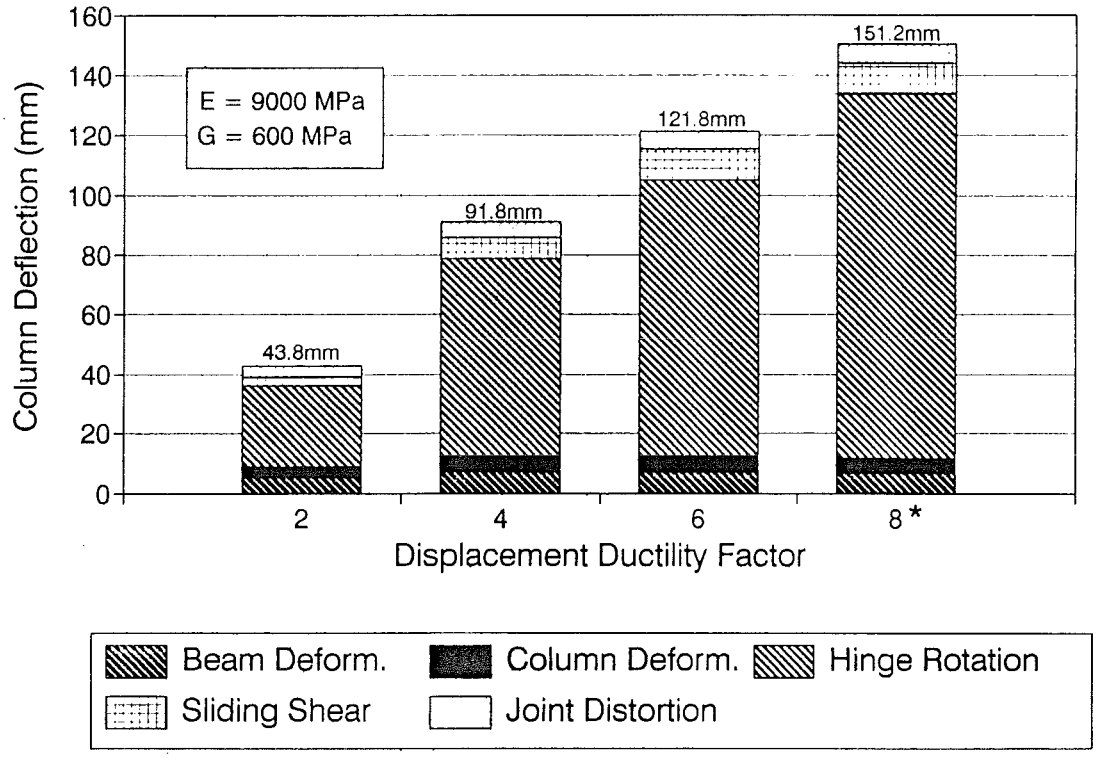

Figure 5.55 Calculated components of column deflection at ductility levels for Unit 6

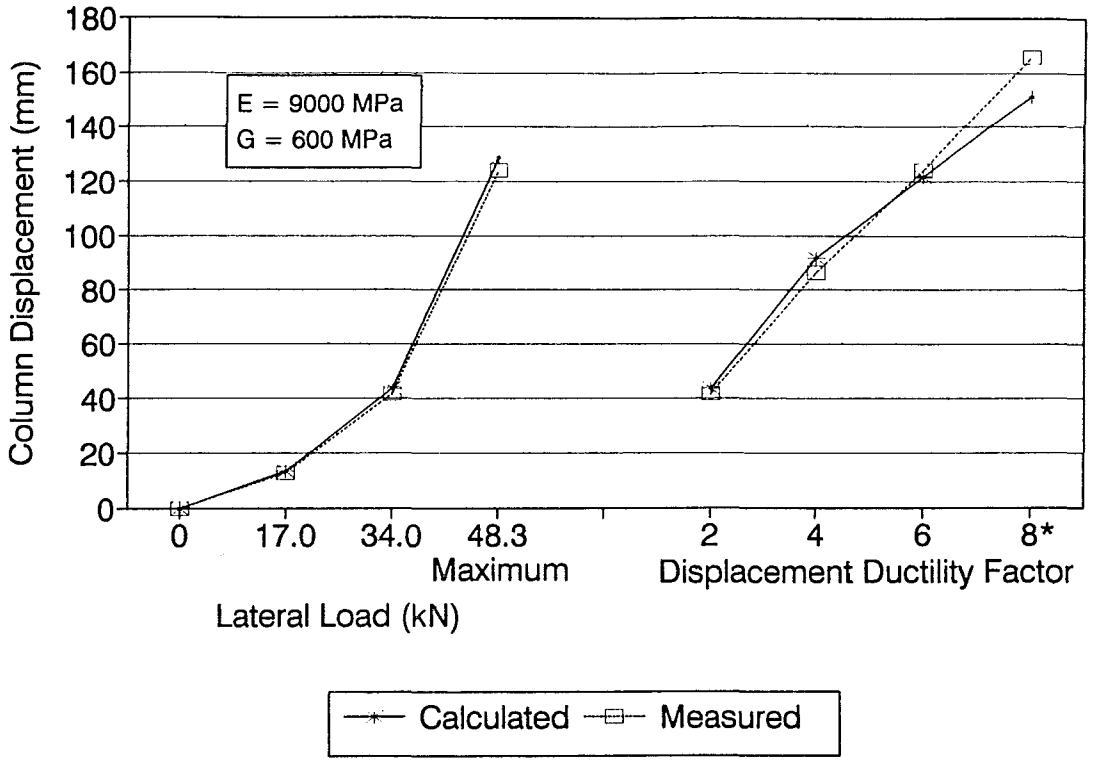

Figure 5.56 Comparision of calculated and measured column deflections for Unit 6

5.4.2 UNIT 7

5.4.2.1 DESCRIPTION OF FAILURE MODE

Final failure in this test was a steel failure and not a timber member failure. As the load increased, the webs started to buckle diagonally between the stiffeners. At a moment of 70.4 kNm, a flexural crack formed at the south top corner of the joint region at the level of the threaded rods. At the formation of the crack, the flexural stresses in the beams and column were 13.2 MPa and 9.6 MPa respectively. The shear stresses in the column, beams and joint core were 0.9 MPa, 0.9 MPa and 4.3 MPa.

As the column cracked, it was decided that further any loading would only be in one direction. Cyclic loading was only conducted in the positive direction up to a lateral load of 70.0 kN, when a series of weld failures occurred at the stiffeners. The connection was cycled back in the other direction until another series of weld failures occurred at the stiffeners and the web began to tear. As the load carrying capacity dropped off, the test was ended.

A photograph of the overall connection at the end of the test is shown in Figure 5.57. Details of the side brackets at the end of test are shown in Figure 5.58.

Figure 5.57 Overall view of Unit 7 at the end of test

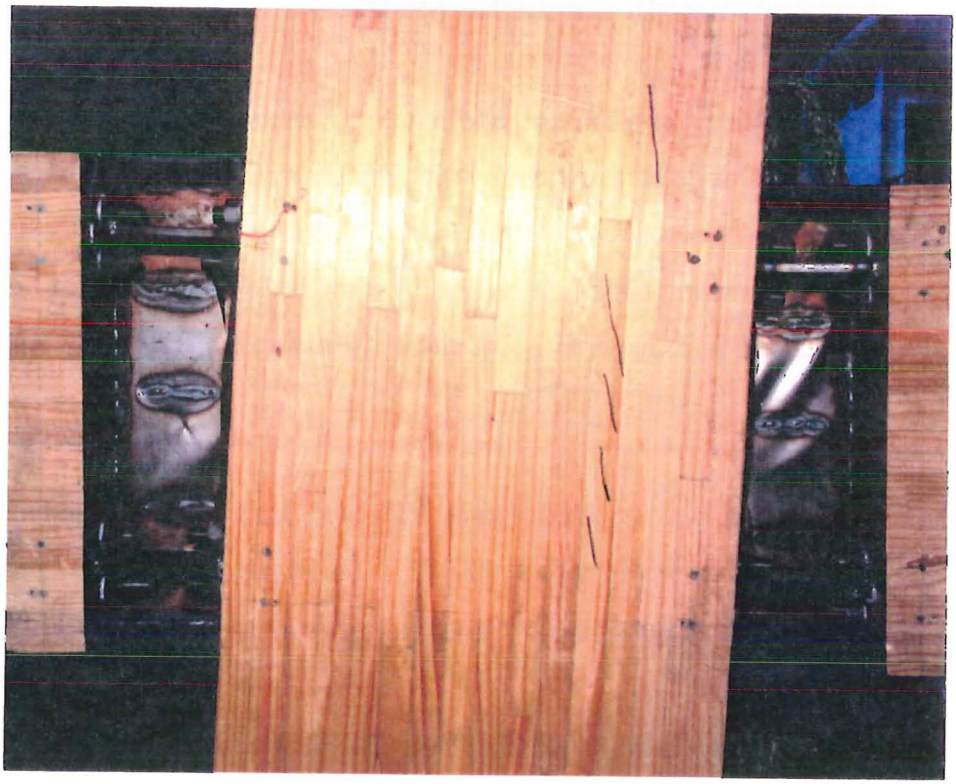

Figure 5.58 View of the joint region of Unit 7 at the end of the test

5.4.2.2 RESULTS

The initial stiffness for Unit 7 was 1.41 kN/mm. The load-deflection plot for Unit 7 is shown in Figure 5.59 and displays linear behaviour up to fracture of the weld at a load bearing stiffener. The saw tooth pattern seen in the plot is due to the other welds fracturing in succession. The plot of the load versus the joint shear distortion as a component of column deflection is shown in Figure 5.60. This graph shows linear behaviour up to the end of the test.

The calculated components of column deflection are shown in Figure 5.61. Note that the asterisk in Figure 5.61 and Figure 5.62 indicates that the hinge rotation of the beams was estimated since the gauges measuring this deformation went offscale.

The graph in Figure 5.61 shows several trends: the deformations due to joint distortion, beam and column deformations and sliding shear all increase by similar proportions as the load is increased. Generally sliding shear deformations are small; the exception is at failure where the deformations double in size. The deformations due hinge rotation increase linearly as the load level increases; except at failure when the hinge rotation increases dramatically.

A comparison of the calculated and measured components of column deflections is shown in Figure 5.62. This graph shows that the calculated components are in good agreement with the overall measured deflection.

5.4.2.3 DISCUSSION

This type of connection did not behave very well. The side plates were too strong, resulting in a flexural wood failure in the column. Using a web to for shear yielding is probably not a practical method to achieve ductility as the shear forces acting on the web are too small, resulting in small plate thicknesses. Using stiffeners to prevent lateral buckling made the side plates too strong.

The weld failures were due to poor penetration of the weld into the flanges.

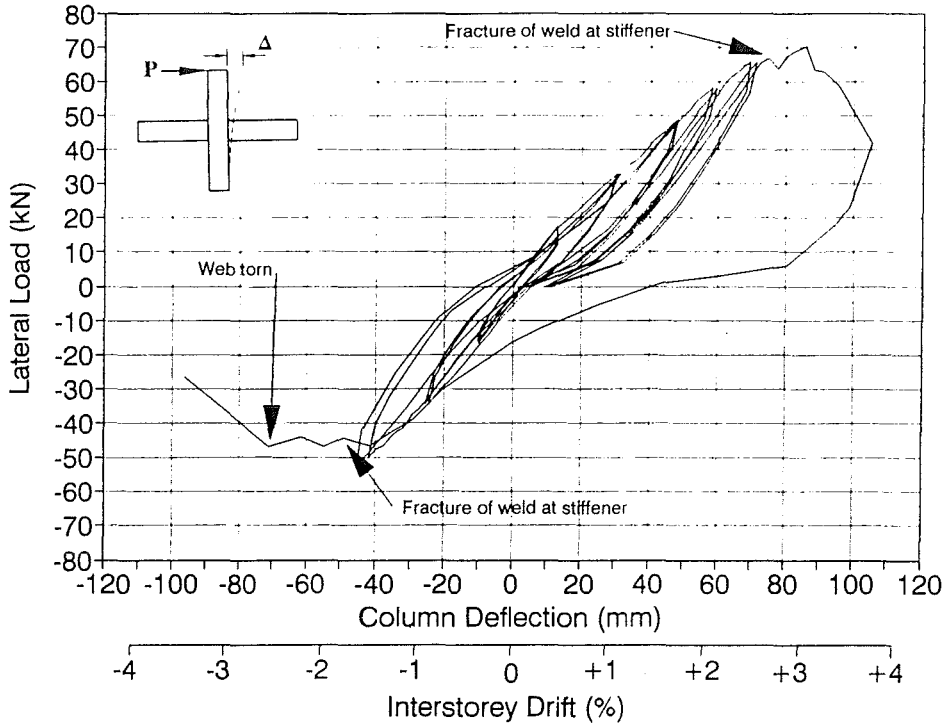

Figure 5.59 Load-deflection plot for Unit 7

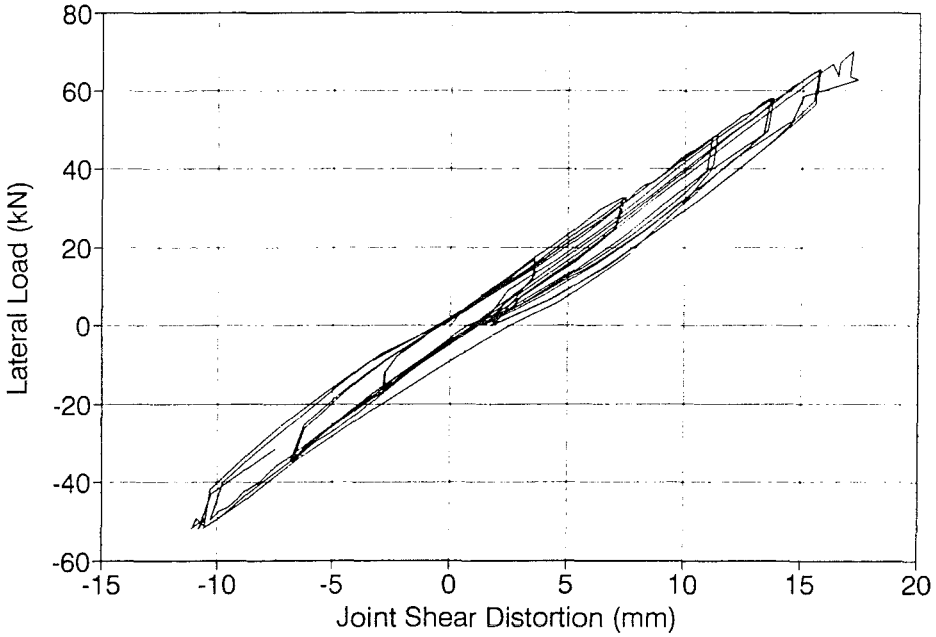

Figure 5.60 Load-joint shear distortion plot for Unit 7

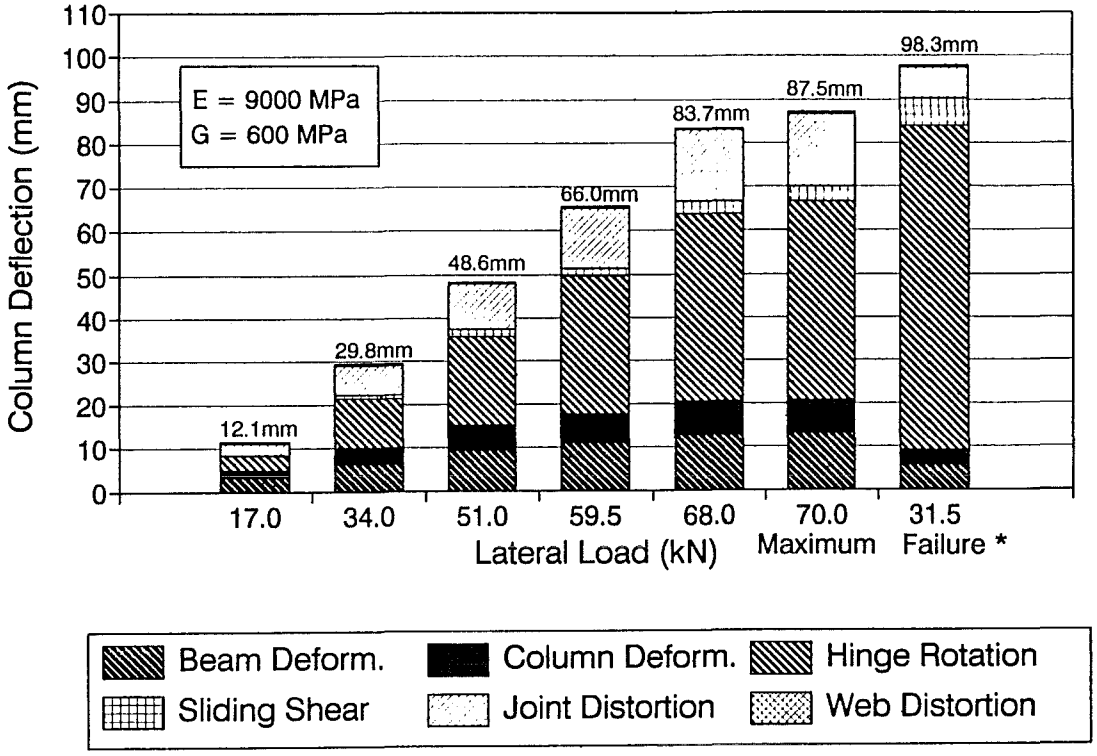

Figure 5.61 Calculated components of column deflection for Unit 7

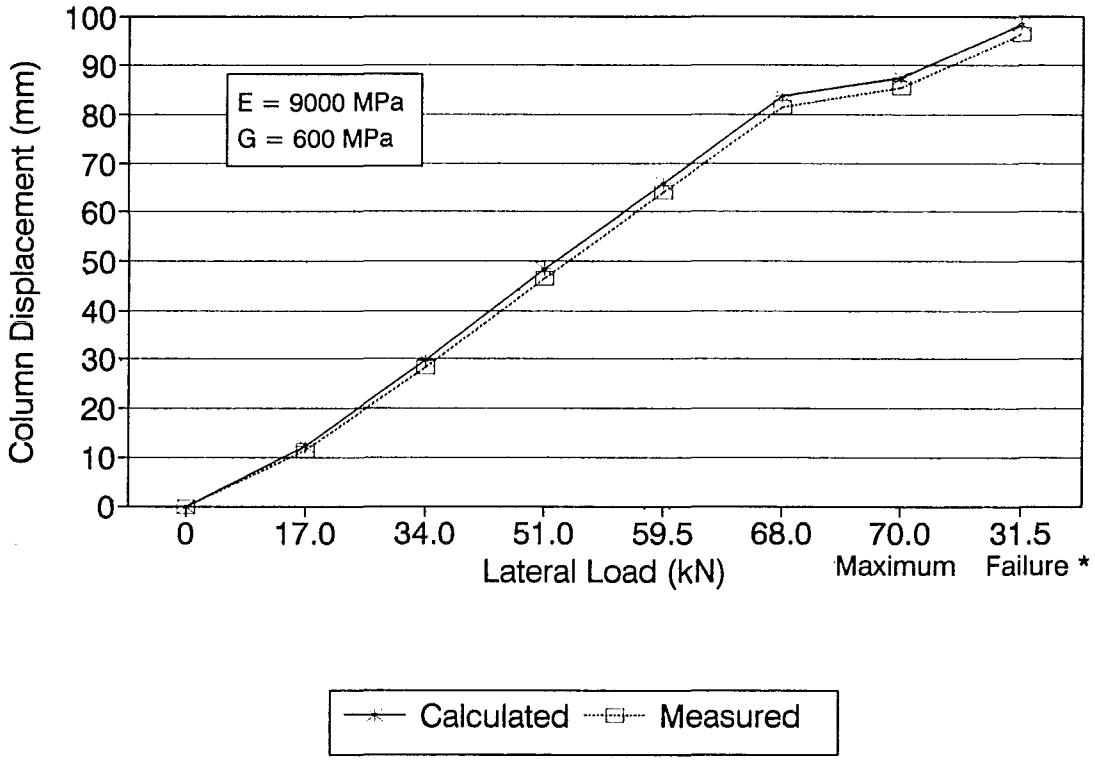

Figure 5.62 Comparision of calculated and measured column deflections for Unit 7

5.4.3 SUMMARY AND DISCUSSION OF RESULTS FOR TYPE C JOINTS

Both the connections were loaded until failure. Failure in both cases consisted of weld failures in the steel side plates. There was also a flexural failure in the column joint of Unit 7. A summary of failure loads and stresses are shown in Table 5.12.

Table 5.12 Summary of failure loads and stresses for joint type C

			UNIT 6	UNIT 7
Initial Stiffness		kN/mm	1.49	1.41
Maximum Loads	**Lateral**	kN	48.2	70.0
	Moment	kNm	67.5	98.1
Maximum Flexural Stresses	**Beam**	MPa	9.73	14.14
	Column		8.95	12.99
Maximum Shear Stresses	**Beam**	MPa	0.80	1.17
	Column		0.80	1.17
	Joint		4.01	5.82
Maximum Column Deflection		mm	166.1	96.3
Maximum Interstorey Drift		%	5.93	3.44
Failure Mode			Weld failure in steel plate	Weld failure in steel plate

As can be seen in Table 5.12, the initial stiffness of Units 6 and 7 were approximately the same.

Two different types of joint behaviour were seen: elastic and ductile behaviour. Unit 6 exhibited excellent ductile behaviour up to a displacement ductility of $\pm$ 8 and Unit 7 behaved elastically up to failure.

The graphs showing the calculated components of column deflection displayed similar trends. The beam and column deformations were of similar proportions and the sliding shear was generally small. The hinge rotation increased as the load increased and escalated once yielding of the connection occurred. Joint distortion was small for Unit 6, but was somewhat larger for Unit 7 as this connection reached higher load levels. Both the connections had very good agreement between the calculated and measured column deformations.

5.5 SUMMARY OF RESULTS

All the connections were loaded to failure or until the expected ductility capacity of the connection was reached. Failure in 7 of the tests was a wood failure in either the beams by flexure (Units 2 and 8), in the column by flexure only (Unit 7), in the columns by flexure (Unit 4) and shear (Units 4) and in the joint region by flexure and shear (Units 1 and 3). Only 1 test (Unit 6) did not have a timber failure; it failed at welds in the steel side bracket. No pullout of the epoxied steel bars occurred, but in Unit 4, the bars and the surrounding wood were pulled out. One failure (Unit 8) was due to poor bonding of the bars into the timber, resulting in stress concentrations which precipitated a wood failure. Several more failures were due to poor quality wood in the joint region (Units 1 and 3).

In most cases, the stresses in the wood at the onset of first cracking were below the code permissible values for No. 1 framing grade radiata pine glulam timber. The low stresses are probably due to a complex stress distribution forming around the bars. In all cases, the timber quality is of vital importance to the performance of the connection. Finger joints in the outer laminations of the timber should not be near the epoxied steel bars. If finger joints happened to be near the bars, usually failure was initiated at that finger joint.

A single layer of bars down the section is better than two layers; as less cross sectional area is removed in the joint where the stresses are high. Using a single layer of bars provides little lateral restraint of the beams, hence staggering the bars down the section would be a better alternative.

A summary of the failure loads and stresses for all the connections are shown in Table 5.13.

Table 5.13 Summary of failure loads and stresses

CONNECTION			Type A				Type B		Type C	
			UNIT 1	UNIT 2	UNIT 3	UNIT 8	UNIT 4	UNIT 5	UNIT 6	UNIT 7
Initial Stiffness		kN/mm	1.41	1.54	1.44	1.48	2.67	2.11	1.54	1.41
Failure Loads	Lateral	kN	60.8	67.9	49.2	52.0	64.4	80.7	48.2	70.0
	Moment	kNm	85.1	95.1	68.8	72.8	70.8	88.8	67.5	98.1
Flexural Stresses at failure	Beam	MPa	13.6	14.9	11.0	11.5	13.9	17.4	9.7	14.1
	Column		12.2	13.7	9.7	9.7	9.4	11.8	9.0	13.0
Shear Stresses at failure	Beam	MPa	1.0	1.1	0.8	0.9	1.1	0.8	0.8	1.2
	Column		1.0	1.2	0.8	0.9	1.1	0.8	0.8	1.2
	Joint		4.9	5.5	5.3	4.1		4.0	4.0	5.8
Maximum Column Deflection		mm	53.9	54.3	56.9	131.6	40.2	85.2	166.1	96.3
Maximum Interstorey Drift		%	1.93	1.94	2.03	4.70	1.44	3.04	5.93	3.44
Predominant Failure Mode			Column Flexure & Joint Shear	Beam Flexure	Column Flexure & Joint Shear	Steel Yielding	Column Flexure	Column Shear	Steel Yielding	Column Flexure

The calculated initial stiffness of the connection was very consistent; it ranged from 1.41 to 1.54 kN/mm. The exception was the much stiffer connections using the central steel hub (Units 4 and 5). In all cases the interstorey drift percentages were very high, ranging from about 2%.

The behaviour of the connections can be put into three categories: elastic, very limited ductility, and ductile behaviour. Units 1 and 4 showed linear behaviour up to failure. Units 2,3 and 5 showed some ductility (up to a displacement ductility of 2). Excellent ductile behaviour was shown by Unit 6 (ductility of 8) and Unit 8 (ductility of 6). The bars in Unit 8 were debonded using insulation tape to increase the length of the bar yielding.

The graphs of the calculated components showed some interesting trends.

- If some of the reinforcement remained elastic, sliding shear was small, but if considerable yielding occurs, the sliding shear component becomes much larger. Shear reinforcement must be provided in ductile connections in which the outer bars yield.
- The shear distortion of the joint core was large for connections having all the bars concentrated at the ends. Conversely, the shear distortion of the joint was much smaller for connections with bars spread down the depth of the beams. This trend implies that bars spread down the joint improves the shear stiffness of the joint, but there was no increase in shear strength.
- The hinge rotation component was significant for connections exhibiting ductile behaviour.
- The beam and column deformations were only significant for connections showing elastic behaviour.

The type of washers used in the prefabricated steel brackets influenced the behaviour of the joint. High strength washers locally increased the stiffness of the flange plates at the bolt holes, increasing the yield strength of the plate. This made the flanges too strong, hence the timber failed before the yielding commenced in the connection. Using mild steel washers rectified the problem

CHAPTER 6

CONCLUSIONS

6.1 INTRODUCTION

In New Zealand, there have been very few multi-storey timber buildings built, even though these types of buildings are not only technically feasible but economically viable. One of the reasons for this indifference is the shortage of design information on suitable beam-column connections. This report looks at several new types of moment-resisting connections assembled using epoxied steel dowels embedded into timber. Use of this technique enables steel bars to be placed at the top and bottom of the beams, forming a compression/tension steel couple which resists the moment with the shear carried by dowel action.

Several advantages can be gained by epoxy bonding steel dowels into timber:

- the steel components are protected from corrosion
- allows high strength connections to be made, utilizing the full strength of the timber
- the epoxy provides a bond stronger than the timber
- increased stiffness of the joint
- excellent aesthetic appearance
- excellent fire resistance since the timber member protects the connection

6.2 CONCLUSIONS

The conclusions from the tests were as follows:

GENERAL

1. Strong and stiff moment-resisting connections can be made using epoxied steel rods in a variety of different geometries.

2. Excellent ductility can be achieved provided that relative strengths are such that brittle fracture of the wood is prevented. This requires high quality glulam timber and preferably no finger joints in the critical regions.
3. A "capacity design" approach to sizing the members and connections is necessary if ductile behaviour is to be achieved.
4. Glulam timber failures occurred in several tests at stresses much less than predicted by the timber design code.
5. The two types of epoxy performed very well as there were no pull-out of the bars.

CONCLUSIONS FOR CONNECTIONS USING EPOXIED STEEL DOWELS ONLY

6. Excellent ductile behaviour can be achieved using only deformed reinforcing bars epoxied into the timber provided that the timber quality is sufficient to prevent premature fracture. Ductility results from axial yielding of bars in tension and compression.
7. A single layer of bars on the column centreline is better than two layers because there is less weakening of the column which could lead to premature failure.
8. Shear failures can occur in the joint region if shear stresses become too large.

CONCLUSIONS FOR CONNECTIONS USING THE STEEL BRACKETS

9. Ductile connections can also be constructed using prefabricated steel plates designed for yielding of the beam flanges.
10. For ductile behaviour, capacity design is necessary to ensure that yielding of the steel connector bracket occurs rather than any timber failure.
11. The steel plate thickness and types of washers have a major influence on the expected ductility.
12. The connection using the prefabricated steel hub was substantially stiffer than the other types of connections.

6.3 FURTHER RESEARCH

This testing has identified some detailed items which would benefit from further study. These include:

- the steel plate thickness required to achieve ductile yielding
- the size and thickness of steel washers
- yield penetration along the epoxied reinforcing bars
- the prevention of wood splitting failures
- shear transfer through dowel action
- the effect of local debonding on sliding shear transfer.

Major issues which will affect the use of these connections in real buildings are the following:

- seismic response of multistorey timber frame buildings, especially the ductility demand.
- building displacements under wind and earthquake loading
- fire resistance of epoxied connections.

REFERENCES

1. Advent, R.R., 1986. "Factors Affecting Strength of Epoxy Repaired Timber", Journal of the Structural Division, American Society of Civil Engineers, New York, Volume 112, No. 2, pp 207-221.

2. Batchelar, M.L. and Hunt, R.D., 1991. "Composite Plywood and Steel Gusset Plates for Moment-Resisting Joints in Timber Frames", Proceedings of the 1991 International Conference on Timber Engineering, London, United Kingdom, Volume 3, pp 3.104-3.110.

3. Boult, B.F., 1988. "Multi-Nailed Moment-Resisting Joints", Proceedings of the 1988 International Conference on Timber Engineering, Seattle, USA, Volume 2, pp 329-338.

4. Buchanan, A.H. and Dean, J.A, 1988. "Practical Design of Timber Structures to Resist Earthquakes", Proceedings of the 1988 International Conference on Timber Engineering, Seattle, USA, Volume 1, pp 813-822.

5. Buchanan, A.H. and Fletcher, M.R., 1989. "Glulam Portal Frame Swimming Pool Construction", Proceedings of the Second Pacific Timber Engineering Conference, Auckland, New Zealand, 1989, Volume 1 pp 245-249.

6. Buchanan, A.H. and Townsend, P.K., 1990. Unpublished Report on "Portal Frame Knee Joints with Epoxied Steel Dowels", Canteprise, University of Canterbury.

7. Buchanan, A.H., Deam, B.L. and Dean J.A., 1991. "Multi-Storey Timber Buildings", Proceedings of the 1991 IPENZ Conference, Auckland, Volume 1, pp 221-232.

8. Buchanan, A.H., Moss, P.J. and Townsend, P.K., 1990. "Reinforced Bars Epoxy Bonded in Glue Laminated Timber", Proceedings of the 1990 International Conference on Timber Engineering, Tokyo, Japan, Volume 2, pp 601-610.

9. Bulleit, W.M., 1989. "Classic Wood Structures", Task Committee on Classic Wood Structures of the Committee on Wood of the Structural Division of the American Society of Civil Engineers, American Society of Civil Engineers, New York.

10. Ceccotti, A. and Vignoli, A., 1988. "The Effects of Seismic Events on the Behaviour of Semi-Rigid Joint Timber Structures - A Simulation of the Influence of Structural Scheme and of Joint Characteristic", Proceedings of the 1988 International Timber Engineering Conference, Seattle, USA, Volume 1, pp 823-837.

11. Clark, W.D. and Mulligan, R.J., 1984. "Use of Pinus Radiata in the Foundation Reconstruction of Historic Wooden Government Building, Wellington", Proceedings of the Pacific Timber Conference, Auckland, Volume 1, pp 239-254.

12. Crews, K.I., 1991. "Joints and Connections: Timber Engineered Structures", Australian Forest Industries Journal, November 1991, pp 32-37.

13. Doyle, 1985. "Wood Frame Economises Anchorage Mixed Use Project", New Zealand Journal of Timber Construction, Volume 1, Number 4, pp 4-7.

14. Frost, K.D., 1990. "Epoxy and Steel Dowel 'Bolt' Joints in Glulam Timber", Research Report, School of Architecture, Victoria University of Wellington, November 1990.

15. Gardner, G.P., 1989. "A Reinforced Glued Laminated Timber System", Proceedings of the Second Pacific Timber Engineering Conference, Auckland, New Zealand, 1989, Volume 2, pp 295-300.

16. Gardner, G.P., 1991. "A Reinforced Glued Laminated Timber System", Proceedings of the 1991 International Conference on Timber Engineering, London, United Kingdom, Volume 3, pp 3.218-3.225.

17. Gopu, V.K.A., 1981. "Repaired Pitch-Cambered Glulam Beams, Journal of the Structural Division, American Society of Civil Engineers, New York, Volume 107, No. 7, pp 1251-1262.

18. Gotz, K., Hoor, D., Mohler, K. and Natterer, J., 1989. "Timber Design and Construction Sourcebook - A Comprehensive Guide to Methods and Practice", McGraw-Hill Publishing Company.

19. Gougeon Brothers, 1980. "The Gougeon Brothers on Boat Construction; Wood and the West System Materals", Gougeon Brothers, Michigan, U.S.A, pp 261-271.

20. Gougeon Brothers, 1988. "WEST SYSTEM Products Technical Manual", Beckett Printing Ltd, Auckland.

21. Halliday, M.A.L., 1991. "Feasibility of Medium Rise Timber Office Buildings", Research Report 91-3, Department of Civil Engineering, University of Canterbury.

22. Hilti, 1990. "Hilti Fastening Manual - Anchoring", Hilti Corporation, October 1990 Issue, pp 223-228.

23. Hunt, R.D. and Bryant, A.H., 1988. "Moment-Resisting Nail Plate Joints - Recent Developments at Auckland University", Proceedings of the 1988 International Conference on Timber Engineering, Seattle, USA, Volume 1, pp 251-256.

24. Inayama, M. and Sakamoto, I., 1989. "Development Research of New Wooden Rigid Frame Structure", Proceedings of the Second Pacific Timber Engineering Conference, Auckland, New Zealand, Volume 2, pp 19-23.

25. Kauri Timber Company, 1990. "Safe Load Tables for Structural Timber", R. and J. McTaggart and Company, Pialba, Queensland.

26. Komatsu, K., 1989. "Performance of Timber Moment-Resisting Joints", Proceedings of the Second Pacific Timber Engineering Conference, Auckland, New Zealand, Volume 2, pp 25-30.

27. Komatsu, K., Kawamoto, N. and Uesugi, S., 1990. "Performance of Glulam Moment-Resisting Joints", Proceedings of the 1990 International Conference on Timber Engineering, Tokyo, Japan, Volume 2, pp 626-632.

28. Komatsu, K., Kawomoto, N., Kazumi, H. and Harada, M., 1991. "Modified Glulam Moment-Resisting Joints", Proceedings of the 1991 International Conference on Timber Engineering, London, United Kingdom, Volume 3, pp 3.111-3.118.

29. Law, P.W. and Yttrup, P.J., 1989. "Epoxy Injected Bolts in Shear", Proceedings of the Second Pacific Timber Engineering Conference, Auckland, New Zealand, 1989, Volume 3, pp 85-91.

30. Lembke, C.A., 1991. "Multi-storey Wood Frame Worldwide!", Australian Forest Industries Journal, October 1991, pp 8-9.

31. Ohashi, Y. and Sakamoto, I., 1989. "Study on Laminated Timber Moment-Resisting Joint", Proceedings of the Second Pacific Timber Engineering Conference, Auckland, New Zealand, 1989, Volume 2, pp 38-42.

32. New Zealand Journal of Timber Construction, 1986. "Prime Award - Glue Laminated Timber Space Frame Enclosing Rankine Brown Courtyard", Volume 2, Number 3, pp 3-4.

33. Nielson, P.C., 1988. "Wooden Blades for Large Turbine Rotors", Proceedings of the 1988 International Conference on Timber Engineering, Seattle, USA, Volume 1, pp 564-569.

34. Packer, J.A. and Morris, L.J., 1977. "A Limit State Design Method for the Tension Region of Bolted Beam-Column Connections", The Structural Engineer, Volume 55, Number 10, October 1977, pp 446-458.

35. Park, R., 1989. "Evaluation of Ductility of Structures and Structural Assemblages from Laboratory Testing", Bulletin of the New Zealand National Society for Earthquake Engineering, Volume 22, Number 3, September 1989, pp 155-166.

36. Park, R. and Paulay, T., 1975. "Reinforced Concrete Structures", John Wiley and Sons, New York.

37. Riberholt, H., 1986. "Glued Bolts in Glulam", Department of Structural Engineering, Technical University of Denmark, Series R, Number 210.

38. Riberholt, H., 1988a. "Glued Bolts in Glulam - Part 2", Department of Structural Engineering, Technical University of Denmark, Series R, Number 228.

39. Riberholt, H., 1988b. "Glued Bolts in Glulam - Proposals for CIB Code", International Council for Building Research Studies and Documentation Working Commission W18 -Timber Structures, Meeting 21, Vancouver, Canada, September 1988, 17pp.

40. Rodd, P.D., 1988. "Timber Joints Made With Improved Circular Dowel Fasteners", Proceedings of the 1988 International Conference on Timber Engineering, Seattle, USA, 1988, Volume 1, pp 26-37.

41. Rodd, P.D., Hilson, B.O. and Spriggs, R.A., 1989. "Resin Injected Mechanically Fastened Timber Joints", Proceedings of the Second Pacific Timber Engineering Conference, Auckland, New Zealand, 1989, Volume 2, pp 131-136.

42. Rodd, P.D., Hilson, B.O. and Spriggs, R.A., 1991. "Prediction of Embedment Characteristics for Laterally Loaded Resin Injected Bolts in Timber", Proceedings of the 1991 International Timber Engineering Conference, London, United Kingdom, Volume 3, pp 3.50-3.57.

43. SANZ, 1990. "NZS 3603:1990 - Code of Practice for Timber Design", Standards Association of New Zealand, Wellington.

44. Smith, P.C., 1982. "Design Aspects of a Four Storey Timber Building", New Zealand Timber Design Society Newsletter, No. 8, pp 7-28.

45. Syme, D.R., 1989. "Timber Jointing Systems in Europe", Proceedings of the Second Pacific Timber Engineering Conference, Auckland, New Zealand, 1989, Volume 2, pp 138-142.

46. Thomas, G.C., 1991. "The Feasibility of Multistorey Light Timber Frame Buildings", Research Report 91-2, Department of Civil Engineering, University of Canterbury.

47. Townsend, P.K., 1990. "Steel Dowels Epoxy Bonded In Glulam Timber", Research Report 90-11, Department of Civil Engineering, University of Canterbury.

48. Touliatos, P.G., 1991. "Design Problems of the Timber Framed Construction in Seismic Zones", Proceedings of the 1991 International Timber Engineering Conference, London, United Kingdom, Volume 4, pp 4.275-4.282.

49. Tukovsky, S.B., 1991. "Use of Glued-In bars for Reinforcement of Wood Structures", Proceedings of the 1991 International Timber Engineering Conference, London, United Kingdom, Volume 3, pp 3.143-3.148

50. Tukovsky, S.B., Lukyanov, E.I and Poporeltsev, A.A., 1991. "Use of Glued-In bars for Reinforcement of Wood Structures", Proceedings of the 1991 International Timber Engineering Conference, London, United Kingdom, Volume 3, pp 3.212-3.217

51. van Resburg, B.W.J, Cillié, C du T and Ebersöhn, W., 1984. "Steel Reinforced Timber Structural Elements", Proceedings of the Pacific Timber Engineering Conference, Auckland, New Zealand, 1984, Volume 1 pp 97-108.

APPENDIX 1 YIELD AND ULTIMATE STRENGTH OF THREADED RODS

The threaded rods were made from 3/4" (19mm) diameter high strength round bar, according to AISI 4140 which is supplied in a heat treated condition with an ultimate tensile strength in the range of 850-1000 MPa. The steel has excellent toughness and is readily machineable.

TESTING

Specimen Size:

Thread Size	=	3/4" BSW x 400 mm
Stress Area	=	196 mm^2

The threads were machine cut onto the round bars using a screw cutting machine using a 3/4" BSW die. The testing was done on the large Avery Testing Machine and gave the following results:

RESULTS

Sample Size	=	2
Ultimate Tensile Strength	=	173.5 kN, 181.3 kN
Mean Ultimate Tensile Strength	=	177.4 kN
Standard Deviation	=	$\pm$ 3.9 kN

ANALYSIS

The analysis of the charts showed that the bars exhibited no well defined yield point and a brittle failure mode. The stress area was used to calculate the yield and ultimate stresses in the threaded rods. The 0.2% strain and 0.5% fracture strain offset methods were used to determine the yield strength of the bar. Both methods gave the same results.

Sample	f_y(MPa)	f_u (MPa)	f_y/f_u
1	715	885	0.808
2	775	925	0.838
Mean	745	905	0.823

CONCLUSIONS

For design, assume a ratio of yield stress to ultimate stress of 0.80 and a nominal ultimate tensile strength of 850 MPa which gives an nominal yield strength of 680 MPa.

APPENDIX 2 YIELD AND ULTIMATE STRENGTH OF DEFORMED BARS

The deformed bars were all grade 250 mild steel bars. Two sizes were tested; D16 bars and D20 bars.

TESTING

The testing was completed on the large Avery Testing Machine with a Data Logger linked to measure the load and the extension of the bar.

RESULTS

Bar Designation		P_y (kN)	P_u (kN)
D16	A	64.0	91.0
	B	63.8	91.4
	C	64.6	91.6
	D	65.2	91.2
	E	64.5	91.2
D20	A	102.0	145.5

ANALYSIS

The analysis of the charts showed that the bars exhibited a well defined yield point. For D16 bars, the nett bar area is 201.06 mm^2 and for D20 bars, the bar area is 314.16 mm^2.

Bar Designation		f_y (MPa)	f_u (MPa)
D16	A	318	453
	B	318	455
	C	321	456
	D	324	454
	E	321	454
	Mean	320	454
D20	A	325	463

CONCLUSIONS

For design, assume a yield stress of 320 MPa and 325 MPa for D16 and D20 bars respectively. The overstrength factor for both sets of bars is 1.42.

APPENDIX 3 MOISTURE CONTENT AND DENSITY OF THE TIMBER

The moisture content was measured using a Protimeter 'Timbermaster' Model D184T or by ovendrying small samples of timber.

(a) for large members

Section	B (mm)	D (mm)	L (mm)	Weight (kg)	Density (kg/m^3)	M/C Measured (%)
U1 - COLUMN	180	481	1116	44.3	458	10.0
U2 - BEAM	136	495	1538	50.3	486	9.5
U2 - COLUMN	180	481	2559	111.4	503	10.2
U3 - BEAM	135	492	1066	34.083	481	12.7
U3 - COLUMN	181	487	1016	42.162	471	11.3
U3 - BEAM	134	493	1085	35.359	493	12.9
U4 - COLUMN	179	503	2560	111.8	485	14.0
U4 - BEAM	133	498	1373	48.7	536	15.1
U5 - BEAM	133	497	1380	52.0	570	14.0
U5 - COLUMN	179	500	2198	96.4	490	11.3
U5 - BEAM	133	498	1373	48.7	536	15.1
U8 - BEAM					479	14.0

(b) for small samples:

Section	B (mm)	D (mm)	L (mm)	Wet Weight (kg)	Dry Weight (kg)	Density (kg/m^3)	M/C Calc (%)
U3 - BEAM	135	490	87	2.722	2.451	471	11.1
U3 - COLUMN	180	486	90	3.727	3.340	472	11.6
U4 - COLUMN	180	504	244	10.300	9.052	465	13.8
U8 - COLUMN	179	502	372	16.019	14.384	479	11.4

The average readings for the moisture content and density of the timber are given below:

	Sample Size	Density (kg/m^3)	M/C Calc (%)	M/C Measured(%)
Average	15	503	11.9	12.5

APPENDIX 4 MODULUS OF ELASTICITY OF THE TIMBER

The Modulus of Elasticity was measured using a Metriguard Model 239A stress wave timer.

Section	Propogation Time (μs)	L (mm)	Density (kg/m^3])	E (MPa)
U1 - COLUMN	266.6	1116	458	8036
U2 - BEAM	380.0	1538	486	7960
U2 - COLUMN	629.0	2559	503	8324
U3 - BEAM	278.3	1066	481	7065
U3 - COLUMN	272.4	1016	471	6551
U3 - BEAM	275.6	1085	493	7648
U4 - BEAM	341.7	1380	485	7913
U4 - COLUMN	605.1	2560	536	9588
U5 - BEAM	341.7	1380	570	9300
U5 - COLUMN	536.5	2198	490	8227
U5 - BEAM	342.8	1373	536	8593
U8 - COLUMN	669.2	2936	479	9227

The average Modulus of Elasticity of the timber used is as follows:

	SAMPLE SIZE	DENSITY (kg/m^3)	E (MPa)
Average	12	499	8203

Classn:

BEAM-COLUMN CONNECTIONS FOR MULTI-STOREY TIMBER BUILDINGS

R.H. Fairweather

ABSTRACT: Results are presented for tests of 8 connections constructed using steel dowels epoxy bonded into glulam timber. Tests were under simulated seismic loads. Variables included bar type, steel percentage, glue type and the use of steel connector plates to attach the members.

Department of Civil Engineering, University of Canterbury
Master of Engineering Report, 1992.